Breaking the Limit - Synthesis and Properties of *p*-Amino-Triazatriangulenium, the Most Stable Carbenium Ion

Marko H. Nowack[a], Gennaro Pescitelli[b], Arianna Lanza[a], Bo W. Laursen[a]*

[a] Dr. Marko H. Nowack, Dr. Arianna Lanza, Prof. Bo W. Laursen
Department of Chemistry
University of Copenhagen
Universitetsparken 5, 2100, Copenhagen Ø, Denmark
E-mail: bwl@chem.ku.dk

[b] Prof. Gennaro Pescitelli

Dipartimento di Chimica e Chimica Industriale, Università di Pisa, Via Giuseppe Moruzzi 13, 56124 Pisa, Italy

Table of Contents

1.1 Experimental Section

1.1.1 General

Commercially available reagents were used without purification unless otherwise stated. *N*-octyl-triazatriangulenium tetrafluoroborate ($TATA^+$) was synthesized according to the literature procedure.[1] The solvents acetonitrile (MeCN), dichloromethane (CH_2Cl_2), diethylether (Et_2O), dimethylformamide (DMF), heptane, *iso*-propanol (*i*-PrOH), methanol (MeOH), were HPLC grade and used as received. Anhydrous tetrahydrofuran (THF) and pyrrolidine were purchased from Sigma Aldrich and used as received. NMR spectroscopy was performed on a BRUKER Avance III 500 Ultrashield Plus with a 5 mm CPDCH CryoProbe with improved ^{13}C sensitivity. The magnet is 11.7 Tesla, corresponding to ^{1}H NMR at 500 MHz and ^{13}C NMR at 126 MHz. The chemical shifts are referenced to the ppm scale relative to the residual solvent signal for the following solvents: deuterated acetonitrile (CD_3CN, ^{1}H = 1.94 ppm, ^{13}C = 118.26 ppm), deuterated chloroform ($CDCl_3$, ^{1}H = 7.26 ppm, ^{13}C = 77.36 ppm), and deuterated dimethylsulfoxide (DMSO-d_6, ^{1}H = 2.54 ppm, ^{13}C = 40.45 ppm.[2] The coupling constants are reported in Hertz (Hz). ^{13}C attached proton test (APT) spectra were phased such that negative signals (−) correspond to *C* and CH_2, and positive signals (+) correspond to *C*H and CH_3. HRMS was recorded on a Bruker SolariX XR 7T ESI/MALDI-FT-ICR-MS instrument, using dithranol as the matrix whenever MALDI was the analysis method. Automated flash column chromatography was performed on a Büchi Pure C-850 chromatography system fitted with a UV/Vis detector from 200-800 nm, using pre-packed FlashPure EcoFlex SiO_2 cartridges. The flowrate (FR) and fraction volume (FV) along with the solvent gradients for each purification are reported.

1.1.2 Photophysical Measurements

UV/Vis absorption spectra were recorded on a PerkinElmer Lambda 1050 double beam spectrometer and baseline corrected to pure solvent in a quartz cuvette with a 10 mm path length. Settings were 1 nm slit-width and 1 nm data interval. The molar absorption coefficients were determined from single point measurements in triplicate. Steady-state emission spectra were recorded on a FluoTime300 from PicoQuant using a Xe-lamp as the excitation source. The maximum absorption of the S_0-S_1 transition was less than 0.1 for all emission measurements. Time-resolved fluorescence decays were measured by time-correlated single photon counting (TCSPC) on a FluoTime300 from PicoQuant using a pulsed solid-state laser at 470 nm (LDH-P-C-470), 450 nm (LDH-P-C-450), or 405 nm (LDH-P-C-405) and emission at magic angle (54.7°). The instrument response function (IRF) was recorded at the excitation wavelength using a dilute sample of Ludox scattering suspension. Fluorescence decay histograms were analyzed using the FluoFit software from PicoQuant by iterative reconvolution with a sum of exponentials.

$$I(t) = I_0 \sum_i \alpha_i \, e^{-\frac{t}{\tau_i}}$$

Where α_i is the amplitude and τ_i is the lifetime of the i-th component.

1.1.3 Quantum Yields

The quantum yields of fluorescence were determined using a 6-point dilution method based on the protocol described in *Practical Fluorescence Spectroscopy* by Z. Gryszynski and I. Gryzynski[3] (**Equation S1**) using Rhodamine 6G in EtOH (ϕ_f = 0.94)[4] and Coumarin-153 in EtOH (ϕ_f = 0.54).[5]

$$\phi = \phi_R \cdot \frac{I}{I_R} \cdot \frac{1 - 10^{-OD_R}}{1 - 10^{-OD}} \cdot \frac{n^2}{n_R^2} = \phi_R \cdot \frac{\mathrm{Grad}}{\mathrm{Grad}_R} \cdot \frac{n^2}{n_R^2}$$

Equation S1. Relative quantum yield determination.

ϕ is the quantum yield of the sample, ϕ_R is the quantum yield of the reference dye, I and I_R are the total integrated emission intensities of the sample and the reference dye. OD and OD_R are the optical densities of the sample and the reference dye at the wavelength of excitation. n and n_R are the refractive indexes of the solvent in which the sample and the reference dye are dissolved. Grad is the gradient of I plotted as a function of $1 - 10^{-OD}$. Grad_R is the gradient of I_R plotted as a function of $1 - 10^{-OD_R}$. The refractive index of EtOH (1.3284) and CH_2Cl_2 (1.4244) were used.

1.1.4 Electrochemistry

Cyclic voltammograms (CV) and differential pulse voltammograms (DPV) were obtained using a Nordic Electrochemistry ECi-100 potentiostat and EC4™ DAQ Software with a scan rate of 0.1 V s^{-1} for the CVs. A one compartment cell was used with the three electrodes. Ag/AgCl was used as the reference electrode, a Pt wire was used at the counter electrode, and a glassy carbon (Ø = 2 mm) electrode was used as the working electrode. Measured potentials were referenced to the ferrocene/ferrocenium (Fc/Fc^+) redox couple, measured before and after each experiment using a 1.0 mM solution of Fc in MeCN. Tetrabutylammonium hexafluorophosphate ($TBAPF_6$) was used as the supporting electrolyte (c = 0.1 M) and was recrystallized from boiling EtOH before use. All solutions were purged with MeCN-saturated N_2 before measurements. HPLC grade MeCN was used without further purification as the solvent. Compound concentrations were 1.0 mM. The potentials were extracted by fitting of a Gaussian function to the raw DPV data.

1.1.5 Computational Methods

All calculations were run with Gaussian'16, Rev. C.01.[6] Geometry optimizations were run at B3LYP/6-311+G(2d,p) level, including D3BJ dispersion correction and a continuum solvent model (IEF-PCM) for DCM. The same level of theory was employed for frequency calculations, to verify the nature of the stationary points, and population analyses. ΔG values for the reaction $C^+ + OH^- \rightleftharpoons COH$ were estimated by evaluating the difference in free energies computed for the three species. DDEC6 charges were generated using a dedicated software[7] which operates on .wfx files containing total density Natural Orbitals (NO) generated by Gaussian'16.

1.1.6 Electron Diffraction Methods

The crystallization attempts yielded intense-yellow, flake-like, particles which were relatively large but too thin and polycrystalline for single-crystal x-ray diffraction. Hence, the crystal structure was characterized with electron diffraction (3D ED). As the crystals readily redissolve in their mother liquor at ambient temperature, a drop of suspension was deposited on a glass slide and let to dry in the air. The solid was then resuspended with pentane, drop casted on a 200-mesh copper TEM grid coated with a continuous film of ultrathin amorphous carbon (from EMS) and let to dry again in the air.

3D ED measurements were performed at 173 K and 10^{-5} Pa using a Gatan Elsa Cryoholder on a Rigaku XtaLAB Synergy-ED,[8] equipped with a LaB_6 source operating at 200 kV (λ= 0.0251 Å). Series of diffraction patterns were collected multiple with a Rigaku HyPix-ED detector during continuous rotation of the crystals with a width of

0.15 ° and an exposure time of 0.3 s per frame, using a selected area aperture with an apparent diameter of 2 µm. The program CrysAlisPro[9] was used to control the data collection and to process the diffraction data, for indexing, data reduction and space group determination.

The datasets from 3 crystals were merged to improve data completeness, which however remains limited due to strong preferred orientation of the thin crystals on the sample support. Structure solution and refinement were carried out in Olex2[10]. The crystal structure was solved ab initio with SHELXT[11] in space group *P*-1. Least-squares refinement in kinematic approximation was performed with SHELXL[12] using scattering factors for electrons.[13] An extinction parameter was refined to mitigate the effects of multiple diffraction. Geometrical restraints were applied to the conformationally flexible alkyl chains and to the disordered PF_6^- anion to facilitate convergence to a physically meaningful geometry. Anisotropic atomic displacement parameters were refined for non-hydrogen atoms with the aid of similarity and rigid-body restraints, while H-atoms were placed in geometrically idealized position and described with a riding model, using tabulated distances from neutron diffraction[14] [nd isotropic atomic displacement parameters derived from their parent atom. Results are reported in **§1.9** and **Table S10** and CCDC 2524713 contains the supplementary crystallographic data for this paper. These data can be obtained free of charge from The Cambridge Crystallographic Data Centre via www.ccdc.cam.ac.uk/structures . The final cif file was prepared with CIVET.[15]

1.2 Synthetic Procedures

1.2.1 Synthesis of 3

Modified conditions from Noguchi et al.[16]

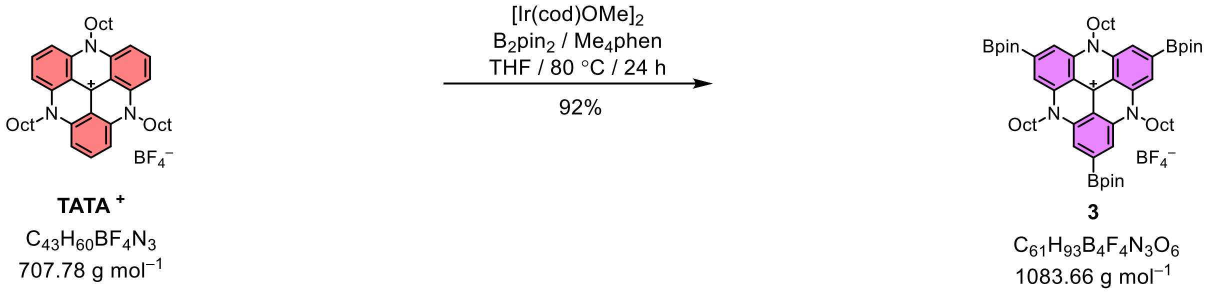

N-octyl-triazatriangulenium (**TATA⁺**) (200 mg, 282 µmol, 1 equiv.), B_2pin_2 (463.4 mg, 1.82 mmol, 6.5 equiv.), 3,4,7,8-tetramethyl-1,10-phenanthroline (Me_4phen) (8.6 mg, 36 μmol, 0.13 equiv.), and bis(1,5-cyclooctadiene)di-μ-methoxydiiridium(I) ($[Ir(cod)OMe]_2$) (10.9 mg, 16 μmol, 0.06 equiv) were added to an oven dried 5 mL microwave vial and sealed. The vial was evacuated and refilled with N_2 three times. Anhydrous, degassed THF (2 mL) was added under N_2. The reaction was stirred at 80 °C, and the progress was continuously monitored by MALDI-TOF MS. After 24 h the reaction mixture was cooled to rt and poured into heptane (100 mL) at 0 °C under stirring. The suspension was stirred at 0 °C for 1 h. The solid was collected by centrifugation of the suspension (4000 rpm, 10 min). The pink solid was washed with heptane (10 mL) by centrifugation (4000 rpm, 5 min), collected, and dried in vacuo o.n. to yield **3** (281 mg, 259 μmol, 92%).

The compound is not analytically pure and further purification was not pursued due to the instability of the boronic esters.

^{1}H NMR ($CDCl_3$): δ (ppm) = 7.53 (s, 6H, 6 × Ar*H*), 4.45 (t, *J* = 8.2 Hz, 6H, 3 × NC*H*$_2$), 1.99 (p, *J* = 7.3 Hz, 6H, 3 × C*H*$_2$), 1.67 (p, *J* = 7.3 Hz, 6H, 3 × C*H*$_2$), 1.57-1.52 (m, 6H, 3 × C*H*$_2$), 1.46-1.39 (m, 42H, 12 × C*H*$_3$ + 3 × C*H*$_2$), 1.38-1.33 (m, 12H, 6 × C*H*$_2$), 0.92 (t, *J* = 6.9 Hz, 9H, 3 × C*H*$_3$). **HRMS** (ESI): Calcd. *m*/*z* for $C_{61}H_{93}N_3O_6^+$ [M$^+$]: 996.7339, Found *m*/*z*: 996.7366

1.2.2 Synthesis of 4

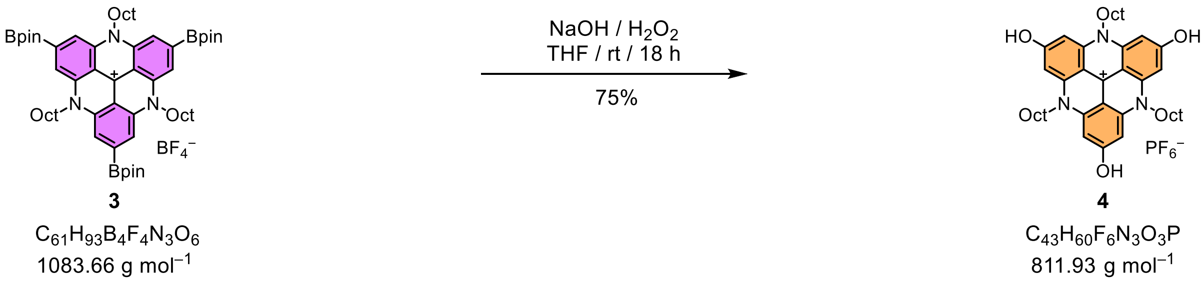

Compound **3** (288 mg, 266 μmol) and NaOH (13.5 mg, 340 μmol) were suspended in THF (20 mL) resulting in a purple solution. H_2O_2 (30% w/w aq., 200 μL, 2.55 mmol) was added where after the solution slowly turned orange. The reaction mixture was stirred at rt for 18 h and poured into KPF_6 acidified with 2 M HCl (0.2 M, 200 mL, pH ≈ 2). The suspension was stirred at rt for 4 h, filtered, and the solid was washed with H_2O (2 × 50 mL). The solid was eluted with MeOH and the solvent was evaporated in vacuo. The solid was purified by automated flash column chromatography (12 g SiO_2 cartridge, FR = 30 mL min^{-1}, FV 10 mL) using a gradient of *i*-PrOH in CH_2Cl_2:MeCN (9:1 v/v): 0−2 CV (0% *i*-PrOH), 2−4 CV (0−2% *i*-PrOH), 4−6 CV (2-10% *i*-PrOH). The fractions containing pure **4** (1-3 CV) as determined by MALDI-TOF-MS were combined and evaporated in vacuo to yield **4** as a yellow solid (163 mg, 201 μmol, 75%).

^{1}H NMR (DMSO-*d*$_6$): *δ* (ppm) = 11.03 (bs, 3H, 3 × ArO*H*), 6.36 (s, 6H, 6 × Ar*H*), 3.80-3.71 (t, *J* = 8.2 Hz, 6H, 3 × NC*H*$_2$), 1.64-1.54 (m, 6H, 3 × C*H*$_2$), 1.48-1.41 (m, 6H, 3 × C*H*$_2$), 1.24-1.37 (m, 24H, 12 × C*H*$_2$), 0.84-0.89 (m, 9H, 3 × C*H*$_3$). **^{13}C NMR** (DMSO-*d*$_6$): *δ* (ppm) = 165.0 (−,*C*$^+$), 141.0 (−, Ar*C*), 135.0 (−, Ar*C*), 102.1 (−, Ar*C*), 92.8 (+, Ar*C*H), 46.9 (−, N*C*H$_2$), 31.2 (−, *C*H$_2$), 28.8 (−, *C*H$_2$), 28.7 (−, *C*H$_2$), 26.1 (−, *C*H$_2$), 24.0 (−, *C*H$_2$), 22.1 (−, *C*H$_2$), 14.0 (+, *C*H$_3$). **HRMS** (ESI): Calcd. *m*/*z* for $C_{43}H_{60}N_3O_3^+$ [M$^+$]: 666.4630, Found *m*/*z*: 666.4640

1.2.3 Synthesis of 2 (MeO-TATA$^+$)

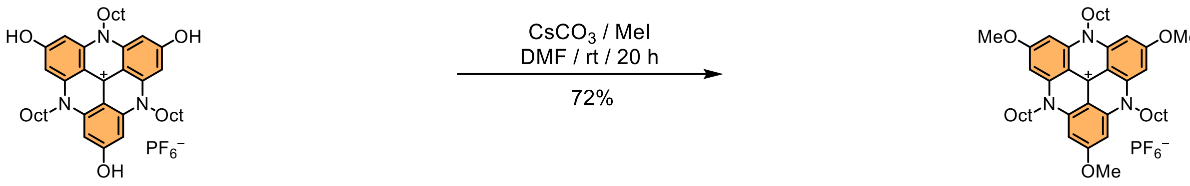

4
$C_{43}H_{60}F_6N_3O_3P$
811.93 g mol^{-1}

2
$C_{46}H_{66}F_6N_3O_3P$
854.02 g mol^{-1}

Compound **4** (163 mg, 201 μmol) and $CsCO_3$ (136 mg, 418 μmol) were suspended in DMF (12 mL), where **4** slowly came into solution. MeI (60 μL, 964 μmol) was added and the reaction mixture was stirred at rt for 20 h. The solution was poured into KPF_6 (0.2 M, 200 mL). The suspension was stirred at rt for 1.5 h, filtered, and the solid was washed with H_2O (2 × 25 mL). The solid was purified by automated flash column chromatography (12 g SiO_2 cartridge, FR = 30 mL min^{-1}, FV = 10 mL) using a gradient of *i*-PrOH in CH_2Cl_2:MeCN (9:1 v/v): 0−2 CV (0% *i*-PrOH), 2−3 CV (0−5% *i*-PrOH), 3−7 CV (5% *i*-PrOH), 7-7.5 (5−27% *i*-PrOH), 7.5-10 (27% *i*-PrOH). The fractions containing pure **2** (3-6.5 CV) (as determined by MALDI-TOF-MS) were combined and evaporated in vacuo to yield **2** as a yellow solid (123 mg, 144 μmol, 72%).

^{1}H NMR (DMSO-*d*$_6$): *δ* (ppm) = 6.47 (s, 6H, 6 × Ar*H*), 4.02 (s, 9H, 3 × OC*H*$_3$), 3.98-3.91 (m, 6H, 3 × NC*H*$_2$), 1.64-1.55 (m, 6H, 3 × C*H*$_2$), 1.51-1.43 (m, 6H, 3 × C*H*$_2$), 1.37-1.24 (m, 24H, 12 × C*H*$_2$), 0.87 (t, *J* = 6.9 Hz 9H, 3 × C*H*$_3$). **^{13}C NMR** (DMSO-*d*$_6$): *δ* (ppm) = 166.0 (−,*C*$^+$), 140.8 (−, Ar*C*), 135.4 (−, Ar*C*), 103.2 (−, Ar*C*), 91.7 (+, Ar*C*H), 56.0 (+, O*C*H$_3$), 46.3 (−, N*C*H$_2$), 31.2 (−, *C*H$_2$), 28.71 (−, *C*H$_2$), 28.66 (−, *C*H$_2$), 25.9 (−, *C*H$_2$), 24.0 (−, *C*H$_2$), 22.1 (−, *C*H$_2$), 13.9 (+, *C*H$_3$). **HRMS** (ESI): Calcd. *m*/*z* for $C_{46}H_{66}N_3O_3^+$ [M$^+$]: 708.5099, Found *m*/*z*: 708.5100

1.2.4 Synthesis of 5

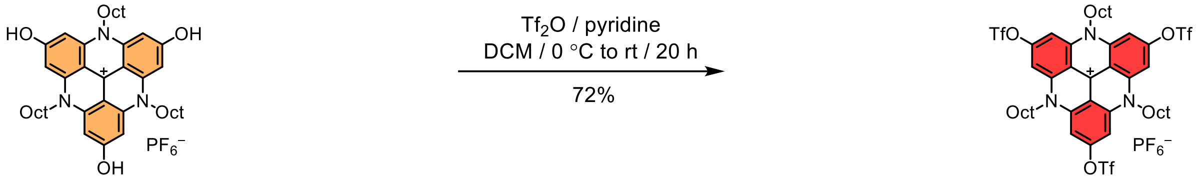

4
$C_{43}H_{60}F_6N_3O_3P$
811.93 g mol^{-1}

5
$C_{46}H_{57}F_{15}N_3O_9PS_3$
1208.10 g mol^{-1}

Compound **4** (156 mg, 192 µmol) was dissolved in anhydrous CH_2Cl_2 (20 mL) and anhydrous pyridine (55 µL, 682 µmol) was added. The mixture was cooled to 0 °C on an ice bath and Tf_2O (160 µL, 951 µmol) was added dropwise over 10 min, where after the cooling was removed. The reaction mixture was stirred at rt for 20 h, diluted with CH_2Cl_2 (20 mL) and transferred to a separatory funnel. The organic phase was washed with $NaHCO_3$ (5% aq. solution, 2 × 25 mL) and dilute HCl (c < 0.1 M, 50 mL). The organic phase was dried ($MgSO_4$) and the solvent was evaporated in vacuo. The resulting solid was dried under vacuum o.n. yielding **5** (140 mg, 116 µmol, 60%).

^{1}H NMR (CD_3CN): *δ* (ppm) = 7.37 (s, 6H), 4.36 (t, *J* = 8.1 Hz, 6H), 1.85 (p, *J* = 8.1 Hz, 6H), 1.58 (p, *J* = 7.5 Hz, 6H), 1.42 (p, *J* = 6.6 Hz, 6H), 1.36 – 1.28 (m, 18H), 0.89 (t, *J* = 6.9 Hz, 9H). **^{13}C NMR** (CD_3CN): δ (ppm) = 156.9 (−, Ar*C*), 143.2 (−, Ar*C*), 140.4 (−,*C*$^+$), 119.7 (q, *J* = 321 Hz, *C*F_3), 111.6 (−, Ar*C*), 101.0 (+, Ar*C*H), 49.8 (+, N*C*H_2), 32.4 (+, *C*H_2), 30.0 (+, *C*H_2), 29.9 (+, *C*H_2), 29.8 (+, *C*H_2), 26.9 (+, *C*H_2), 25.5 (+, *C*H_2), 23.3 (+, *C*H_2), 14.3 (−, *C*H_3). **HRMS** (ESI): Calcd. *m/z* for $C_{46}H_{57}F_9N_3O_9S_3^+$ [M$^+$]: 1062.3108, Found *m/z*: 1052.3146

1.2.5 Synthesis of 1 (A-TATA$^+$)

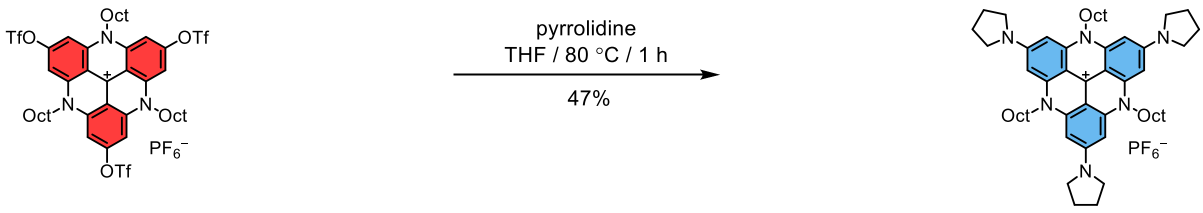

5
$C_{46}H_{57}F_{15}N_3O_9PS_3$
1208.10 g mol^{-1}

1
$C_{55}H_{81}F_6N_6P$
971.26 g mol^{-1}

Compound **5** (41.5 mg, 34.3 µmol) was sealed in an oven dried 5 mL microwave vial. The vial was evacuated and refilled with N_2 three times before anhydrous THF (2 mL) was added under N_2. The vial was heated to 80 °C in a pre-heated aluminum block and anhydrous pyrrolidine (50 µL, 610 µmol) was added. The reaction mixture was stirred at 80 °C and progress was monitored by MALDI-TOF MS. After 1 h the mixture was cooled to rt and the volatiles were evaporated under vacuum. The resulting solid was purified by automated column chromatography (4 g SiO_2 cartridge, FR = 15 mL min^{-1}, FV 10 mL) using a gradient of MeCN in CH_2Cl_2: 0−3 CV (0% MeCN), 3−5 CV (0−10% MeCN), 5−7.5 CV (10% MeCN), 7.5−9.1 CV (10−40% MeCN), 9.1−15.1 CV (40% MeCN). Fractions containing pure **1** (3-5 CV) as determined by MALDI-TOF MS were combined and evaporated in vacuo to yield **1** as a yellow solid (15.7 mg, 16.2 µmol, 47%).

^{1}H NMR (CD_3CN): δ (ppm) = 5.76 (s, 6H), 3.77-3.66 (m, 6H), 3.46-3.42 (m, 12H), 2.11-2.09 (m, 12H), 1.75-1.67 (m, 6H), 1.54-1.50 (m, 6H), 1.47-1.42 (m, 6H), 1.38-1.32 (m, 18H), 0.92 (t, J = 6.8 Hz, 9H). **^{13}C NMR** (CD_3CN): δ (ppm) = 153.0 (−, Ar*C*), 141.7 (−, Ar*C*), 134.0 (−,C^+), 100.7 (−, Ar*C*), 89.1 (+, Ar*C*H), 48.9 (−, NCH_2), 47.6 (−, NCH_2), 32.7 (−, CH_2), 32.6 (−, CH_2), 30.1 (−, CH_2), 29.9 (−, CH_2), 27.4 (−, CH_2), 26.1 (−, CH_2), 24.6 (−, CH_2), 23.4 (−, CH_2), 14.4 (+, CH_3). **HRMS** (ESI): Calcd. *m*/*z* for $C_{55}H_{81}N_6^+$ [M^+]: 825.6518, Found *m*/*z*: 825.6534

1.3 Electrochemistry

The electrochemical experiments were performed according to the method described in section 1.1.4. The potentials were determined relative to the ferrocenium/ferrocene redox couple and converted to SCE by addition of −380 mV, according to the method described by Pavlishchuk and Addison.[17] The voltammograms were recorded at variable scan rates to probe the reversibility of the electrochemical process. The chemical structures of the trianguleniums are shown in Figure S1.

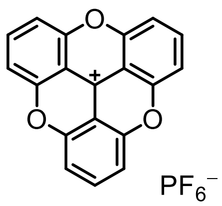

TOTA$^+$

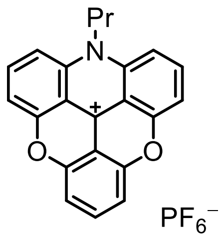

ADOTA$^+$

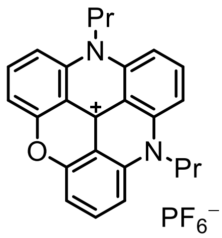

DAOTA$^+$

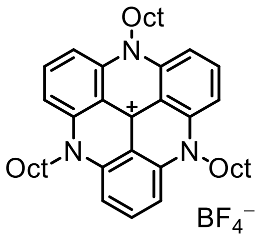

TATA $^+$

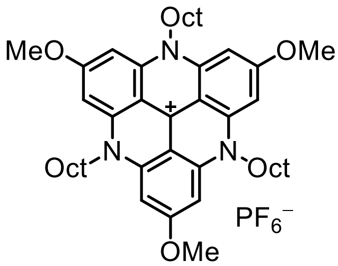

MeO-TATA $^+$ (**2**)

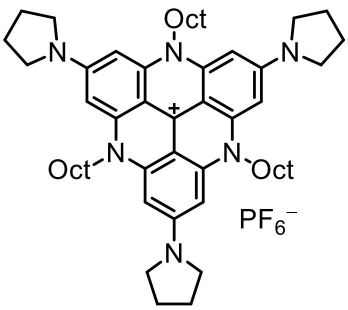

A-TATA $^+$ (**1**)

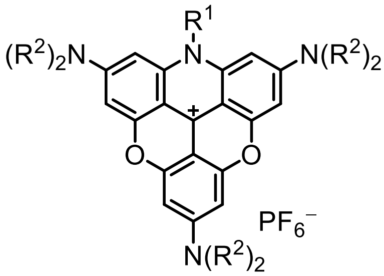

A-ADOTA$^+$

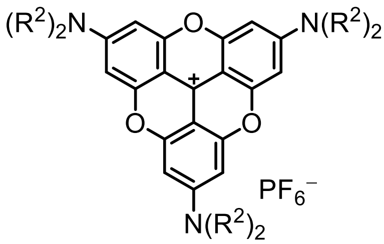

A-TOTA$^+$

Figure S1. Chemical structures of the trianguleniums for which the electrochemical properties are reported below. R^1 = Pr, R^2 = Et

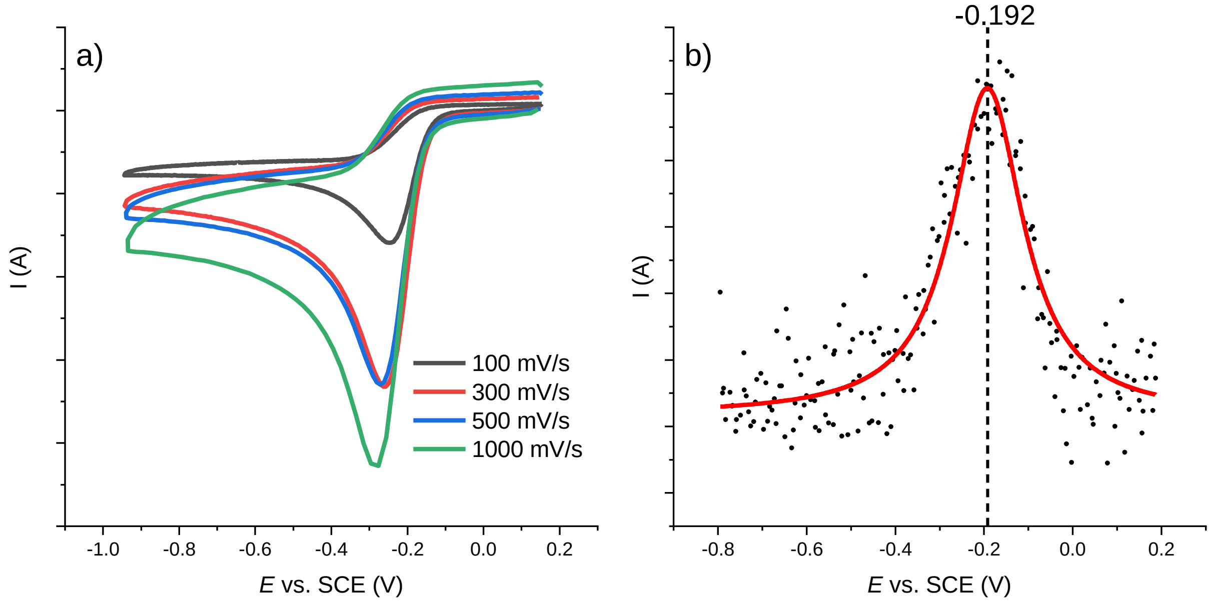

Figure S2. a) CVs of TOTA$^+$ (c = 1 mM) in MeCN (0.1 M $TBAPF_6$) at variable scan rates. b) Raw DPV data and Lorentzian fit (red line) to extract the reduction potential.

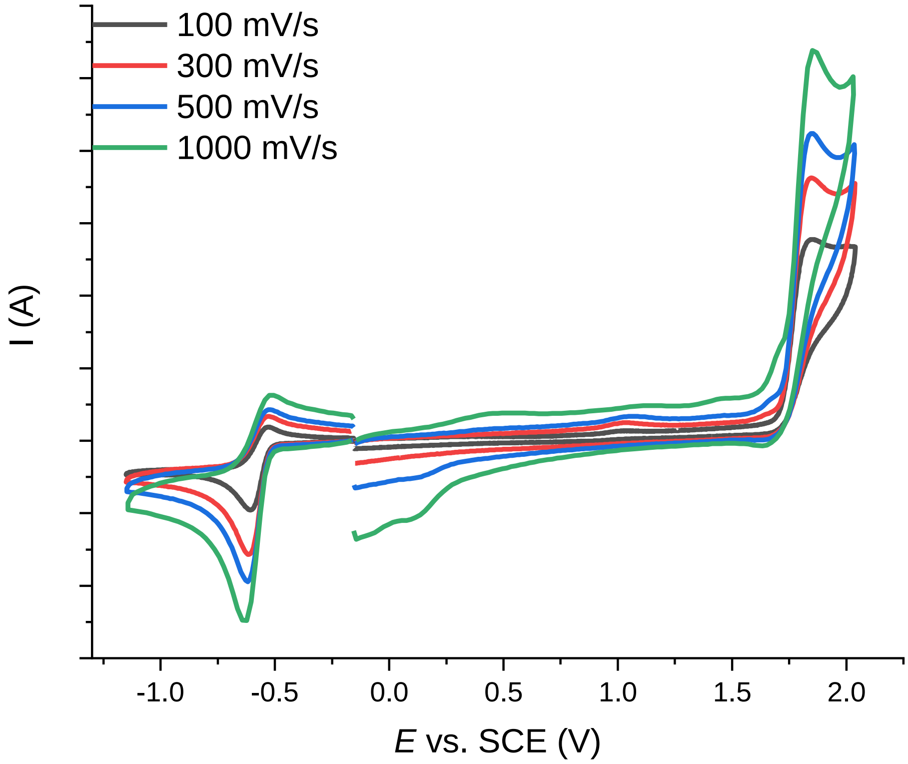

Figure S3. CVs of ADOTA$^+$ (c = 1 mM) in MeCN (0.1 M $TBAPF_6$) at variable scan rates.

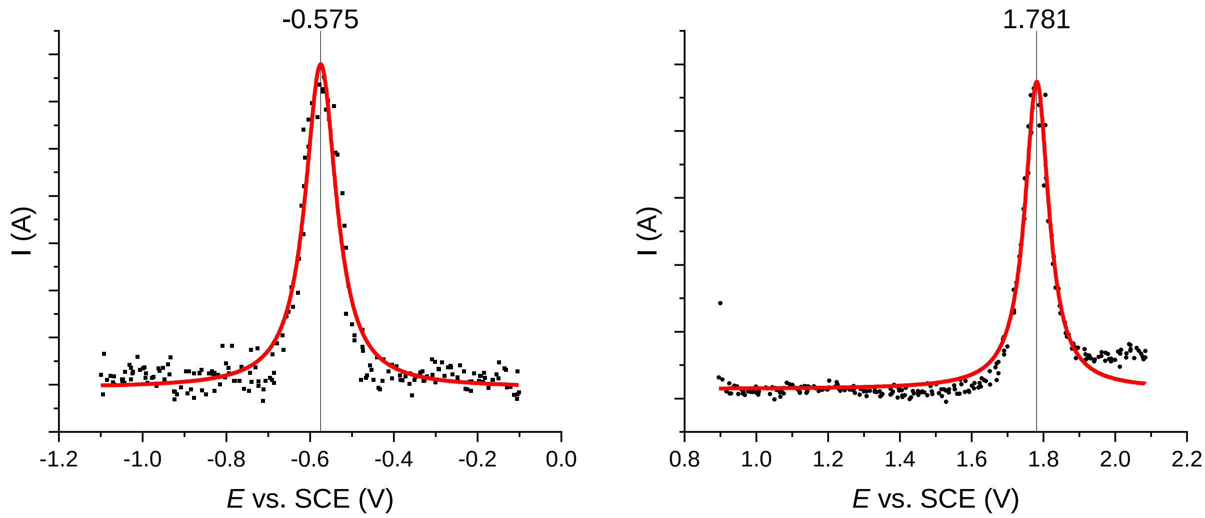

Figure S4. Raw DPV data and Lorentzian fit (red line) to extract the redox potentials for ADOTA⁺.

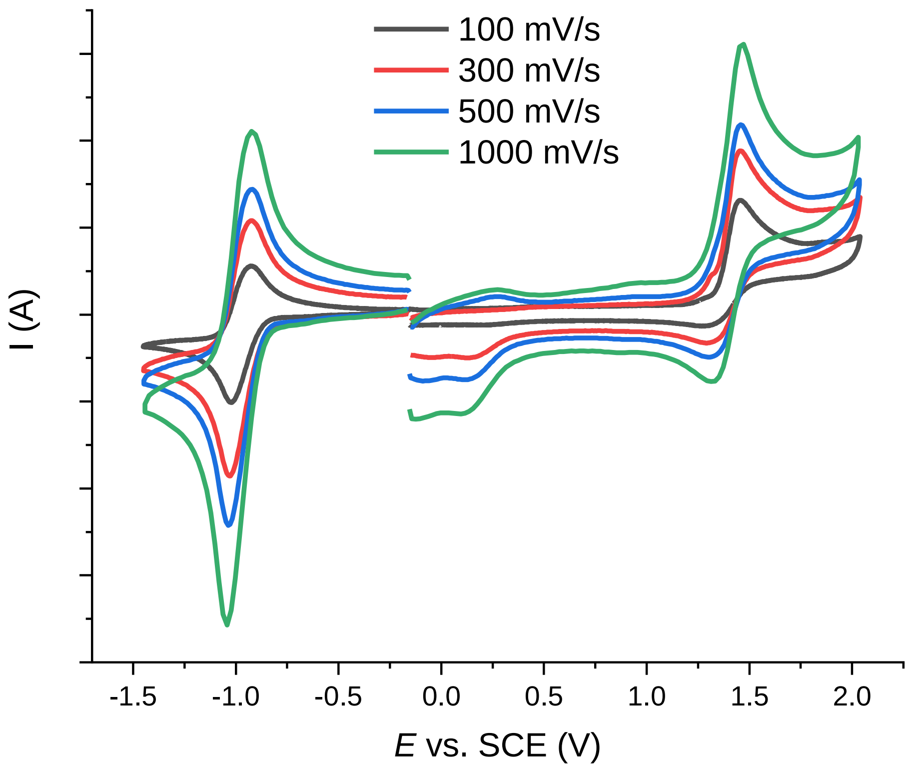

Figure S5. CVs of DAOTA⁺ (c = 1 mM) in MeCN (0.1 M $TBAPF_6$) at variable scan rates.

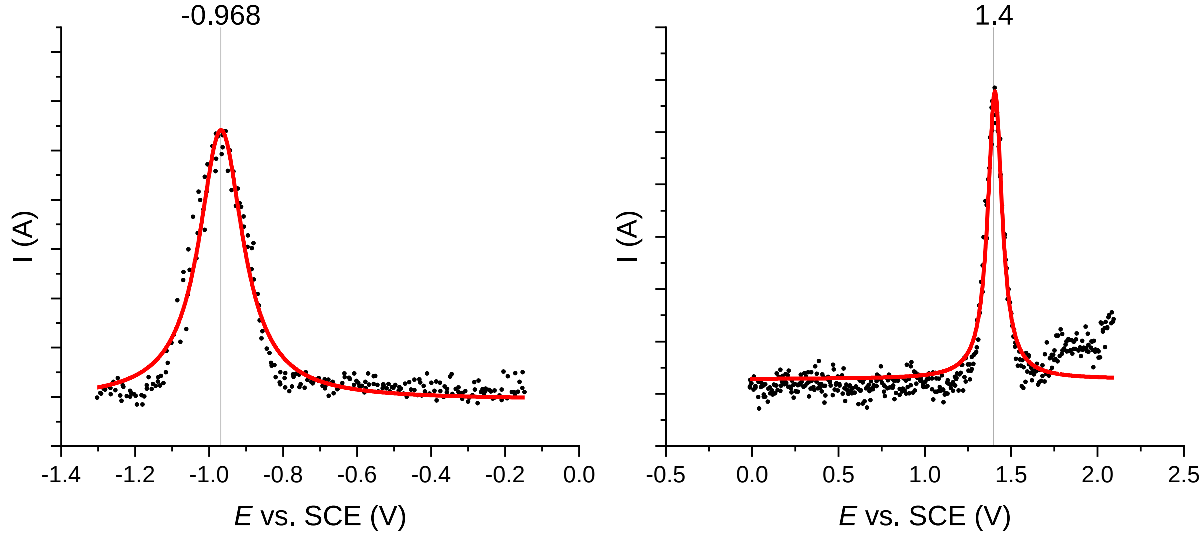

Figure S6. Raw DPV data and Lorentzian fit (red line) to extract the redox potentials for $DAOTA^+$.

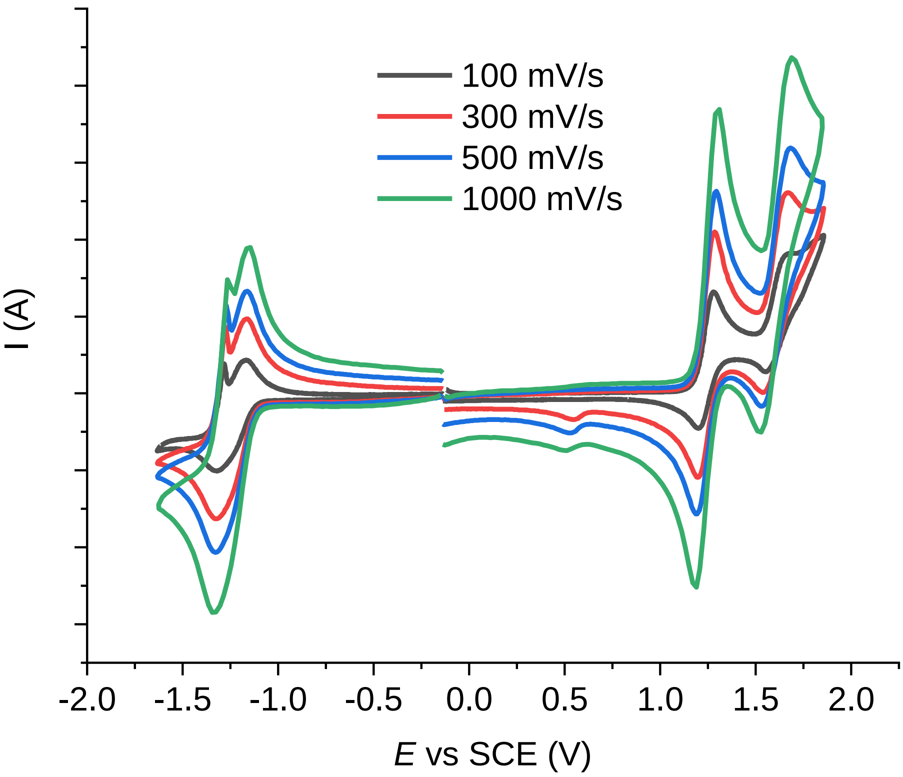

Figure S7. CVs of $TATA^+$ (c = 1 mM) in MeCN (0.1 M $TBAPF_6$) at variable scan rates.

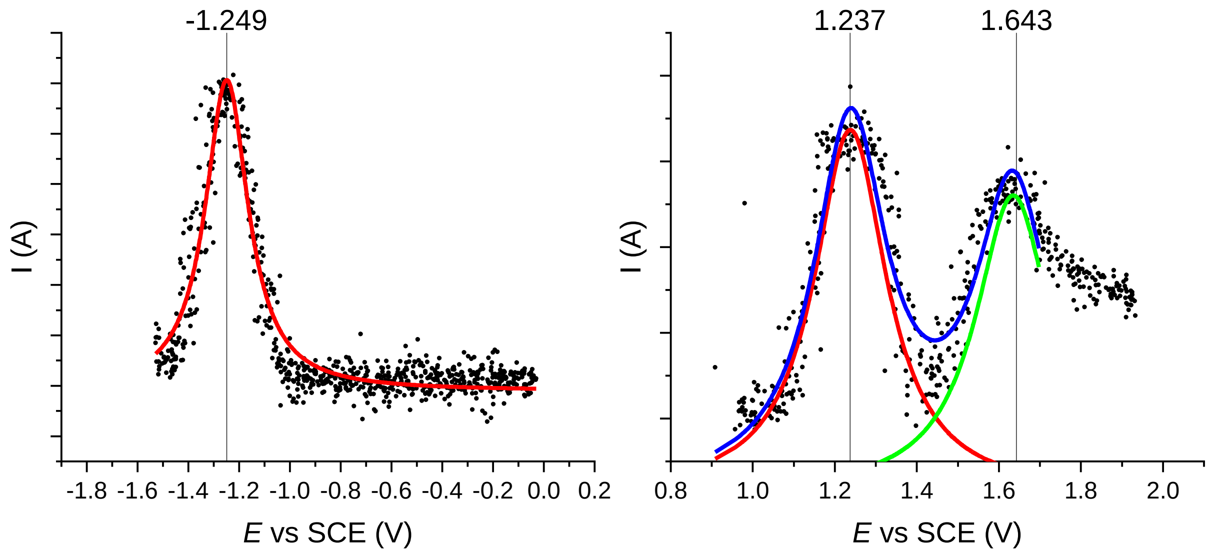

Figure S8. Raw DPV data and Lorentzian fit (red line) to extract the redox potentials for DAOTA$^+$.

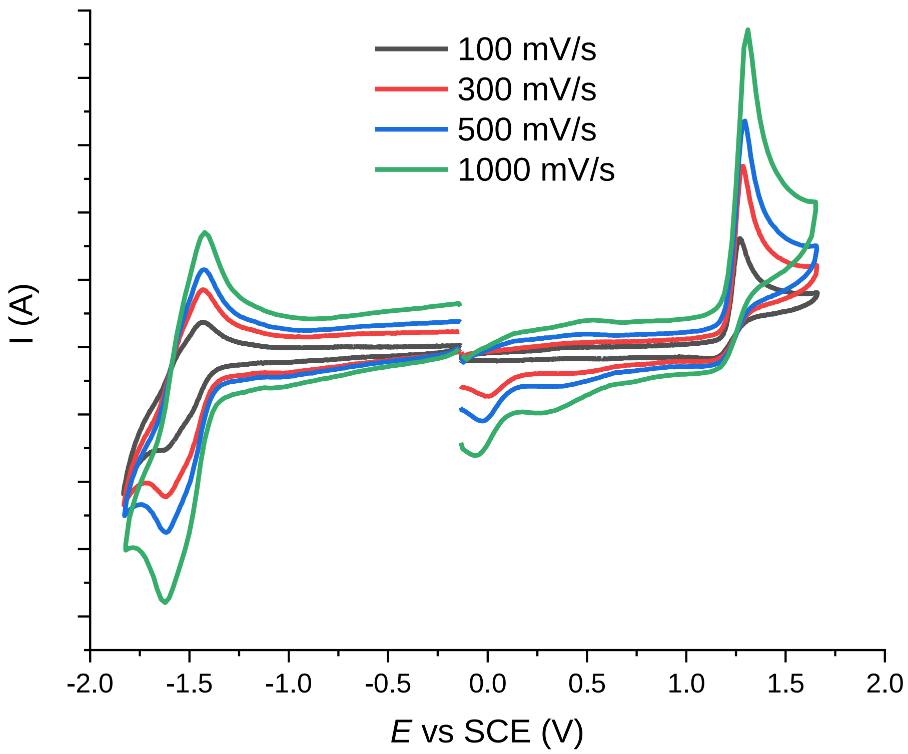

Figure S9. CVs of MeO-TATA$^+$ (**2**) (*c* = 1 mM) in MeCN (0.1 M $TBAPF_6$) at variable scan rates.

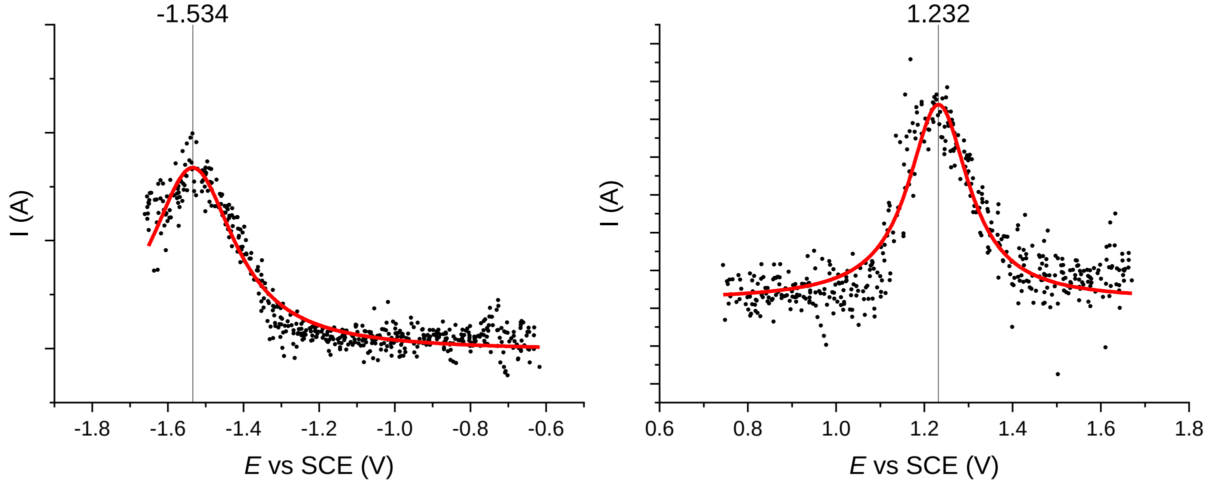

Figure S10. DPVs and Lorentzian fits (red lines) to the raw data to extract redox potentials of MeO-TATA$^+$ (**2**).

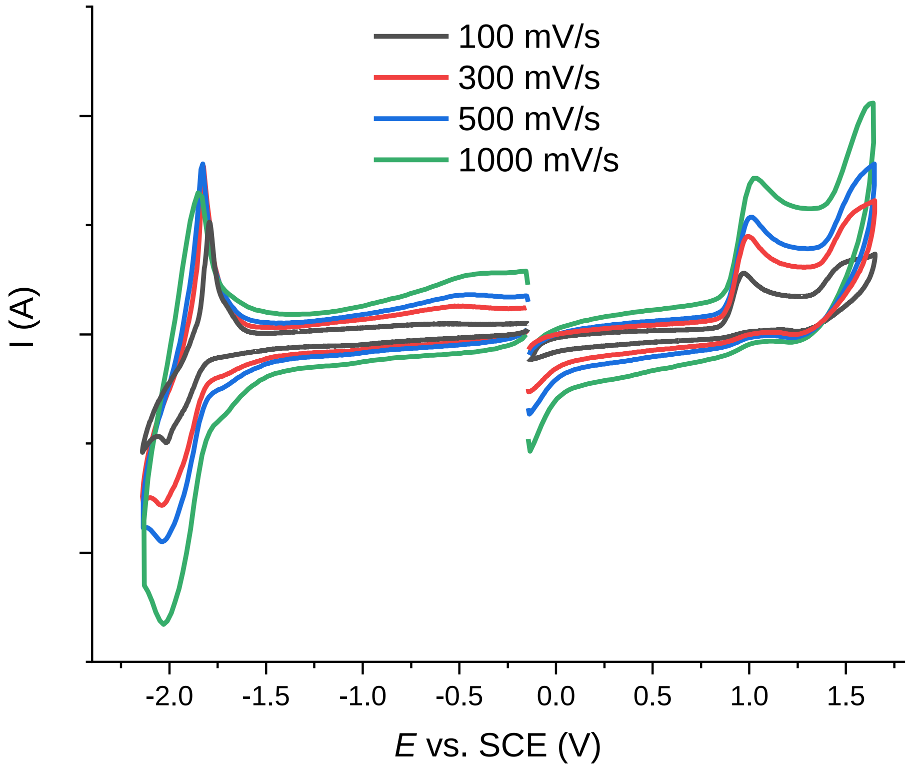

Figure S11. CVs of A-TATA$^+$ (**1**) (*c* = 0.5 mM) in MeCN (0.1 M $TBAPF_6$) at variable scan rates.

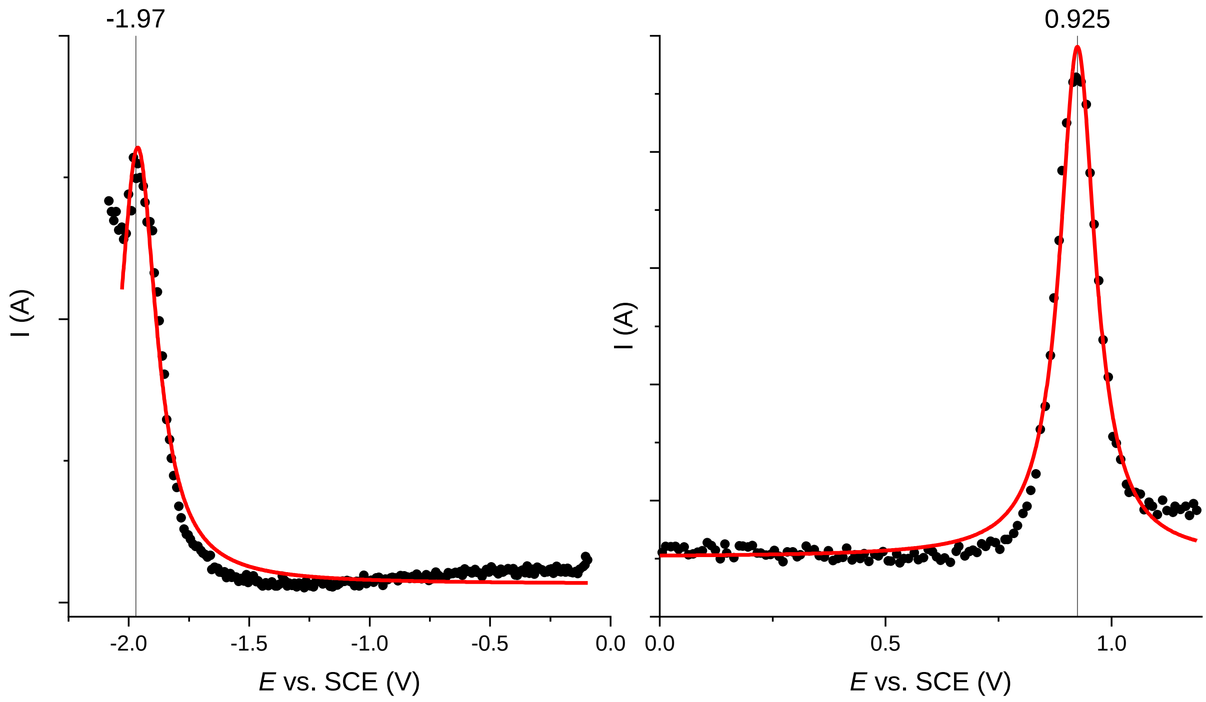

Figure S12. Raw DPV data and Lorentzian fit (red line) to extract the redox potentials for A-TATA$^+$ (**1**).

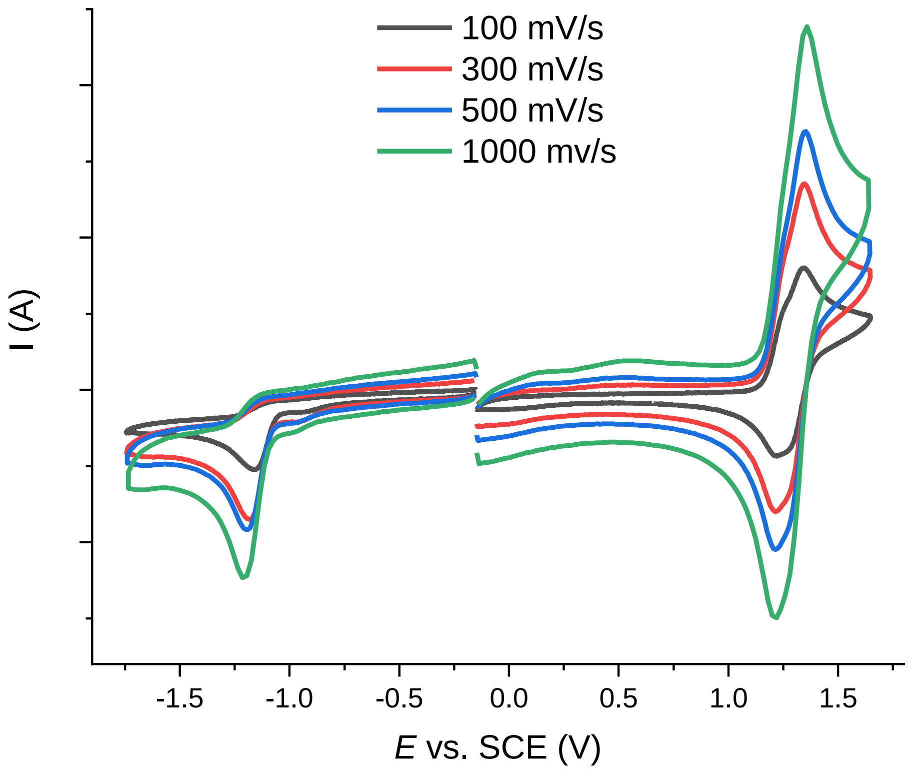

Figure S13. CVs of A-TOTA$^+$ (*c* = 0.5 mM) in MeCN (0.1 M $TBAPF_6$) at variable scan rates.

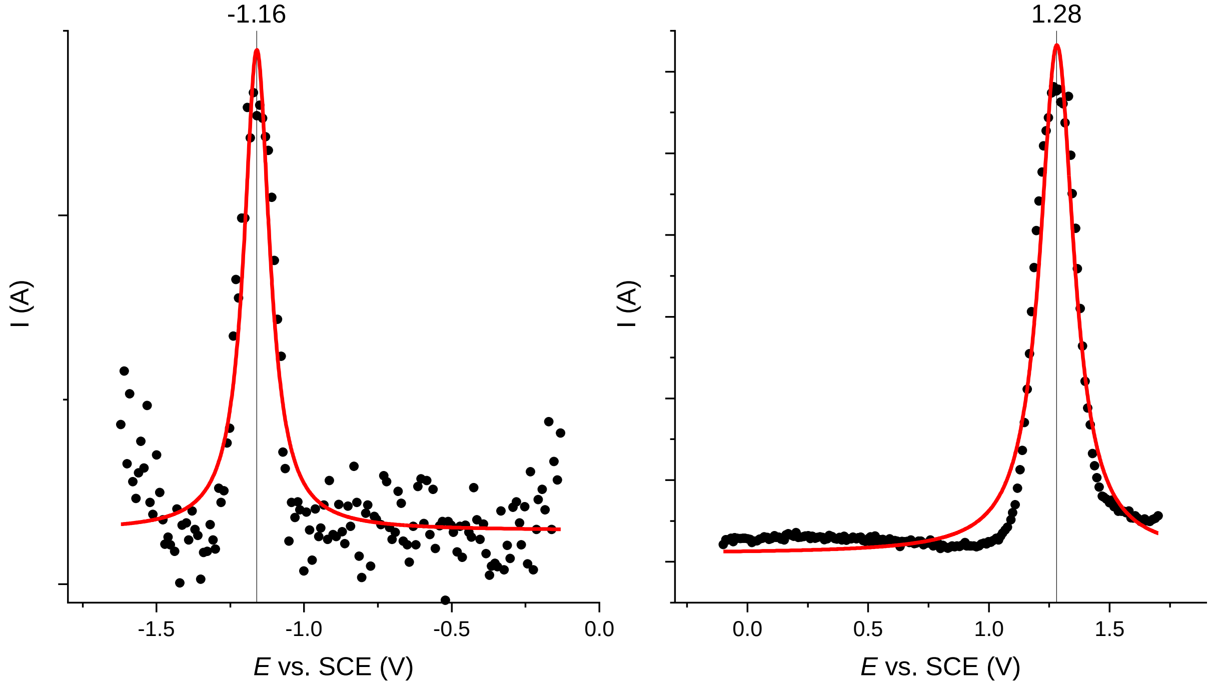

Figure S14. Raw DPV data and Lorentzian fit (red line) to extract the redox potentials for A-TOTA$^+$.

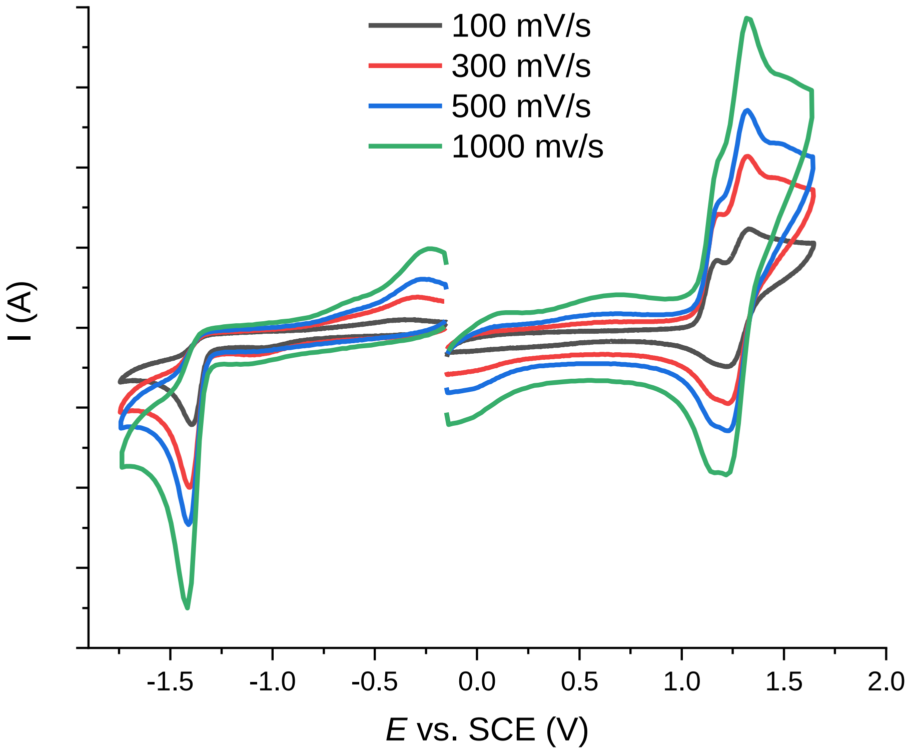

Figure 15. CVs of A-ADOTA$^+$ (c = 0.5 mM) in MeCN (0.1 M TBAPF$_6$) at variable scan rates.

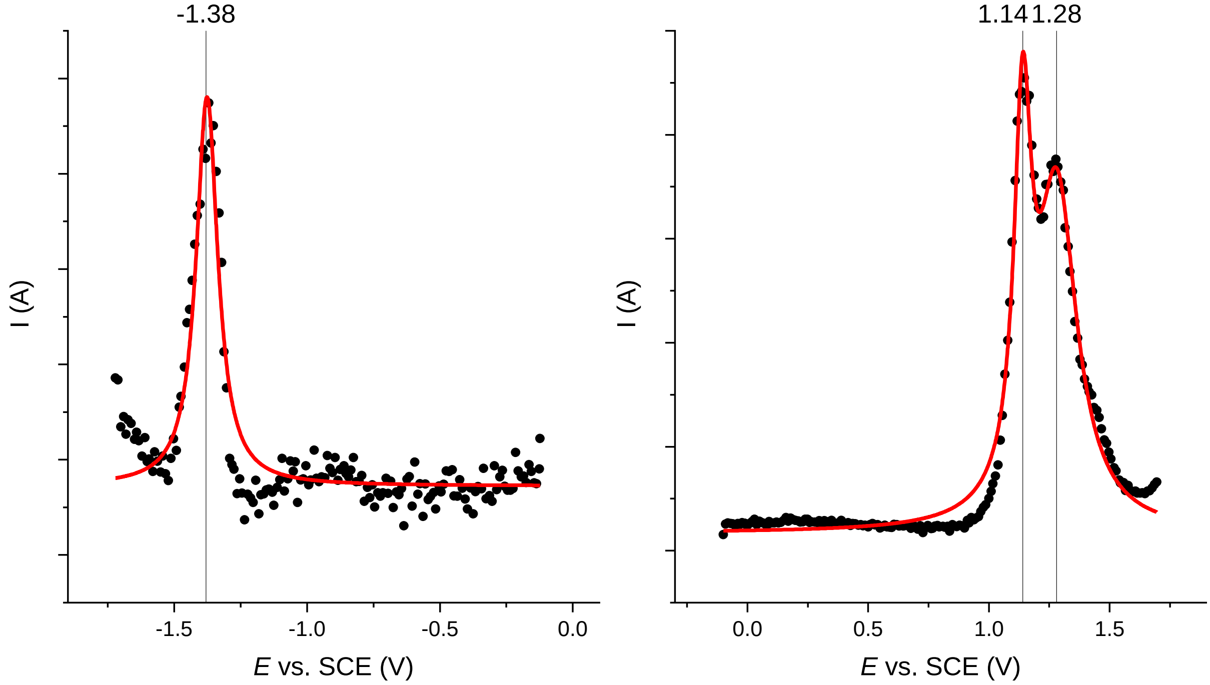

Figure S16. Raw DPV data and Lorentzian fit (red line) to extract the redox potentials for A-ADOTA⁺.

Table S1. Reduction (E_{red}) and oxidation (E_{ox}) potentials vs. SCE for the trianguleniums determined by differential pulse voltammetry (DPV).

	E_{red} vs. SCE [V]	E_{ox} vs. SCE [V]
TOTA⁺	−0.19	−
ADOTA⁺	−0.57	+1.78
DAOTA⁺	−0.97	+1.4
TATA⁺	−1.25	+1.25
MeO-TATA⁺ (**2**)	−1.53	+1.23
A-TATA⁺ (**1**)	−1.94	+0.92
A-TOTA⁺	−1.16	+1.28
A-ADOTA⁺	−1.37	+1.28

1.4 Free Energy Relationships

To illustrate the general applicability of the proportionality between pK_{R+} values and one-electron reduction potentials (E_{red}) for carbenium ions, this relationship is explored for three classes of structurally similar tris-, bis-, and mono-azuleneylmethyl carbenium ions shown in Figure S17. The associated data from three Ito et al. publications[18-20] is shown in Table S2, and the proportionality is illustrated in Figure S18.

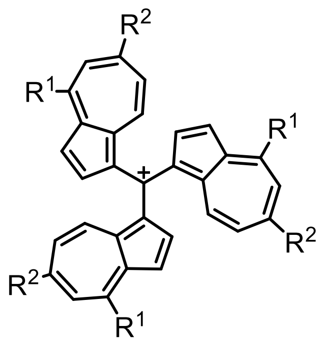

$(Az)_3C^+$

a: $R^1 = R^2 = H$

b: $R^1 = H$, $R^2 = OMe$

c: $R^1 = H$, $R^2 = NMe_2$

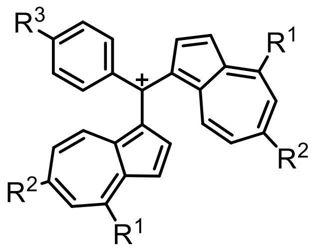

$(Az)_2PhC^+$

a: $R^1 = R^2 = R^3 = H$

b: $R^1 = H$, $R^2 = R^3 = OMe$

c: $R^1 = R^2 = H$, $R^3 = OMe$

d: $R^1 = Me$, $R^2 = H$, $R^3 = OMe$

e: $R^1 = H$, $R^2 = R^3 = NMe_2$

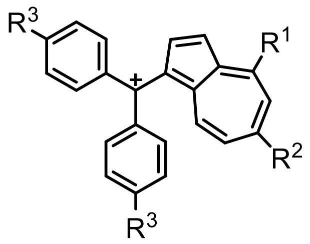

$Az(Ph)_2C^+$

a: $R^1 = R^2 = R^3 = H$

b: $R^1 = R^2 =$ *t*-Bu, $R^3 = OMe$

c: $R^1 = Me$, $R^2 = H$, $R^3 = OMe$

d: $R^1 = R^2 =$ *t*-Bu, $R^3 = H$

e: $R^1 = R^2 = H$, $R^3 = NMe_2$

Figure S17. Chemical structures for the azulenylmethyl carbenium ions from three Ito et al. publications.[18-20]

Table S2. Reduction potentials (E_{red}) and carbocation stability constants (pK_{R+}) for the azulenylmethyl carbenium ions shown in **Figure S17**.

	$(Az)_3C^+$			$(Az)_2PhC^+$			$Az(Ph)_2C^+$	
	E_{red} vs. Ag/Ag^+ [V]	pK_{R+}		E_{red} vs. Ag/Ag^+ [V]	pK_{R+}		E_{red} vs. Ag/Ag^+ [V]	pK_{R+}
a	−1.26	24.3	**a**	−0.66	10.5	**a**	−0.48	3
b	−0.88	14	**b**	−0.80	14	**b**	−0.71	7
c	−0.78	11.3	**c**	−0.71	11.7	**c**	−0.65	6
			d	−0.75	12.2	**d**	−0.59	4.6
			e	−1.22	21.5	**e**	−0.94	12.6

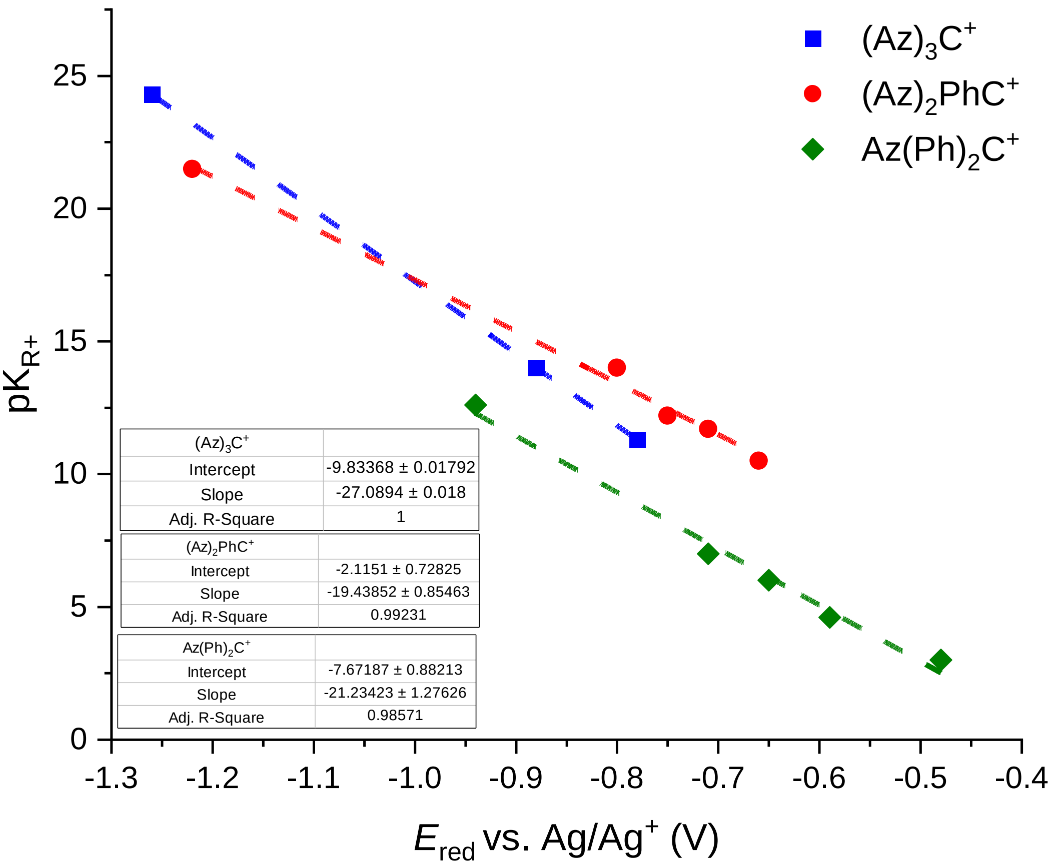

Figure S18. Proportionality of pK_{R+} values and E_{red} for structurally related azulenylmethyl carbenium ions shown in **Figure S17**. The tris-, bis-, and mono-azulenylmethyl carbenium ions are proportional within their respective group, but no relationship exists between the groups.

This general applicability is further explored for the substituted triarylcarbenium ions shown in Figure S19. The associated data from the Arnett et al publication[21] is shown in Table S3, and the proportionality is illustrated in Figure S20.

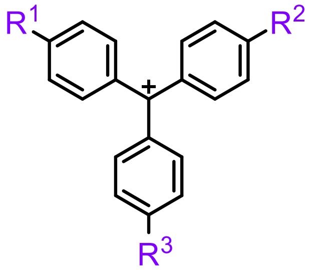

a: $R^1 = R^2 = R^3$ = Cl
b: $R^1 = R^2 = R^3$ = H
c: R^1 = F, $R^2 = R^3$ = H
d: R^1 = Me, $R^2 = R^3$ = H
e: $R^1 = R^2$ = Me, R^3 = H
f: $R^1 = R^2 = R^3$ = H
g: R^1 = OMe, $R^2 = R^3$ = H
h: $R^1 = R^2 = R^3$ = *t*-Bu
i: $R^1 = R^2$ = OMe, R^3 = H
j: $R^1 = R^2 = R^3$ =OMe
k: $R^1 = R^2 = R^3$ = NMe2

Figure S19. Chemical structures for the triarylcarbenium ions used to explore pK_{R+} - E_{red} relationships.

Table S3. Reduction potentials (E_{red}) and carbocation stability constants (pK_{R+}) for the triarylcarbenium ions shown in **Figure S19** from Arnett et al.[21]

Triarylcarbenium Ion	E_{red} vs. NHE [V]	pK_{R+}
a	0.752	−7.74
b	0.542	−6.63
c	0.662	−6.42
d	0.558	−5.41
e	0.535	−4.39
f	0.503	−3.56
g	0.486	−3.4
h	0.451	−6.5
i	0.418	−1.24
j	0.219	0.82
k	−0.366	9.4

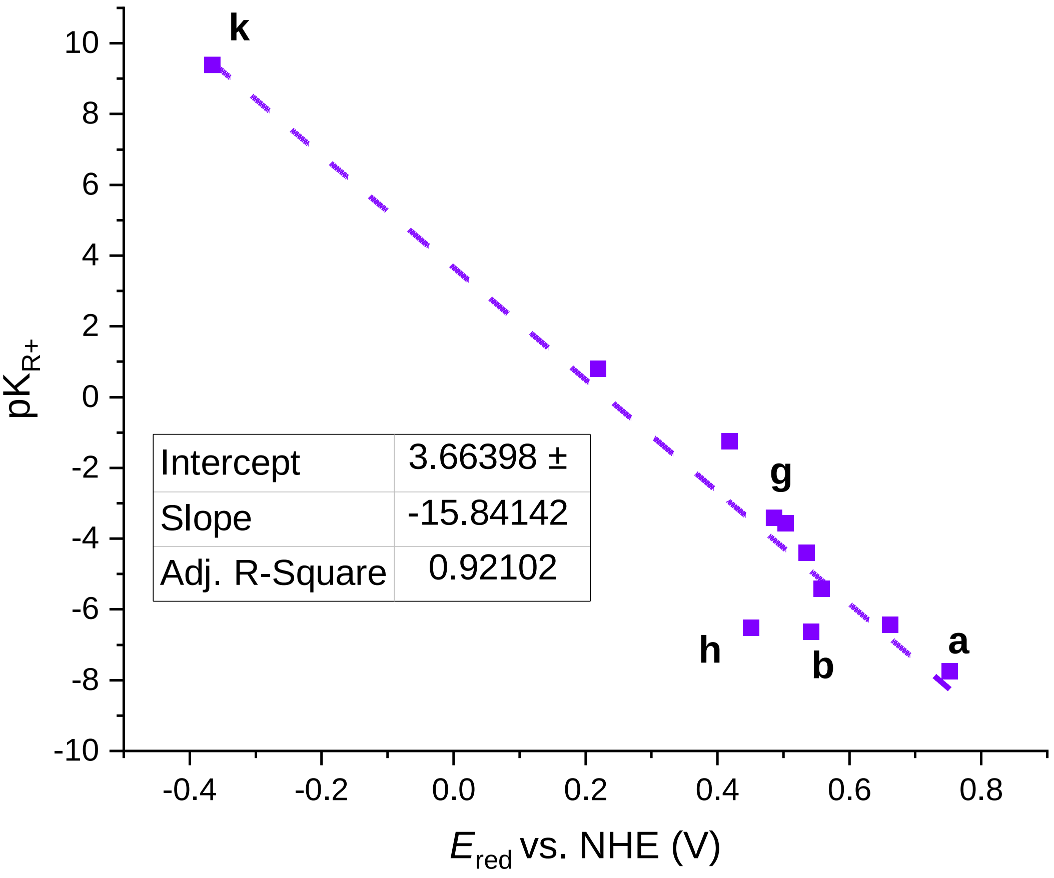

Figure S20. Proportionality of pK_{R+} values and E_{red} for structurally related triarylcarbenium ions shown in **Figure S19**.

Finally, for comparison, the relationships for 5 different classes of carbenium ions are plotted in one graph. The reduction potentials are converted to SCE by addition of −343 mV for the Ag/Ag^+ data, and by addition of +250 mV for the NHE data as described by Pavlishchuk and Addison.[17] This showcases how the different structural features leads to different slopes and intercepts for the E_{red}/pK_{R+} relationships explored herein (Figure S21).

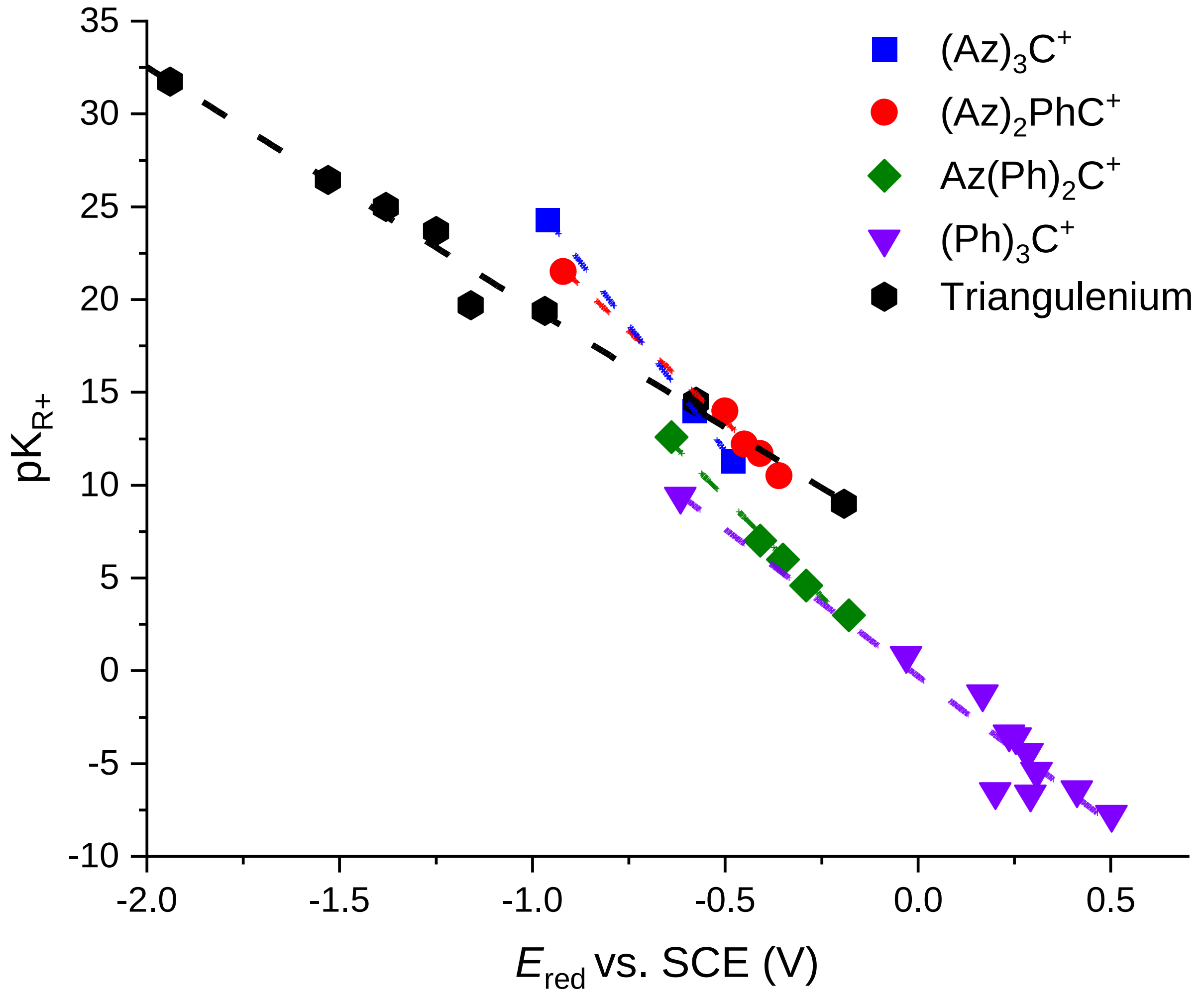

Figure S21. Proportionality of pK_{R+} values and E_{red} for different families of carbenium ions. Illustrating how the proportionality only holds within specific families.

The reduction potentials and carbocation stability constants for the trianguleniums discussed herein in compiled in Table S4.[22-25]

Table S4. Reduction potentials (E_{red}) and carbocation stability constants (pK_{R+}) for the trianguleniums.

Triangulenium	E_{red} vs. SCE [V]	pK_{R+}
$TOTA^+$	−0.19	9
$ADOTA^+$	−0.57	14.5
$DAOTA^+$	−0.97	19.4
$TATA^+$	−1.25	23.4
MeO-$TATA^+$ (**2**)	−1.53	26
A-$TATA^+$ (**1**)	−1.94	32
A-$TOTA^+$	−1.16	19.7
A-$ADOTA^+$	−1.37	25

1.5 Optical Spectroscopy

The following section shows the characterization of the optical properties for MeO-$TATA^+$ (**2**) and A-$TATA^+$ (**1**) in dichloromethane.

1.5.1 Steady State Spectroscopy

To investigate whether the excitation and emission spectra for MeO-$TATA^+$ (**2**) vary as a function of wavelength we recorded excitation and emission spectra at different wavelengths. Normalized excitation spectra at different wavelengths in comparison with absorption spectra are shown in Figure S22. Normalized emission spectra with excitation at different wavelengths are shown in Figure S23.

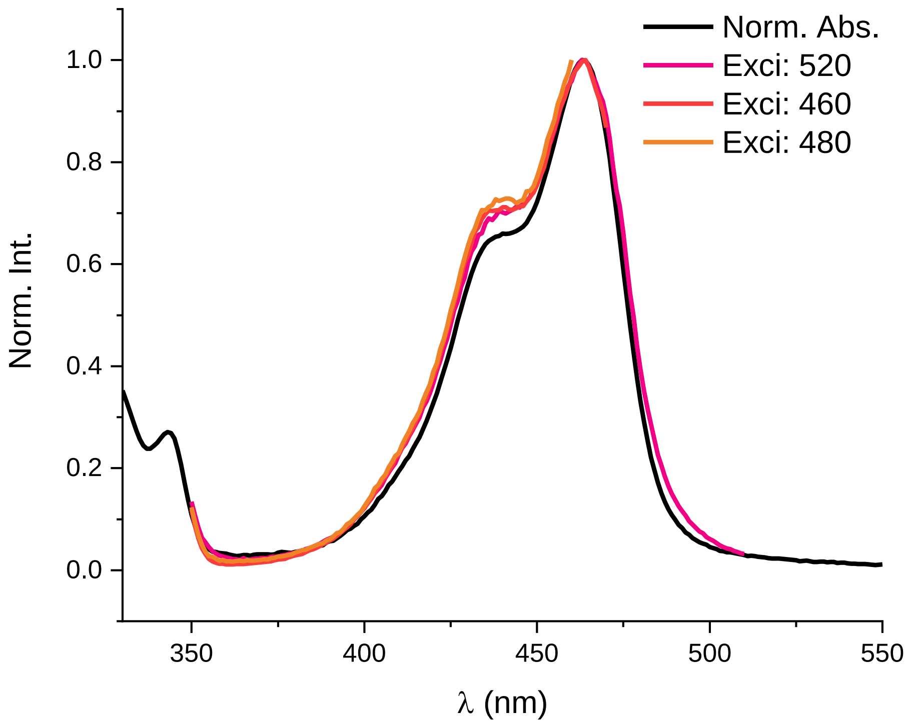

Figure S22. Normalized excitation spectra at three different wavelengths for MeO-TATA$^+$ (**2**) in CH_2Cl_2. The normalized absorption spectra is shown for comparison.

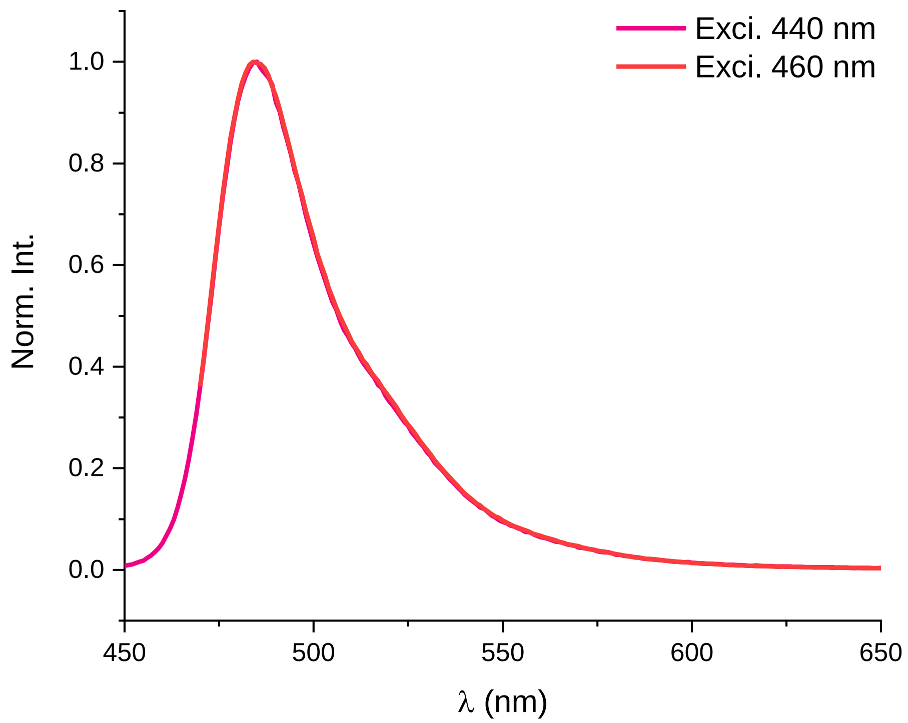

Figure S23. Normalized emission spectra at two different wavelengths for MeO-TATA$^+$ (**2**) in CH_2Cl_2.

The molar absorption coefficient was determined using three single point measurements with a known concentration of MeO-TATA$^+$ (**2**) in CH_2Cl_2 (Figure S24). The average of these three measurements is the determined coefficient.

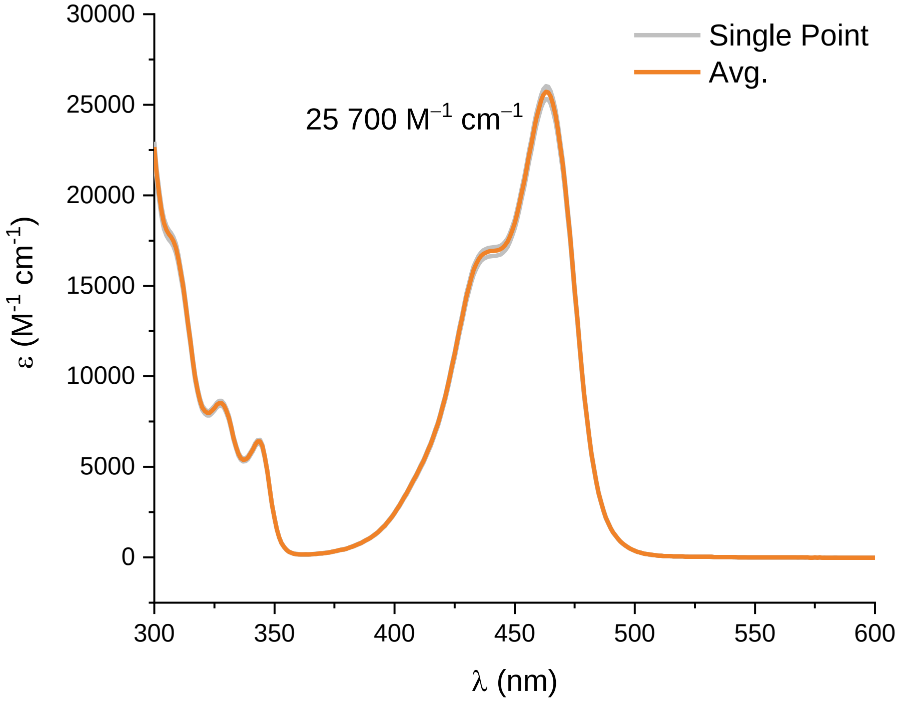

Figure S24. Molar absorption coefficient single point measurements of MeO-TATA$^+$ (**2**) in CH_2Cl_2. The orange line is the average of three single point measurements.

To investigate whether the excitation and emission spectra for A-TATA$^+$ (**1**) vary as a function of wavelength, we recorded excitation and emission spectra at different wavelengths. Normalized excitation spectra at different wavelengths in comparison with absorption spectra are shown in Figure S25. Normalized emission spectra with excitation at different wavelengths are shown in Figure S26.

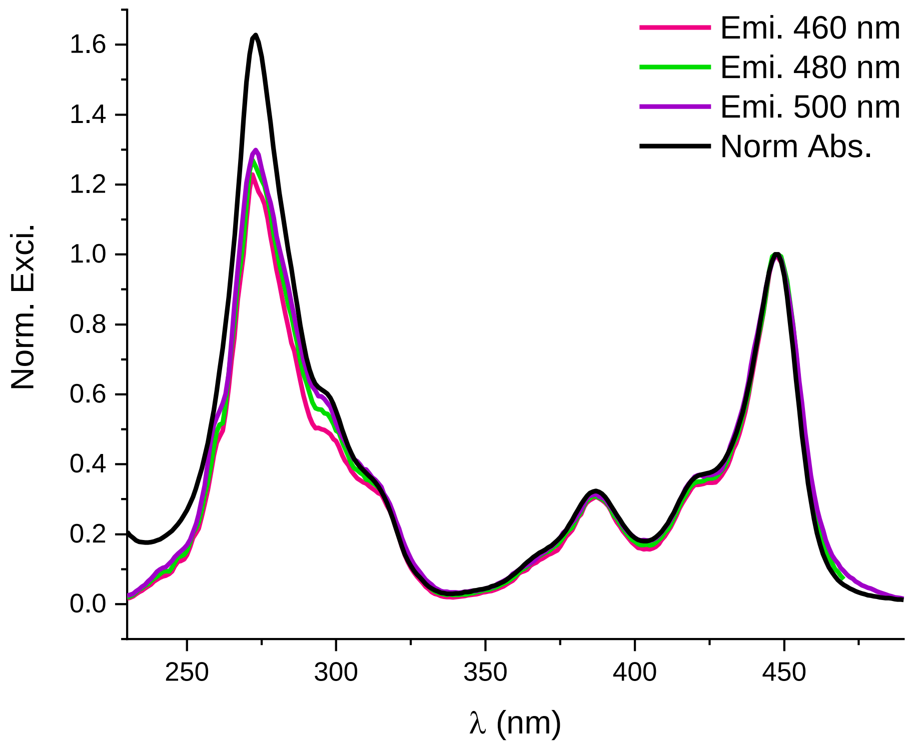

Figure S25. Normalized excitation spectra at four different wavelengths for A-TATA$^+$ (**1**) in CH_2Cl_2. The normalized absorption spectrum is shown for comparison.

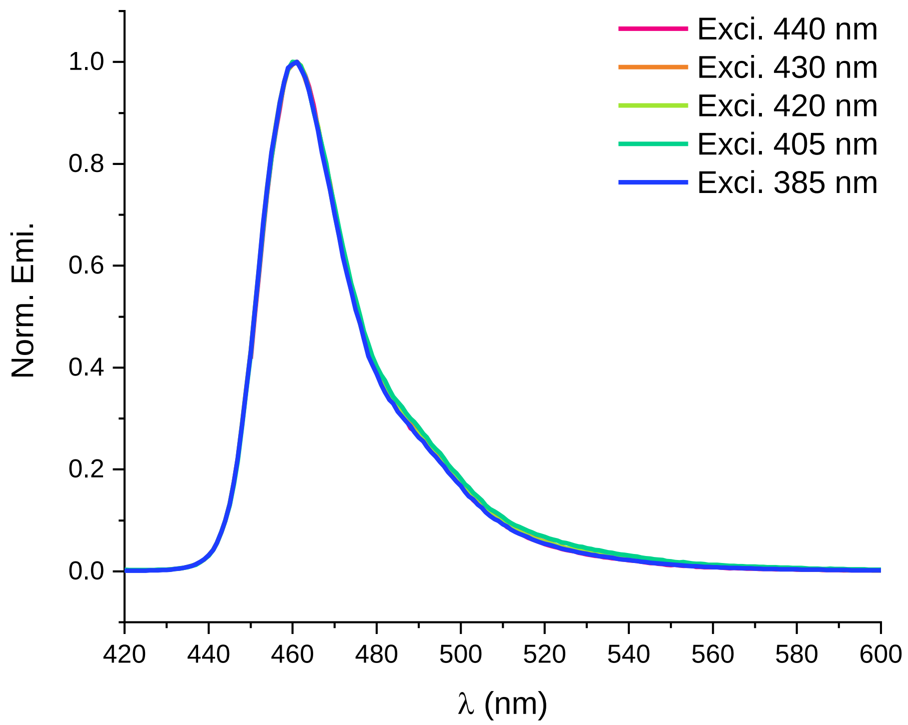

Figure S26. Normalized emission spectra at five different wavelengths for A-TATA$^+$ (**1**) in CH_2Cl_2.

The molar absorption coefficient was determined using four single point measurements with a known concentration of A-TATA$^+$ (**1**) in CH_2Cl_2 (Figure S24). The average of these three measurements is the determined coefficient.

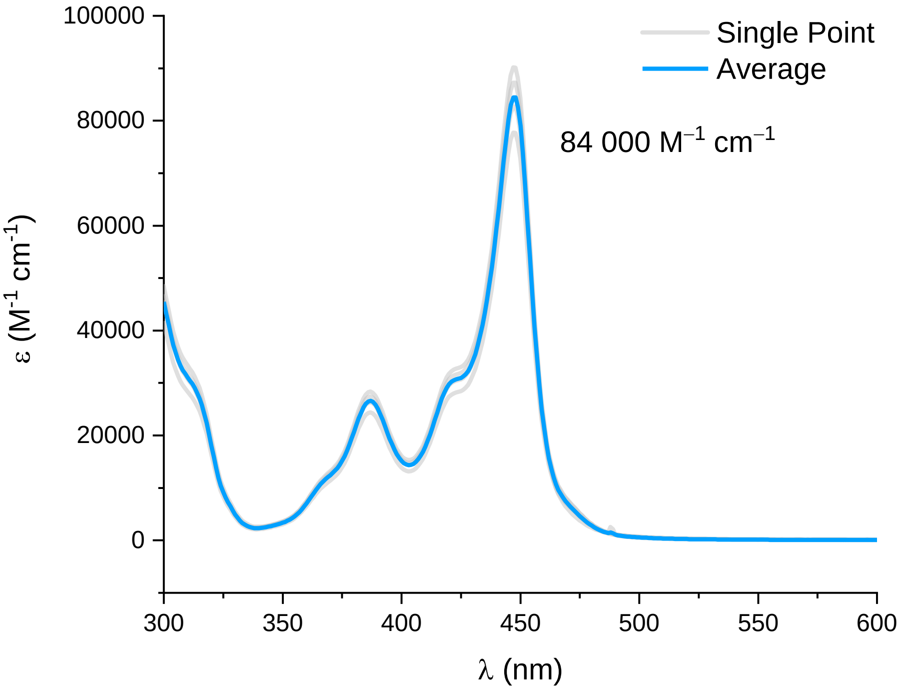

Figure S27. Molar absorption coefficient single point measurements of A-TATA$^+$ (**1**) in CH_2Cl_2. The blue line is the average of four single point measurements.

1.5.2 Quantum Yield Determination

Quantum yield determinations were done using the 6-point dilution method as described above using CH_2Cl_2 as the solvent. The quantum yield for TATA$^+$ was determined relative to Rho-6G in EtOH (ϕ_f = 0.94)[4] while the quantum yields for MeO-TATA$^+$ (**2**), A-TATA$^+$ (**1**), A-TOTA$^+$, and A-ADOTA$^+$ were determined relative to Cou-153 in EtOH (ϕ_f = 0.54).[5] The spectra in the figures below show the absorption and emission profiles of the 6-point dilution series, and the integrated emission intensity as a function of $1-10^{-OD}$. The curve of the latter plot is used to determine the quantum yield relative to the reference fluorophore. The chemical structures of the fluorophores are presented in Figure S28. The determined quantum yields are shown in Table S5.

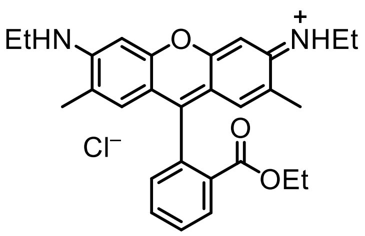

Rho-6G

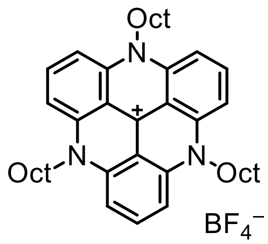

TATA $^{+}$

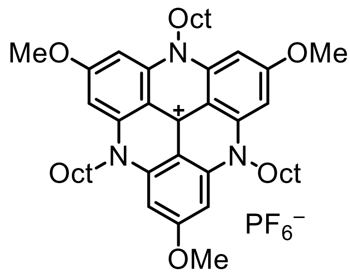

MeO-TATA $^{+}$ (**2**)

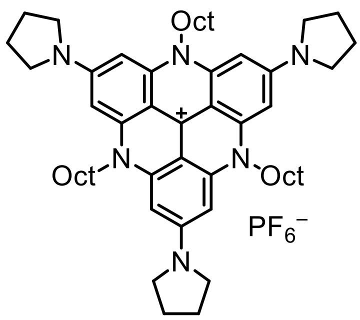

A-TATA $^{+}$ (**1**)

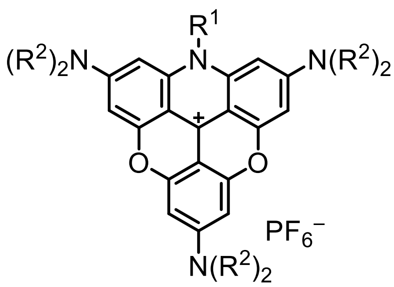

A-ADOTA $^{+}$

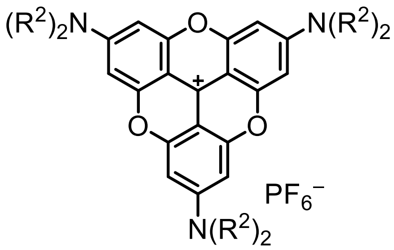

A-TOTA $^{+}$

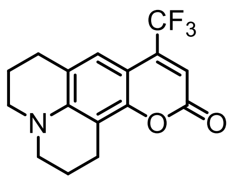

Cou-153

Figure S28. Chemical structures of the fluorophores discussed in Section 1.2.2, Quantum Yield Determination.

Table S5. Relative fluorescence quantum yields (ϕ_f) for the fluorophores in **Figure S28** in CH_2Cl_2.

	ϕ_f [%]
TATA^{+}	21[a]
MeO-TATA^{+} (**2**)	28[b]
A-TATA^{+} (**1**)	45[b]
A-TOTA^{+}	93[b]
A-ADOTA^{+}	73[b]

[a]Relative to Rho-6G in EtOH (ϕ_f = 94%).[4] [b]Relative to Cou-153 in EtOH (ϕ_f = 54%).[5]

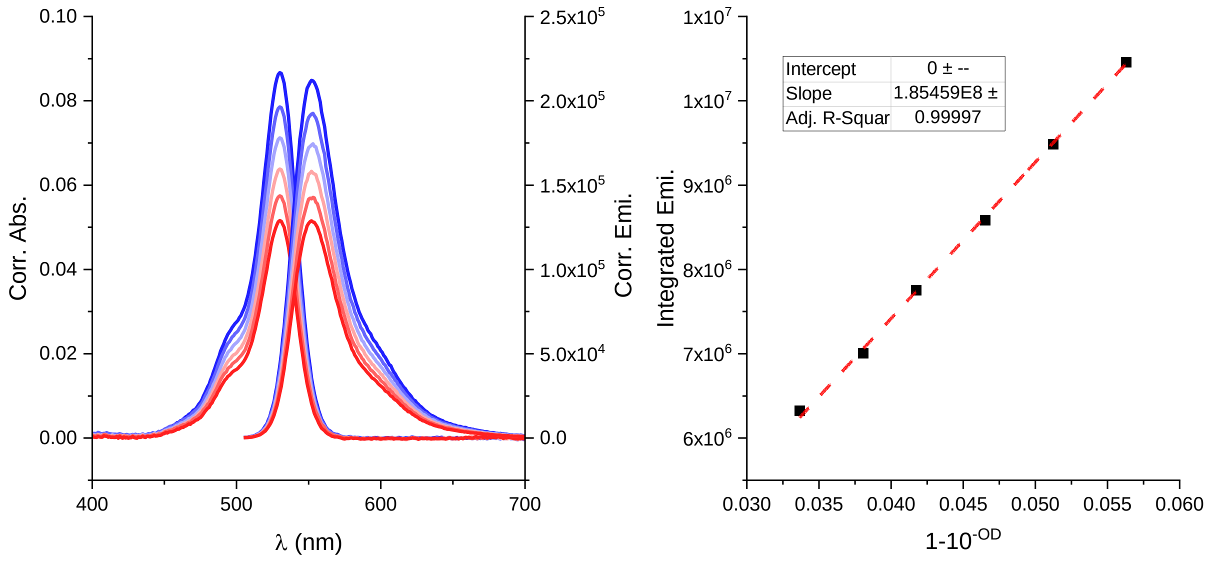

Figure S29. Rho-6G reference fluorophore quantum yield determination in EtOH. Used for the relative quantum yield of $TATA^+$. Excitation wavelength = 495 nm.

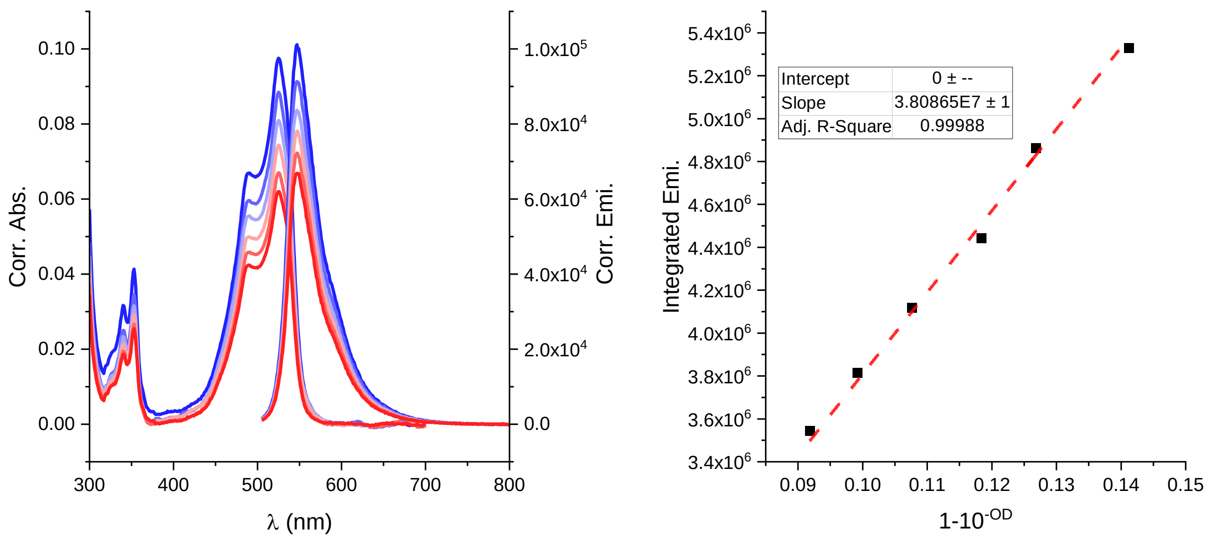

Figure S30. $TATA^+$ quantum yield determination in CH_2Cl_2. Excitation wavelength = 495 nm.

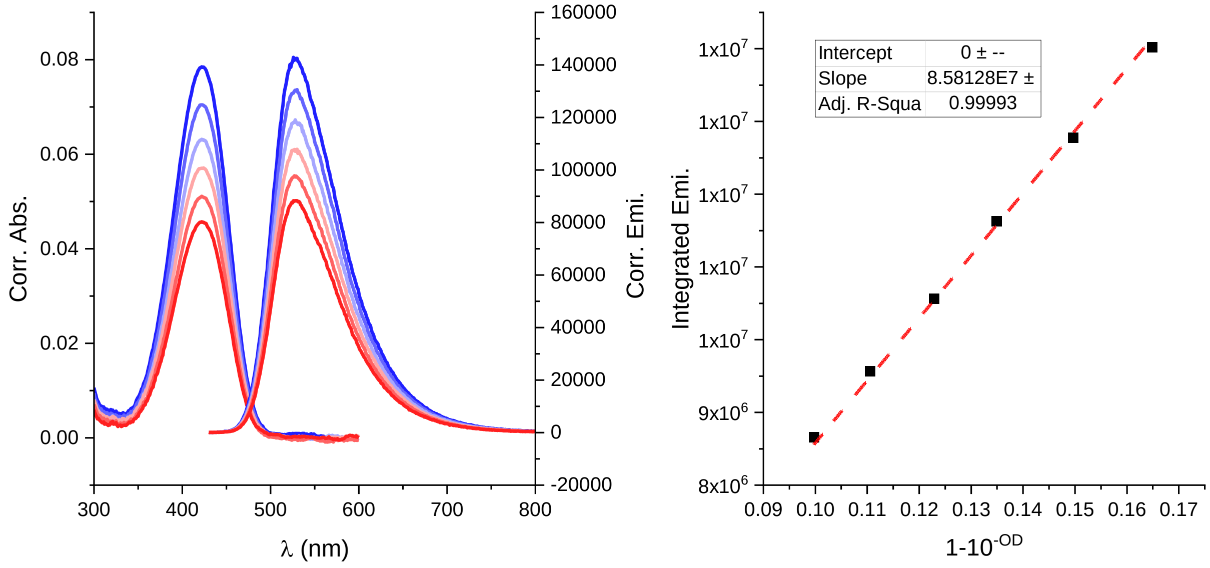

Figure S31. Cou-153 reference fluorophore quantum yield determination in EtOH. Used for the relative quantum yield of A-TATA$^+$ (**1**). Excitation wavelength = 420 nm.

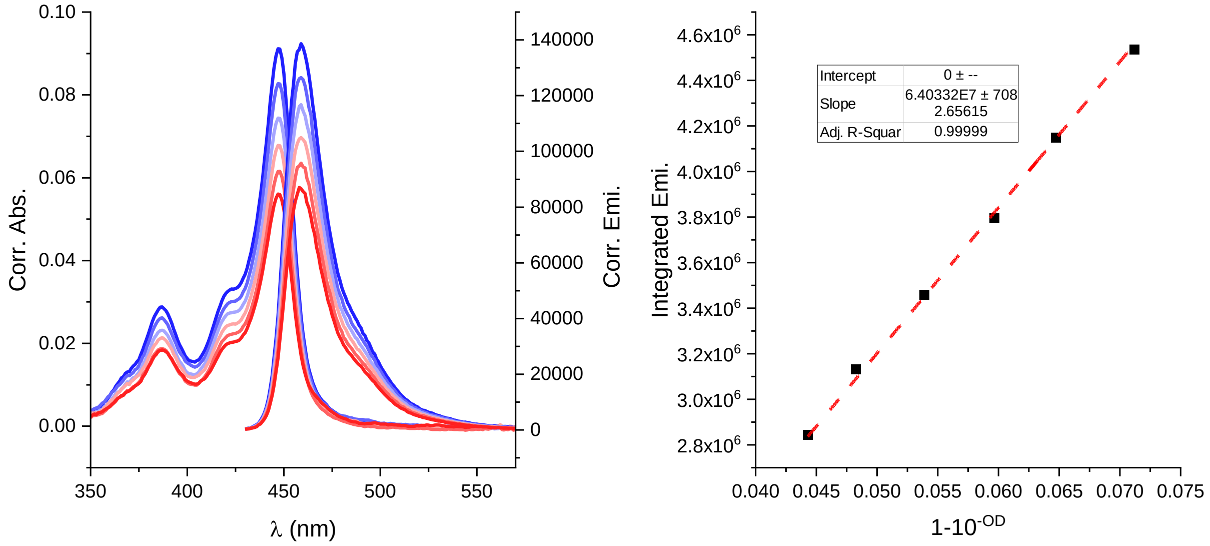

Figure S32. A-TATA$^+$ (**1**) quantum yield determination in CH_2Cl_2. Excitation wavelength = 420 nm.

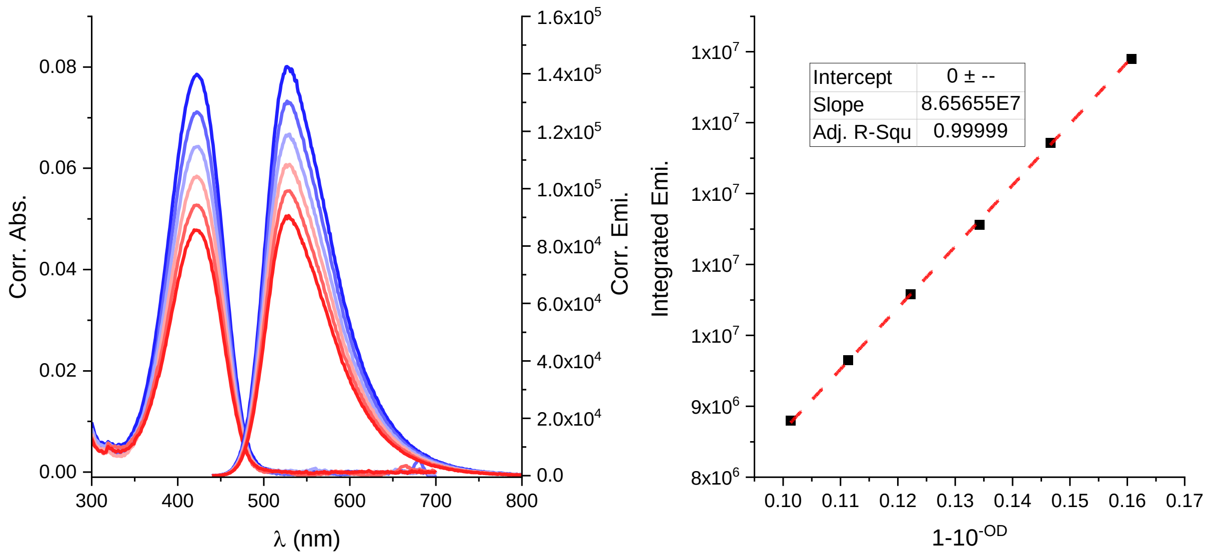

Figure S33. Cou-153 reference fluorophore quantum yield determination in EtOH. Used for the relative quantum yield of MeO-TATA$^+$ (**2**). Excitation wavelength = 430 nm.

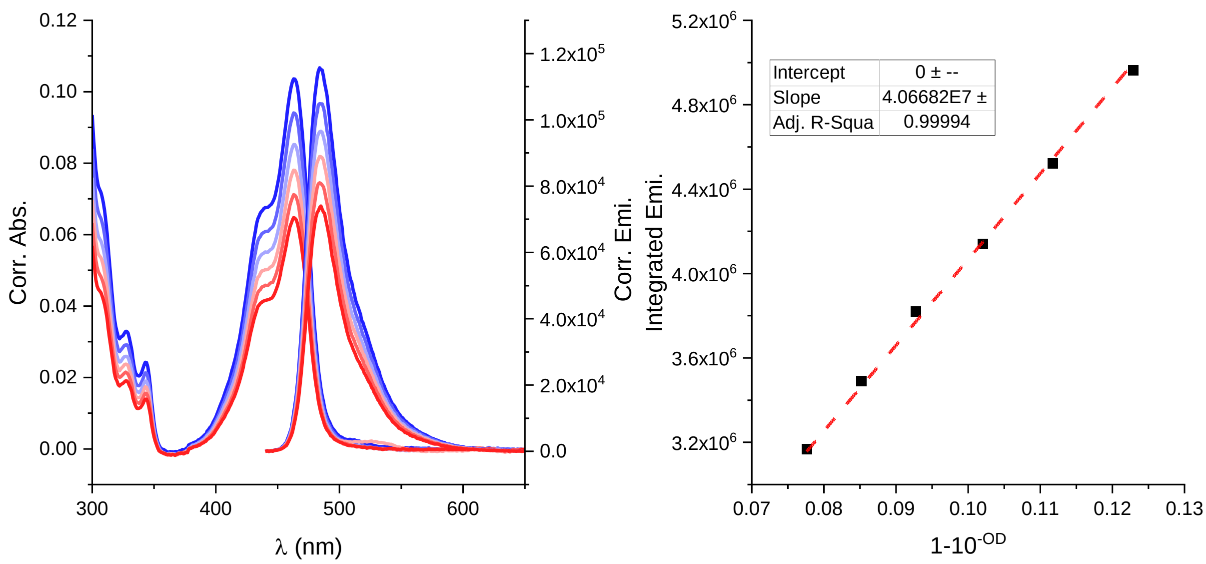

Figure S34. MeO-TATA$^+$ (**2**) quantum yield determination in CH_2Cl_2. Excitation wavelength = 430 nm.

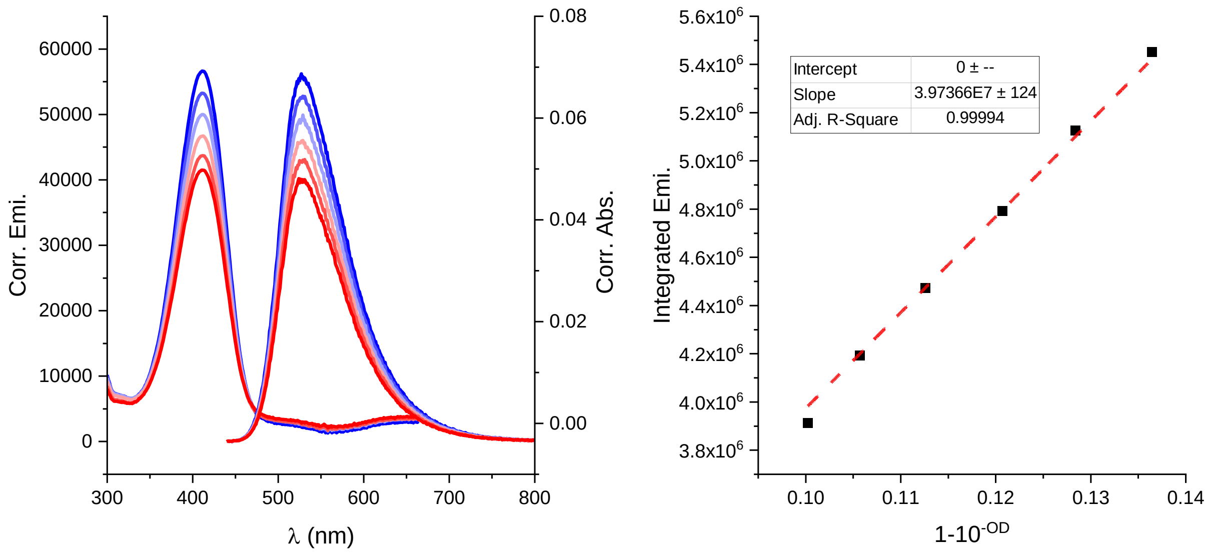

Figure S35. Cou-153 reference fluorophore quantum yield determination in EtOH. Used for the relative quantum yield of A-TOTA$^+$ and A-ADOTA$^+$. Excitation wavelength = 435 nm.

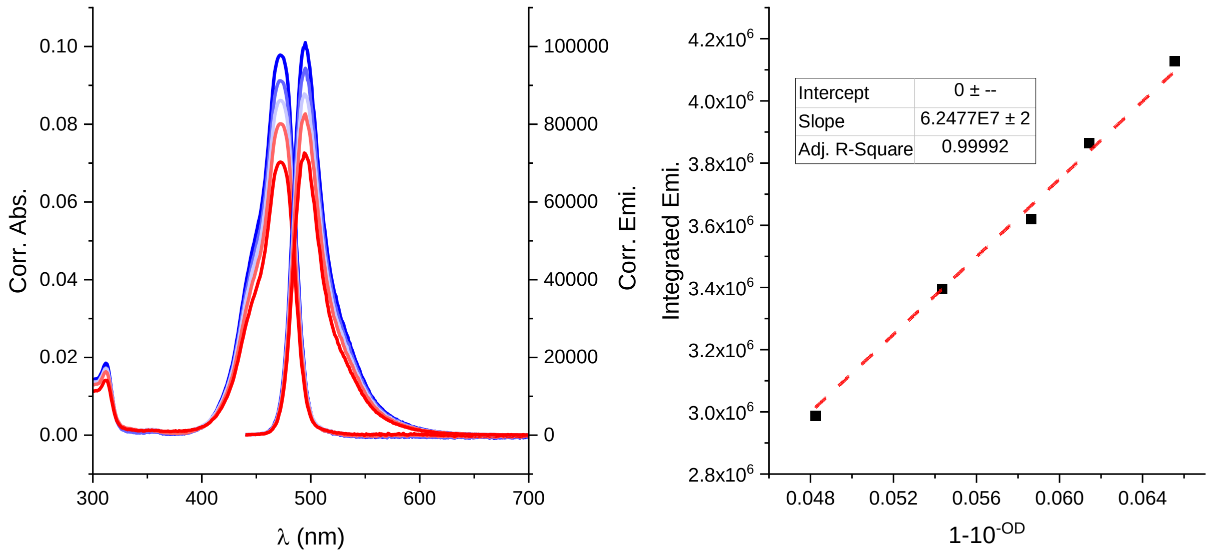

Figure S36. A-TOTA$^+$ quantum yield determination in CH_2Cl_2. Excitation wavelength = 435 nm.

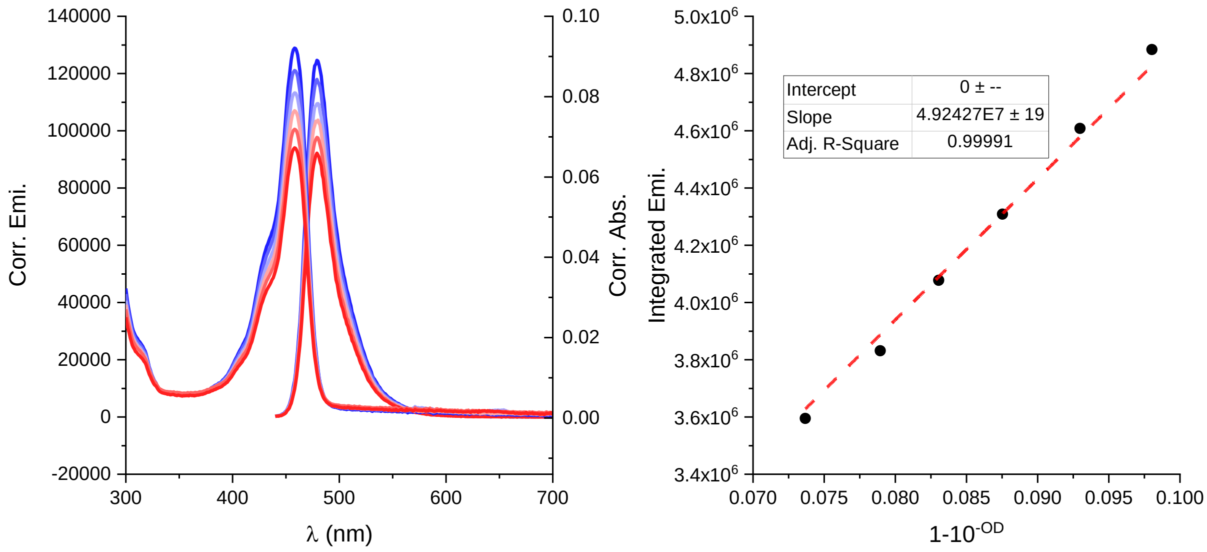

Figure S37. A-ADOTA$^+$ quantum yield determination in CH_2Cl_2. Excitation wavelength = 435 nm.

1.5.3 Fluorescence Lifetime Measurements

The fluorescence lifetimes of the fluorophores were determined as described in section 1.1.2. The decay histograms and the associated exponential fit for the fluorophores in CH_2Cl_2 are shown in Figure S38 and Figure S39 along with the instrument response functions (IRF) for the associated lasers used in the fitting. The goodness of fit parameter (χ^2) for the exponential fit and the fluorescence lifetimes for each fluorophore are shown in Table S6.

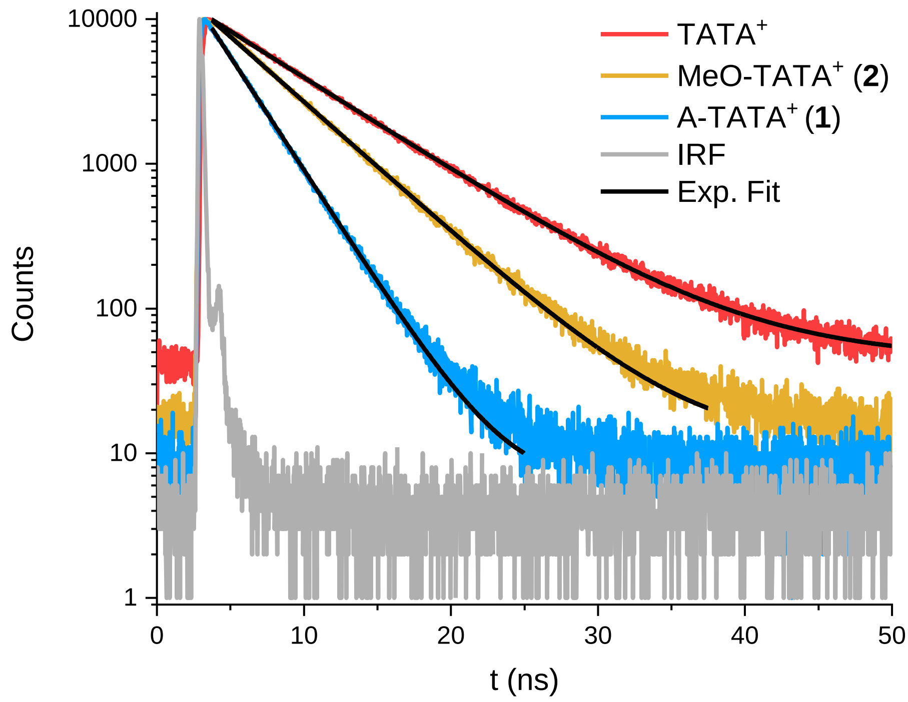

Figure S38. Fluorescence decay histograms for TATA$^+$, MeO-TATA$^+$ (**2**), and A-TATA$^+$ (**1**) in CH_2Cl_2. The IRF for the laser is shown in grey. The exponential fits to the decays are show in black.

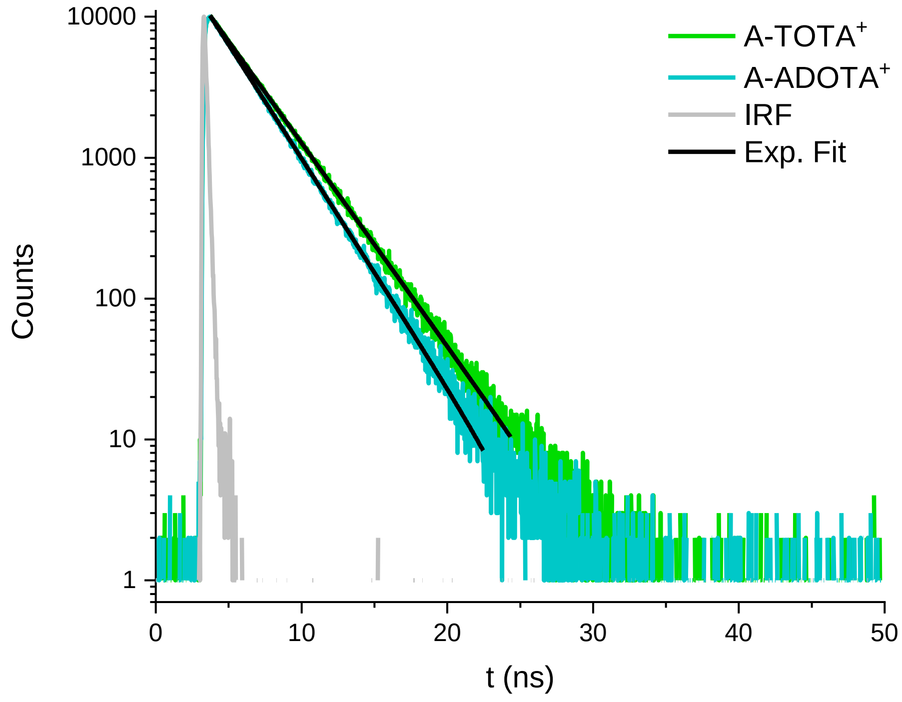

Figure S39. Fluorescence decay histograms for A-TOTA$^+$ and A-ADOTA$^+$ (**2**) in CH_2Cl_2. The IRF for the laser is shown in grey. The exponential fits to the decays are show in black.

Table S6. Fluorescence lifetimes (τ) for the fluorophores in **Figure S28** in CH_2Cl_2. For bi-exponential decays the average amplitude weighted lifetime is reported in τ_{avg}.

	τ_1 [ns]	τ_2 [ns]	τ_{avg} [ns]	χ^2
TATA$^+$	5.9 (95%)	17.4 (5%)	6.6	0.981
MeO-TATA$^+$ (**2**)	4.9 (95%)	2.0 (5%)	4.6	1.099
A-TATA$^+$ (**1**)	2.5 (95%)	4.2 (8%)	2.6	1.066
A-TOTA$^+$	3.0			0.8365
A-ADOTA$^+$	2.7			0.8226

1.6 Computational Data

Table S7. DFT-calculated free energies for the species C$^+$, C-OH, OH$^-$, and free energy difference for the reactions C$^+$+OH$^-$⇌COH. Calculation level B3LYP-D3BJ/6-311+G(2d,p)/PCM(DCM).

	G (au)	ΔG (kcal mol^{-1})
TOTA$^+$	–955.116933	–31.91
TOTA-OH	–1031.121501	
A-TOTA$^+$	–1589.284463	–10.46
A-TOTA-OH	–1665.254850	
DAOTA$^+$	–993.992690	–15.86
DAOTA-OH	–1069.971675	
ADOTA$^+$	–974.557653	–22.80
ADOTA-OH	–1050.547701	
A-ADOTA$^+$	–1608.717999	–5.09
A-ADOTA-OH	–1684.679825	
TATA$^+$	–1013.423884	–9.94
TATA-OH	–1089.393443	
A-TATA$^+$	–1647.576501	+4.07
A-TATA-OH	–1723.523738	
MeO-TATA$^+$	–1357.051559	–4.29
MeO-TATA-OH	–1433.012118	
OH$^-$	–75.953715	

Table S8. DFT-calculated HOMO and LUMO energies and net atomic charge (DDEC6 scheme) for the central carbon of carbenium ions. Calculation level B3LYP-D3BJ/6-311+G(2d,p)/PCM(DCM).

	E_{HOMO} (eV)	E_{LUMO} (eV)	DDEC6 charge
$TOTA^+$	–7.3498	–3.9614	+0.181
$A\text{-}TOTA^+$	–6.0317	–2.7788	+0.152
$DAOTA^+$	–6.3778	–3.3032	+0.129
$ADOTA^+$	–6.7544	–3.6118	+0.150
$A\text{-}ADOTA^+$	–5.8997	–2.5489	+0.135
$TATA^+$	–6.2208	–3.0235	+0.105
$A\text{-}TATA^+$	–5.6518	–2.1075	+0.099
$MeO\text{-}TATA^+$	–6.1669	–2.6294	+0.109

Table S9. TD-DFT-calculated transition energies (in eV, compared with experimental values) and oscillator strengths for the first two transitions of carbenium ions. Calculation level CAM-B3LYP/def2-TZVP/PCM(DCM).[a]

		S_0-S_1 transition		S_0-S_2 transition	
	Exp. energy (eV)[b]	Calc. energy (eV)	Calc. oscill. strength	Calc. energy (eV)	Calc. oscill. strength
$TOTA^+$	2.58	3.21	0.143	3.21	0.143
$A\text{-}TOTA^+$	2.63	3.26	1.000	3.26	1.000
$DAOTA^+$	2.23	2.88	0.248	3.32	0.109
$ADOTA^+$	2.28	2.95	0.225	3.40	0.098
$A\text{-}ADOTA^+$	2.71	3.29	0.833	3.37	0.908
$TATA^+$	2.36	3.02	0.196	3.02	0.196
$A\text{-}TATA^+$	2.77	3.40	0.620	3.40	0.620
$MeO\text{-}TATA^+$	2.68	3.35	0.268	3.35	0.268

[a] See **Figures S40-S41** for data plots. [b] Measured in CH_2Cl_2.

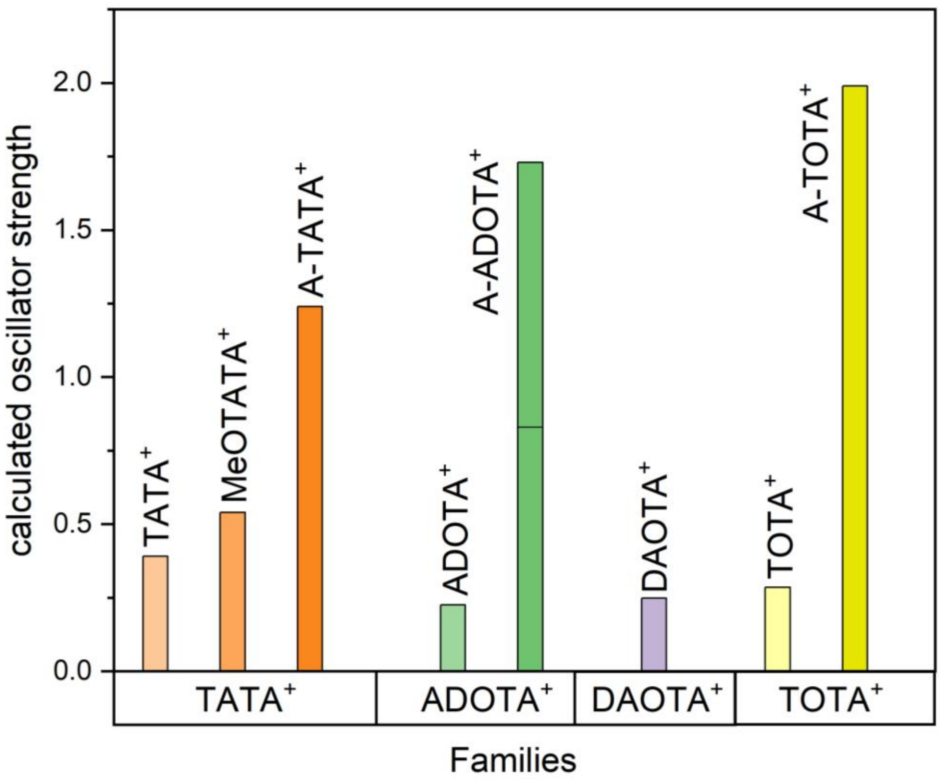

Figure S40. Calculated oscillator strengths for the first transition(s) of carbenium ions. Calculation level CAM-B3LYP/def2-TZVP/PCM(DCM). For compounds with degenerate S_0-S_1 and S_0-S_2 transitions (see **Table S9**), the two contributions are summed. For A-ADOTA$^+$, with quasi-degenerate transitions, the two contributions are shown on top of each other

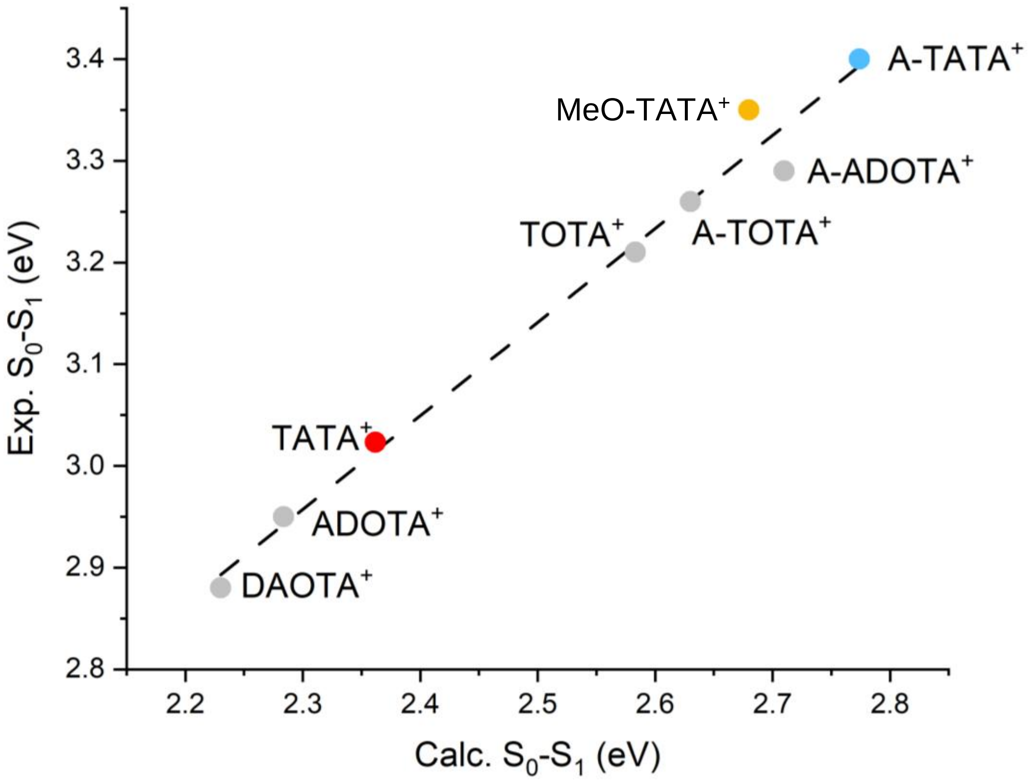

Figure S41. Correlation between experimental transition energies (recorded in CH_2Cl_2) and transition energies for the S_0-S_1 transition of carbenium ions. Calculation level CAM-B3LYP/def2-TZVP/PCM(DCM).

1.7 NMR Spectra

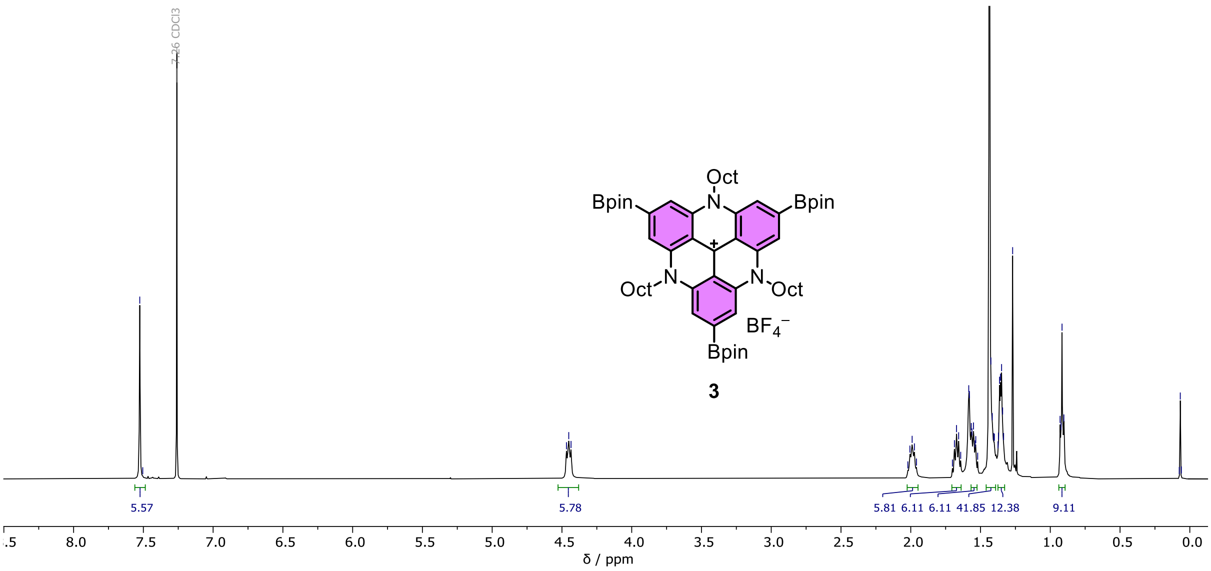

Figure S42. ^{1}H NMR (500 MHz) spectrum of **3** in $CDCl_3$.

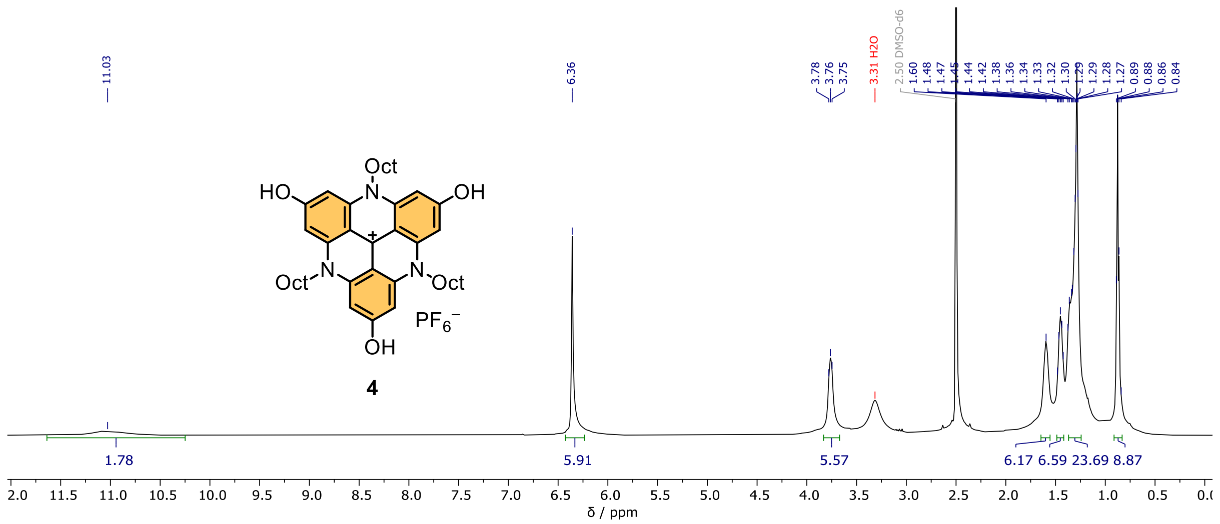

Figure S43. ^{1}H NMR (500 MHz) spectrum of **4** in DMSO-d_6.

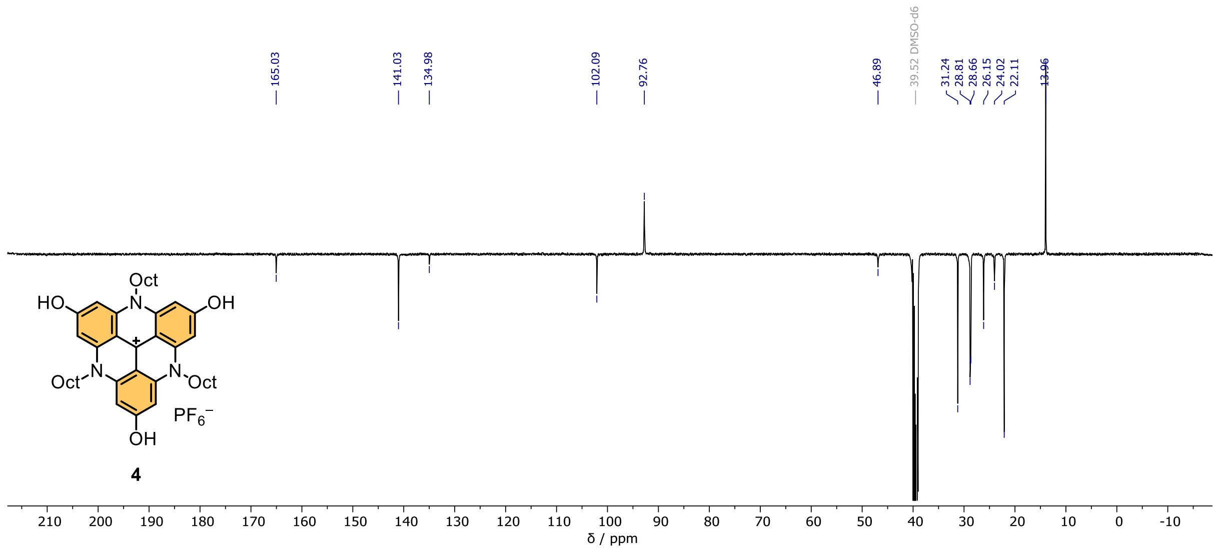

Figure S44. ^{13}C NMR (126 MHz) spectrum of **4** in DMSO-d_6.

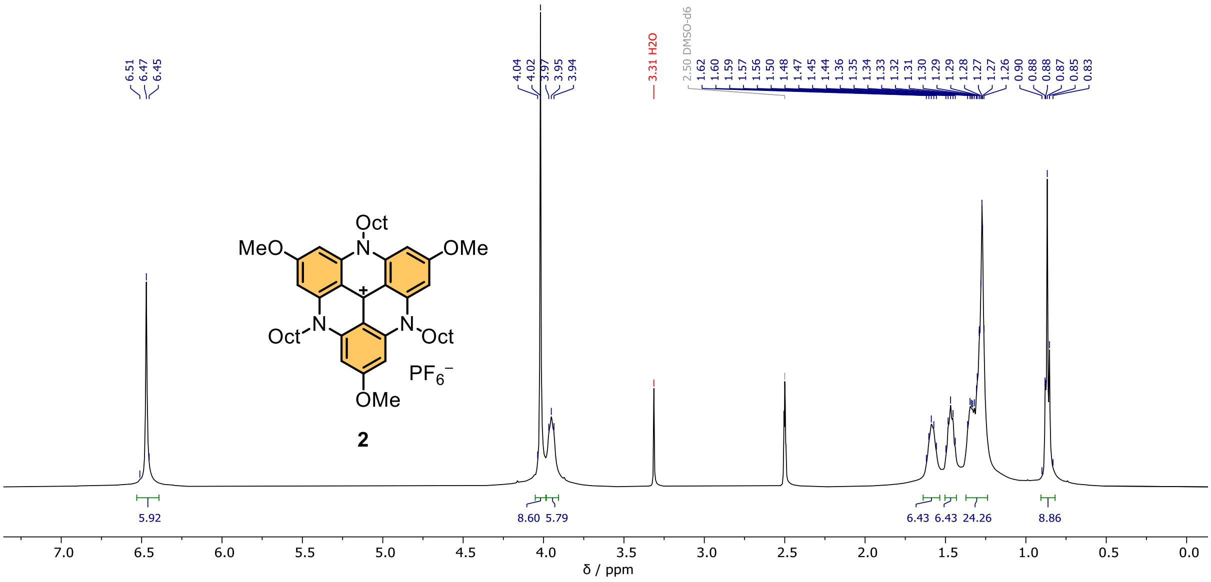

Figure S45. ^{1}H NMR (500 MHz) spectrum of MeO-TATA^{+} (**2**) in DMSO-d_6.

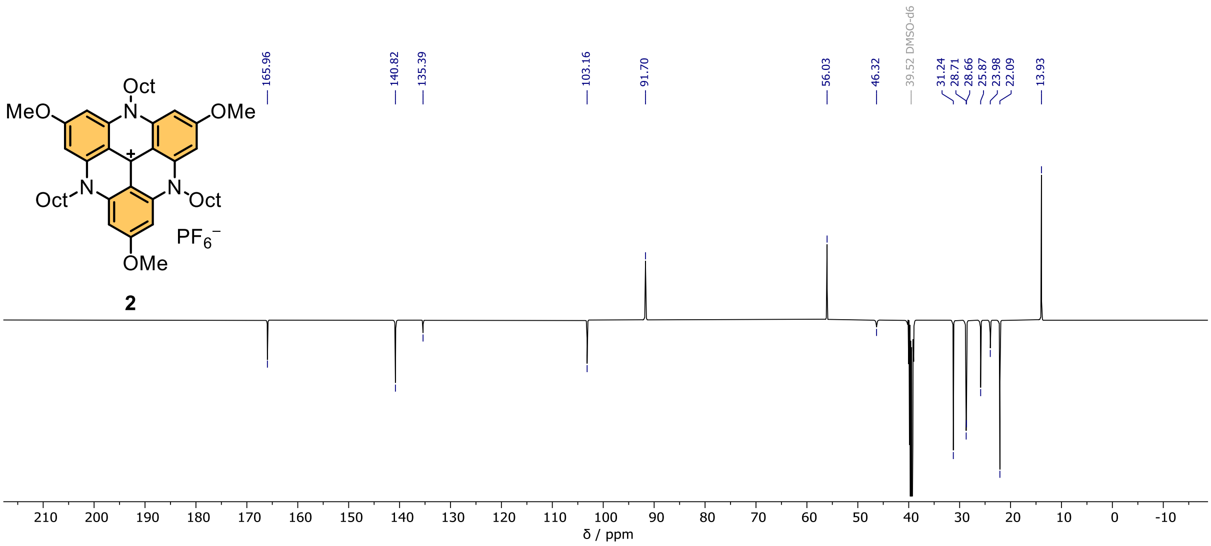

Figure S46. ^{13}C NMR (126 MHz) spectrum of MeO-TATA^{+} (**2**) in DMSO-d_6.

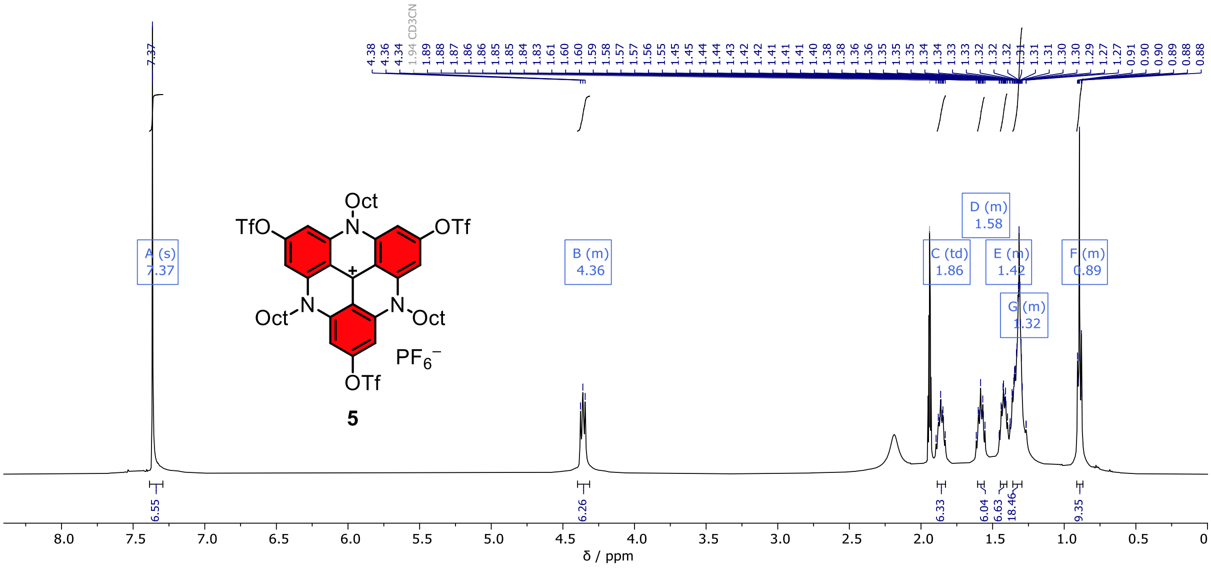

Figure S47. ^{1}H NMR (500 MHz) spectrum of **5** in CD_3CN.

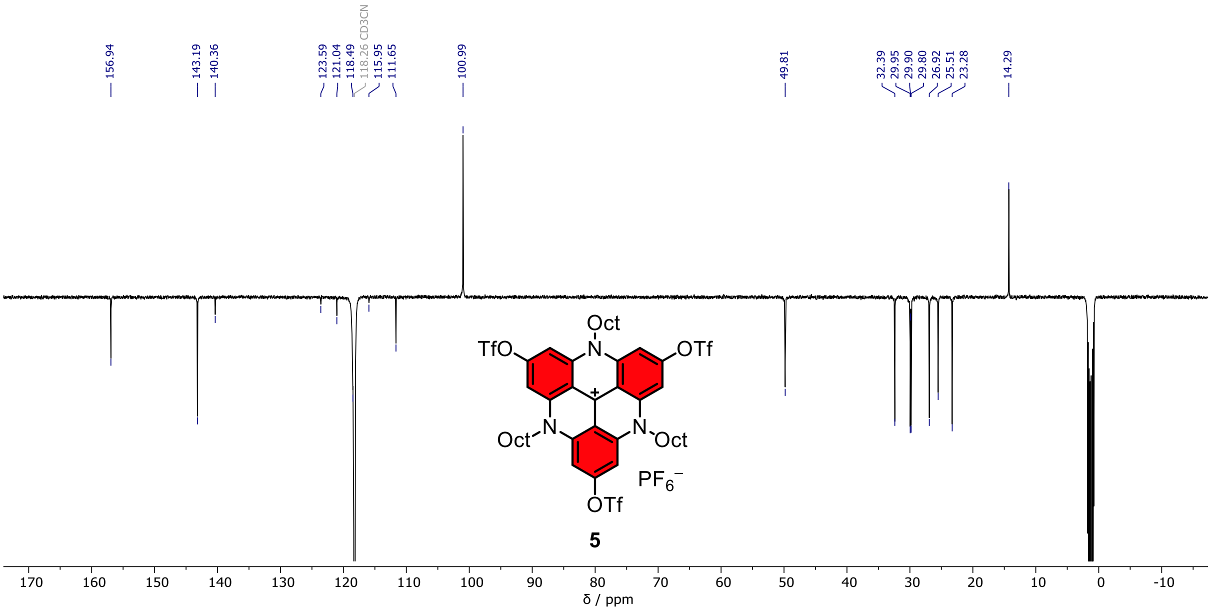

Figure S48. ^{13}C NMR (126 MHz) spectrum of **5** in CD_3CN.

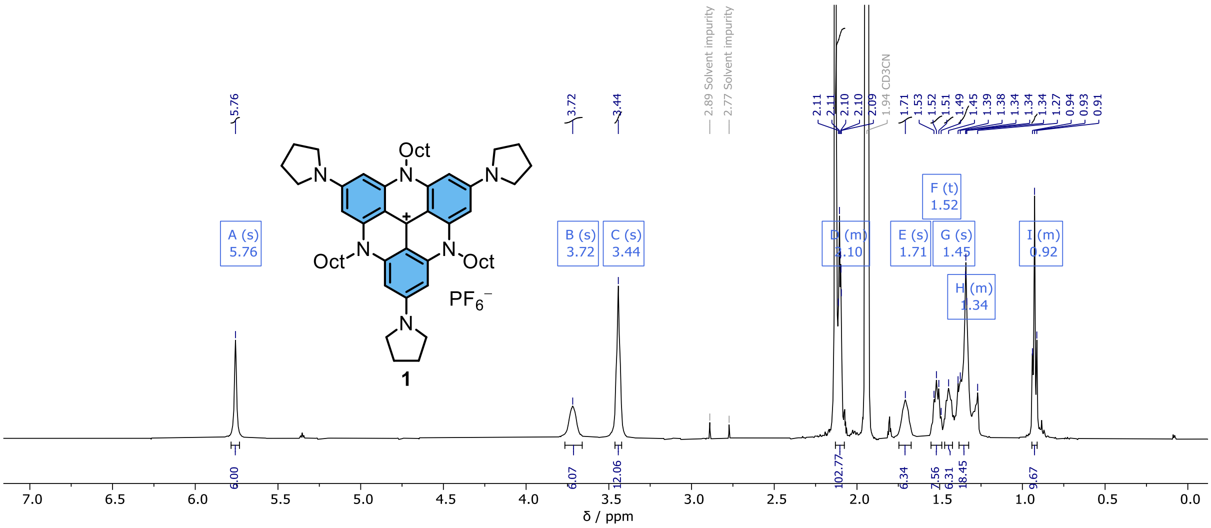

Figure S49. ^{1}H NMR (500 MHz) of A-TATA⁺ (**1**) in CD_3CN.

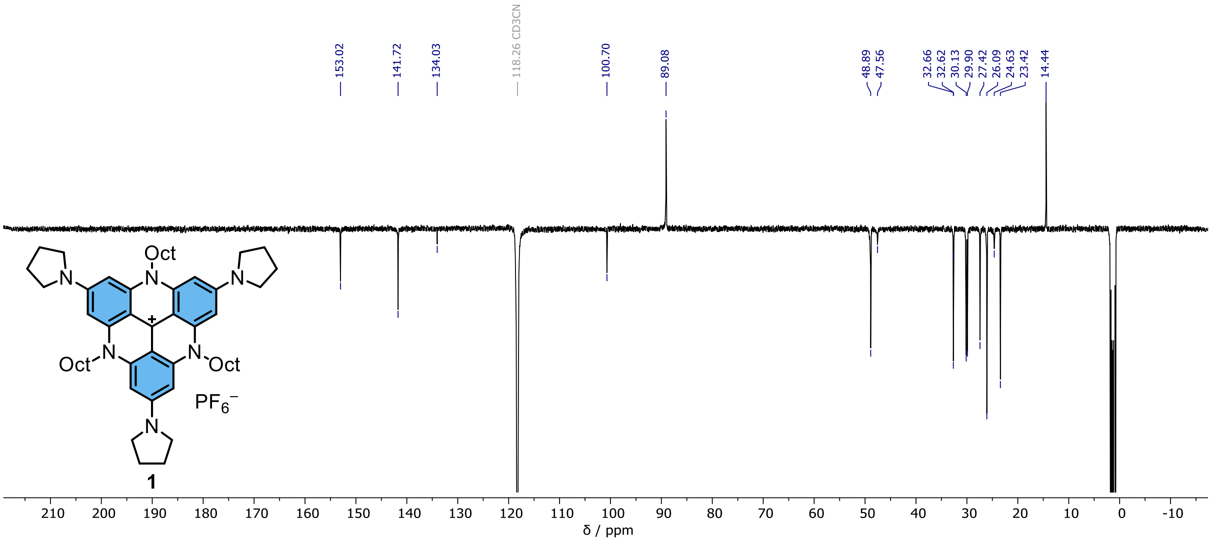

Figure S50. ^{13}C NMR (126 MHz) spectrum of A-TATA⁺ (**1**) in CD_3CN.

1.8 HRMS Spectra

HRMS spectra were recorded according to the description in section 1.1.1.

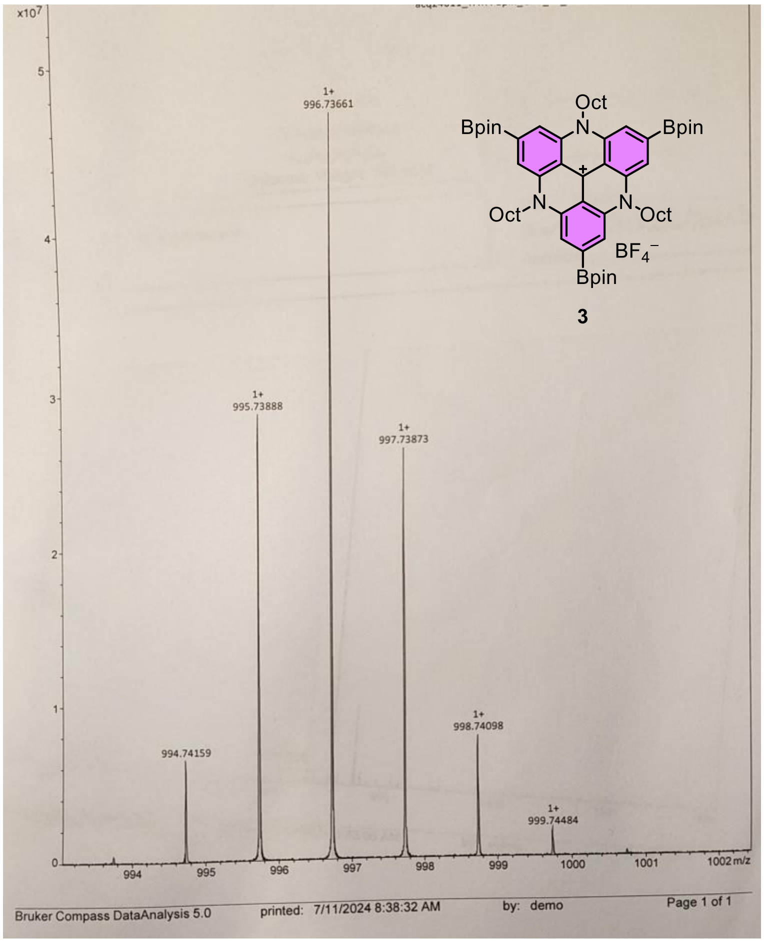

Figure S51. HRMS spectrum of **3**.

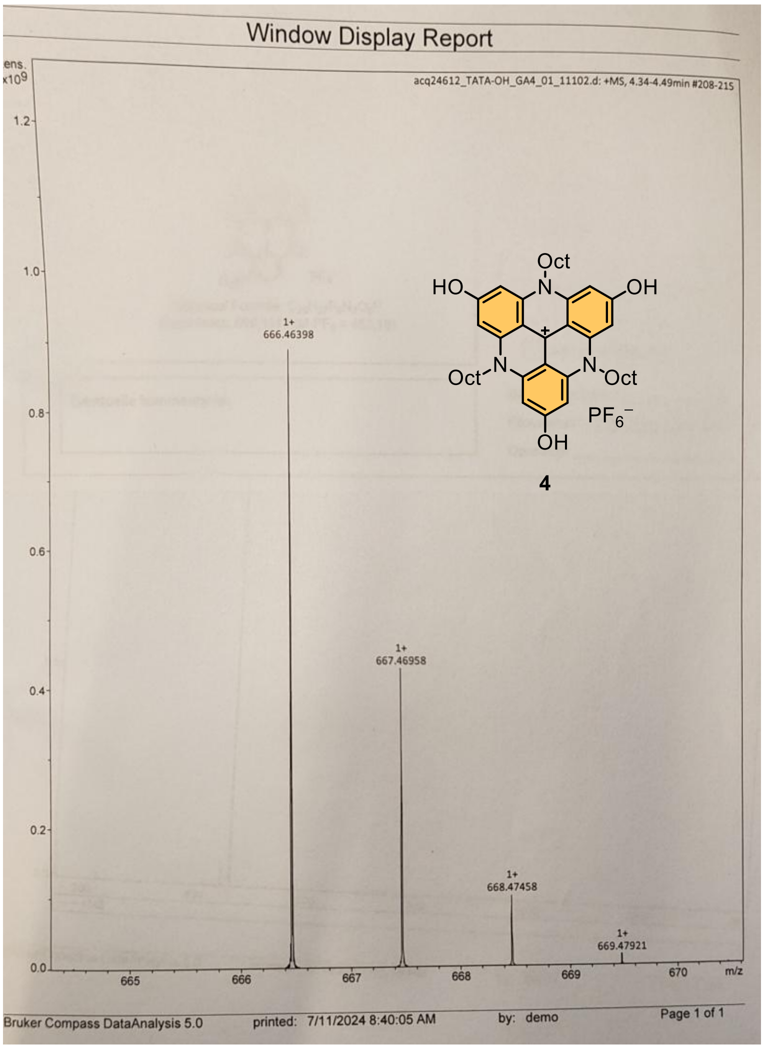

Figure S52. HRMS spectrum of **4**.

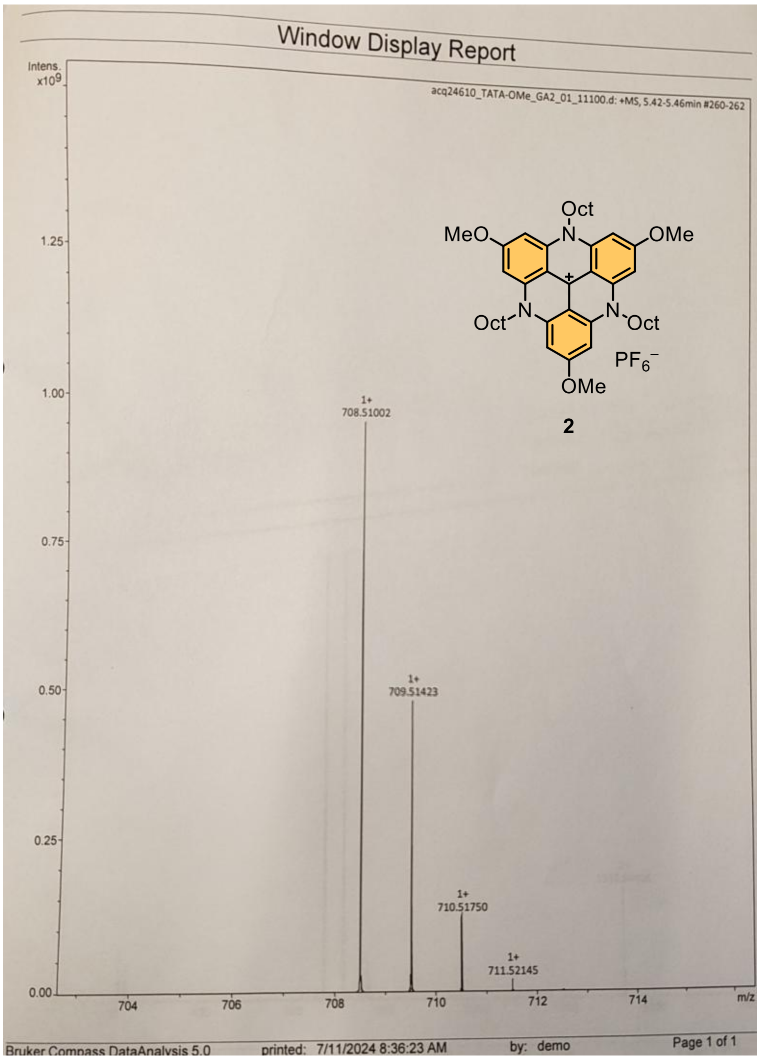

Figure S53. HRMS spectrum of MeO-TATA$^+$ (**2**).

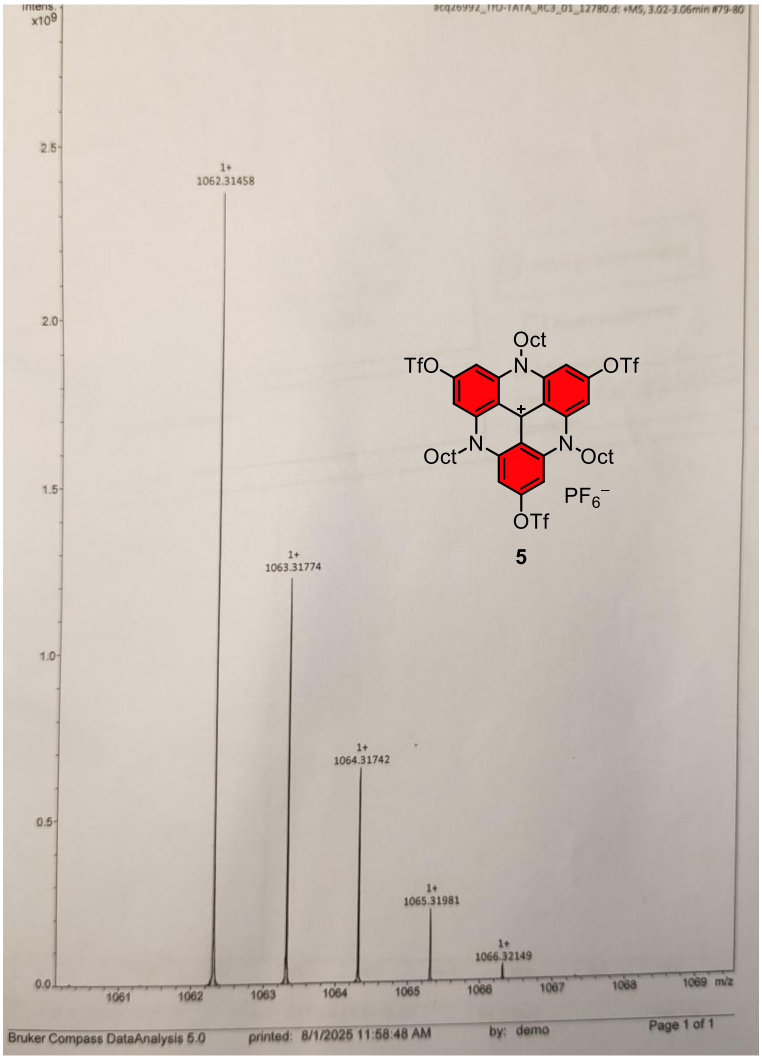

Figure S54. HRMS spectrum of **5**.

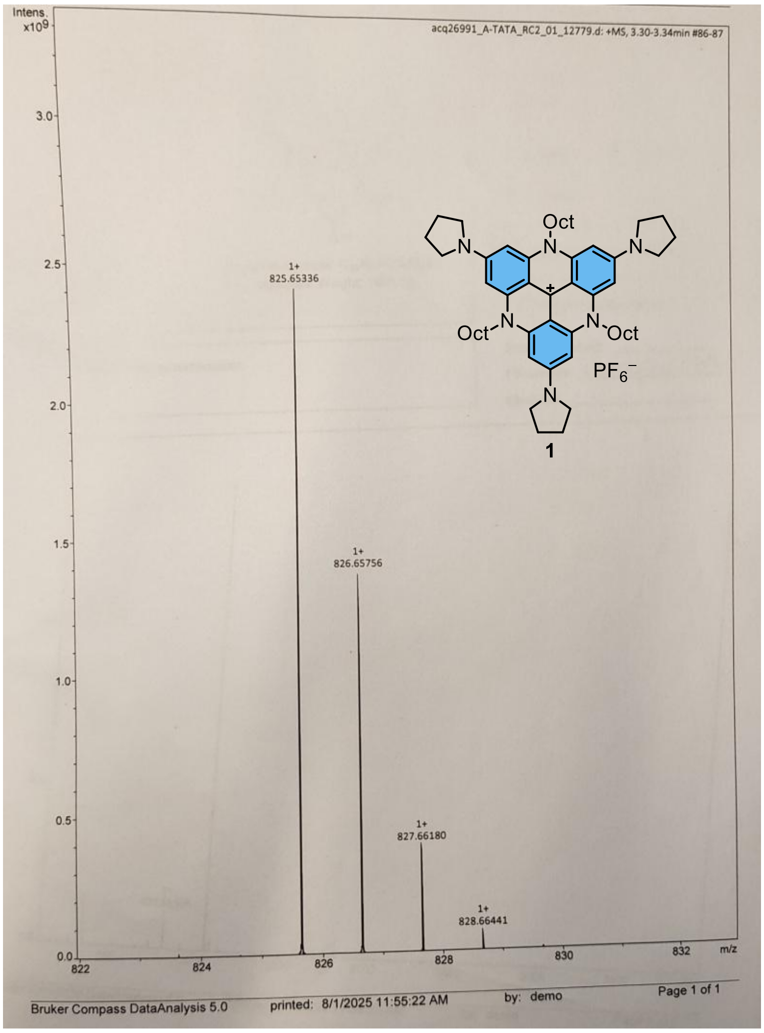

Figure S55. HRMS spectrum of A-TATA⁺ (**1**).

1.9 Electron Diffraction

Table S10. Crystallographic data and structure refinement results for MeO-TATA·PF_6

Compound	**MeO-TATA·PF_6**
CCDC	2524713
Formula	$C_{46}H_{66}F_6N_3O_3P$
$D_{calc.}$/ g cm^{-3}	1.278
Formula Weight	853.99
Colour	yellow
Shape	plate
T/K	173
Crystal System	triclinic
Space Group	*P*-1
a/Å	9.1861(10)
b/Å	15.0323(11)
c/Å	16.919(2)
a/°	107.194(10)
b/°	94.929(12)
g/°	91.656(7)
V/Å^3	2220.0(4)
Z, Z'	2, 1
Wavelength/Å	0.0251
Radiation type	electron
$\theta_{min} - \theta_{max}$ /°	0.050 – 0.902
Resolution /Å	0.8
Measured Refl. (3 crystals merged)	29564
Independent Refl.	6358
Reflections with I > 2(I)	3376
R_{int}	0.2149
Parameters	590
Restraints	2491
Largest Peak /Å^{-2}	0.285
Deepest Hole /Å^{-2}	-0.249
GooF	1.063
wR_2 (all data)	0.5896
wR_2	0.5489
R_1 (all data)	0.2725
R_1	0.2170

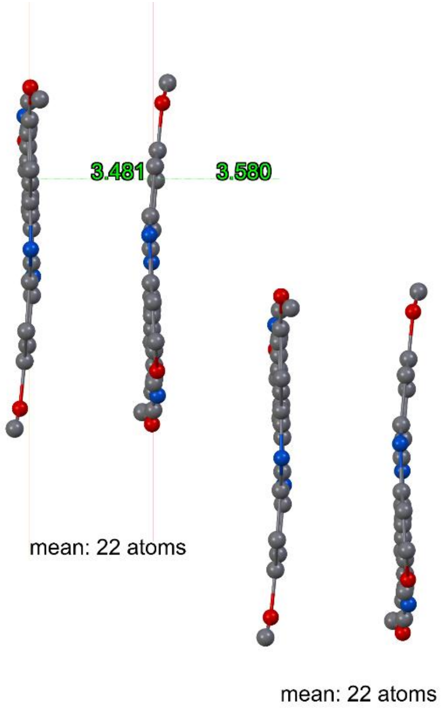

Figure S56. Side view of the stacked triangulenium cores of MeO-TATA+, with H-atoms, octyl chains and anions omitted for clarity. The 22 atoms of the triangulenium core adopt the expected planar geometry with average rms deviation of 0.0617 Å and maximum deviation of 0.14(6) Å from the mean plane (calculated with SHELXL).[12] The trianguleniums are stacked pairwise in a staggered fashion, with alternating distances (reported in the figure in Å).

1.10 Atomic Coordinates

Atom coordinates of DFT-optimized structures for all compounds. Level of calculation: B3LYP-D3BJ/6-311+g(2d,p) with IEF-PCM for dichloromethane. In all cases, no imaginary frequencies were found. E and G represent, respectively, the electronic energy and the free (Gibbs) energy.

$TOTA^+$, E = −955.306752 au, G = −955.116933 au

Symbol	X	Y	Z
H	0.0000000	2.1623830	−4.0113560
C	0.0000000	1.2309380	−3.4635600
C	0.0000000	−1.2258300	−2.0827780
C	0.0000000	0.0000000	−4.1244410
C	0.0000000	1.2258300	−2.0827780
C	0.0000000	0.0000000	−1.3931720
C	0.0000000	−1.2309380	−3.4635600
H	0.0000000	0.0000000	−5.2065680
H	0.0000000	−2.1623830	−4.0113560
C	0.0000000	0.0000000	−0.0000610
C	0.0000000	1.2062990	0.6964330
C	0.0000000	2.4165180	−0.0201440
O	0.0000000	2.4037120	−1.3877110
C	0.0000000	3.6147870	0.6658550
C	0.0000000	3.5716520	2.0623050
C	0.0000000	2.3838140	2.7977560
C	0.0000000	1.1906400	2.1028820
H	0.0000000	4.5549420	0.1331300
H	0.0000000	4.5088120	2.6033460
H	0.0000000	2.3923890	3.8783160
C	0.0000000	−1.2062990	0.6964330
C	0.0000000	−3.5716520	2.0623050
C	0.0000000	−2.4165180	−0.0201440
C	0.0000000	−1.1906400	2.1028820
C	0.0000000	−2.3838140	2.7977560
C	0.0000000	−3.6147870	0.6658550
H	0.0000000	−4.5088120	2.6033460
H	0.0000000	−2.3923890	3.8783160
H	0.0000000	−4.5549420	0.1331300
O	0.0000000	0.0000000	2.7755170
O	0.0000000	−2.4037120	−1.3877110

ADOTA$^+$, E = −974.785616 au, G = −974.557653 au

Symbol	X	Y	Z
H	0.0663320	0.1689440	4.5516170
C	0.0495800	−0.3917040	3.6280550
C	−0.0025090	−1.9009560	1.2133110
C	0.0781840	−1.7894140	3.6183970
C	0.0122160	0.2565720	2.4158650
C	−0.0072650	−0.4803660	1.2100280
C	0.0559030	−2.5456810	2.4554640
H	0.1256470	−2.3099620	4.5661220
H	0.1028400	−3.6194180	2.5336030
C	−0.0190920	0.2090850	0.0000000
C	−0.0195550	1.6162450	0.0000000
C	−0.0157310	2.3123450	1.2162870
O	−0.0020850	1.6244240	2.3967470
C	−0.0198820	3.6945420	1.2260430
C	−0.0237030	4.3609070	0.0000000
C	−0.0198820	3.6945420	−1.2260430
C	−0.0157310	2.3123450	−1.2162870
H	−0.0175500	4.2357090	2.1615290
H	−0.0263490	5.4429980	0.0000000
H	−0.0175500	4.2357090	−2.1615290
C	−0.0072650	−0.4803660	−1.2100280
C	0.0781840	−1.7894140	−3.6183970
C	−0.0025090	−1.9009560	−1.2133110
C	0.0122160	0.2565720	−2.4158650
C	0.0495800	−0.3917040	−3.6280550
C	0.0559030	−2.5456810	−2.4554640
H	0.1256470	−2.3099620	−4.5661220
H	0.0663320	0.1689440	−4.5516170
H	0.1028400	−3.6194180	−2.5336030
N	−0.0546670	−2.5680890	0.0000000
O	−0.0020850	1.6244240	−2.3967470
C	−0.1581750	−4.0318990	0.0000000
H	−0.7127920	−4.3529240	−0.8743880
H	−0.7127920	−4.3529240	0.8743880
H	0.8306420	−4.4919380	0.0000000

DAOTA$^+$, E = −994.260453 au, G = −993.992690 au

Symbol	X	Y	Z
H	4.1266490	−0.0635850	2.3216770
C	3.0468160	−0.0385260	2.3548930
C	0.2107170	0.0251470	2.4484020
C	2.3475560	−0.0545990	3.5618650
C	2.3140710	−0.0057260	1.1888940
C	0.9067180	0.0241770	1.2146630
C	0.9624520	−0.0275630	3.6295320
H	2.9077700	−0.0990600	4.4868450
H	0.4891770	−0.0705680	4.5965270
C	0.1972880	0.0357560	0.0000000
C	0.9067180	0.0241770	−1.2146630
C	2.3140710	−0.0057260	−1.1888940
O	2.9855970	−0.0114660	0.0000000
C	3.0468160	−0.0385260	−2.3548930
C	2.3475560	−0.0545990	−3.5618650
C	0.9624520	−0.0275630	−3.6295320
C	0.2107170	0.0251470	−2.4484020
H	4.1266490	−0.0635850	−2.3216770
H	2.9077700	−0.0990600	−4.4868450
H	0.4891770	−0.0705680	−4.5965270
C	−1.1965150	0.0086400	0.0000000
C	−3.9401350	−0.1925410	0.0000000
C	−1.8945080	−0.0163130	1.2442820
C	−1.8945080	−0.0163130	−1.2442820
C	−3.2847460	−0.1306440	−1.2224570
C	−3.2847460	−0.1306440	1.2224570
H	−5.0169310	−0.3041520	0.0000000
H	−3.8614440	−0.2035830	−2.1295060
H	−3.8614440	−0.2035830	2.1295060
N	−1.1730780	0.0711270	2.4246230
C	−1.9071140	0.1983240	3.6868750
H	−1.2950210	0.7259010	4.4089950
H	−2.1814100	−0.7803370	4.0838030
H	−2.8017790	0.7900470	3.5221140
N	−1.1730780	0.0711270	−2.4246230
C	−1.9071140	0.1983240	−3.6868750

H	−1.2950210	0.7259010	−4.4089950
H	−2.1814100	−0.7803370	−4.0838030
H	−2.8017790	0.7900470	−3.5221140

TATA^{+}, E = −1013.731717 au, G = −1013.423884 au

Symbol	X	Y	Z
H	−0.1933540	−4.5928500	−0.1898720
C	−0.6968530	−3.6435840	−0.1131240
C	−2.1258750	−1.2117180	−0.0015020
C	−2.0818430	−3.6065790	−0.1746560
C	0.0138930	−2.4468880	−0.0012110
C	−0.7036800	−1.2190330	0.0245810
C	−2.8066190	−2.4257280	−0.1138830
H	−2.6201810	−4.5390410	−0.2877980
H	−3.8804590	−2.4647630	−0.1912200
C	0.0000140	0.0000000	0.0524760
C	1.4076590	0.0001270	0.0245930
C	2.1123590	−1.2352660	−0.0012520
N	1.3955900	−2.4168590	0.0795880
C	3.5041260	−1.2177810	−0.1134030
C	4.1642470	0.0003760	−0.1744410
C	3.5039060	1.2184140	−0.1134040
C	2.1121360	1.2356470	−0.0012520
H	4.0752420	−2.1279710	−0.1904860
H	5.2409230	0.0004730	−0.2876230
H	4.0748580	2.1287070	−0.1904860
C	−0.7039000	1.2189060	0.0245810
C	−2.0824940	3.6062030	−0.1746560
C	−2.1260940	1.2113340	−0.0015020
C	0.0134510	2.4468910	−0.0012110
C	−0.6975110	3.6434580	−0.1131240
C	−2.8070570	2.4252210	−0.1138830
H	−2.6210010	4.5385680	−0.2877970
H	−0.1941830	4.5928150	−0.1898720
H	−3.8809040	2.4640620	−0.1912200
N	−2.7908590	−0.0002520	0.0795580
N	1.3951530	2.4171110	0.0795880
C	2.1237540	−3.6777100	0.2352700

H	2.3755190	−4.1163280	−0.7320430
H	1.5164250	−4.3743810	0.8032600
H	3.0319020	−3.4987440	0.8009510
C	−4.2468520	−0.0003840	0.2354240
H	−4.5462010	0.8747270	0.8023680
H	−4.5460430	−0.8755480	0.8023680
H	−4.7525610	−0.0004290	−0.7319780
C	2.1230900	3.6780930	0.2352690
H	2.3747750	4.1167580	−0.7320430
H	3.0312690	3.4992920	0.8009510
H	1.5156340	4.3746550	0.8032600

MeO-TATA$^+$, E = −1357.445784 au, G = −1357.051559 au

Symbol	X	Y	Z
H	0.3829830	−4.5687530	0.1176170
C	0.8582270	−3.6085540	0.0370430
C	2.1777670	−1.1148080	−0.0769500
C	2.2477430	−3.5128400	0.0968860
C	0.1029490	−2.4412670	−0.0764210
C	0.7572550	−1.1829370	−0.1065270
C	2.9131550	−2.2856580	0.0343270
H	3.9874520	−2.2956580	0.1130070
C	0.0000040	0.0000500	−0.1361150
C	−1.4031450	−0.0642770	−0.1067480
C	−2.0544410	−1.3285650	−0.0772960
N	−1.2798170	−2.4782920	−0.1591180
C	−3.4362430	−1.3799180	0.0324030
C	−4.1664480	−0.1900950	0.0939880
C	−3.5544670	1.0611150	0.0348430
C	−2.1657690	1.1315550	−0.0768890
H	−3.9822390	−2.3051620	0.1110300
H	−4.1481600	1.9529780	0.1146050
C	0.6459210	1.2473160	−0.1064770
C	1.9186560	3.7031030	0.0960260
C	2.0629200	1.3098770	−0.0776950
C	−0.1233340	2.4434220	−0.0754410
C	0.5231210	3.6656310	0.0353720
C	2.6963080	2.5476690	0.0347930

H	−0.0054180	4.6007980	0.1152740
H	3.7656170	2.6160320	0.1137400
N	2.7862050	0.1307390	−0.1607990
N	−1.5063380	2.3476890	−0.1575540
C	−1.9483070	−3.7706980	−0.3089340
H	−2.1716320	−4.2226400	0.6596640
H	−1.3154070	−4.4383300	−0.8848780
H	−2.8695040	−3.6347570	−0.8657140
C	4.2395840	0.1970710	−0.3126060
H	4.5012910	1.0784130	−0.8894440
H	4.5809630	−0.6693200	−0.8693330
H	4.7440160	0.2298150	0.6552000
C	−2.2910450	3.5734130	−0.3046100
H	−2.5707150	3.9905410	0.6649540
H	−3.1858380	3.3607150	−0.8808200
H	−1.7126190	4.3044470	−0.8596810
O	2.4435540	4.9387280	0.2309560
O	3.0554060	−4.5851710	0.2319750
O	−5.4990960	−0.3535020	0.2278690
C	3.8650830	5.0851250	0.3077370
H	4.0429720	6.1524110	0.4025530
H	4.2627910	4.5671130	1.1824640
H	4.3436280	4.7116160	−0.5994650
C	2.4717140	−5.8896020	0.3081820
H	3.3070700	−6.5770260	0.4049510
H	1.8224390	−5.9752400	1.1814910
H	1.9107370	−6.1176910	−0.5999840
C	−6.3370330	0.8040890	0.3057850
H	−6.2528880	1.4064350	−0.6006970
H	−7.3501660	0.4240550	0.4000640
H	−6.0876880	1.4065360	1.1812530

A−TOTA^{+}, E = −1589.781641 au, G = −1589.284463 au

Symbol	X	Y	Z
H	2.4269640	3.8359910	−0.0102190
C	2.4261090	2.7575050	0.0026670
C	2.4166880	−0.0544940	−0.0031120
C	3.6465980	2.0187920	0.0006180

C	1.2366020	2.0772850	0.0030830
C	1.2145950	0.6725900	−0.0002770
C	3.6246100	0.5923920	−0.0019600
H	4.5389790	0.0205510	0.0111400
C	0.0000290	0.0001880	−0.0007810
C	−1.1896470	0.7158720	−0.0005540
C	−1.1610750	2.1204670	−0.0020670
O	0.0499800	2.7780800	0.0009470
C	−2.3253680	2.8429820	−0.0006280
C	−3.5716310	2.1487710	0.0001110
C	−3.6010050	0.7224840	0.0007410
C	−2.4171250	0.0325320	0.0012570
H	−2.2874660	3.9206790	0.0131800
H	−4.5354180	0.1840080	−0.0121910
C	−0.0249520	−1.3879100	−0.0014420
C	−0.0749500	−4.1672170	−0.0016960
C	1.1805690	−2.1093320	0.0010820
C	−1.2556210	−2.0654480	−0.0044760
C	−1.2993470	−3.4349900	−0.0038900
C	1.1749550	−3.4795630	0.0000630
H	−2.2518470	−3.9408380	0.0088880
H	2.1084500	−4.0196000	−0.0127920
O	2.3807120	−1.4320870	−0.0011230
O	−2.4306590	−1.3454870	−0.0019180
N	−0.0990690	−5.5136770	−0.0009500
N	−4.7256480	2.8428690	0.0010620
N	4.8249060	2.6708080	0.0005690
C	−1.3276670	−6.3126400	−0.0965260
H	−1.9624410	−5.9457000	−0.9041620
H	−1.8937130	−6.2510510	0.8390770
C	1.0998370	−6.3562390	0.0979210
H	1.6679360	−6.3191730	−0.8377570
H	1.7476640	−6.0092360	0.9040360
C	6.1308600	2.0061880	−0.0987200
H	6.1282140	1.2728980	−0.9063220
H	6.3635000	1.4851370	0.8361290
C	4.9555820	4.1302860	0.0997070
H	4.3338390	4.5175230	0.9080750
H	4.6365450	4.6039670	−0.8348480

C	−4.8036110	4.3064610	−0.0938070
H	−4.1658560	4.6737620	−0.8989540
H	−4.4706750	4.7656060	0.8431760
C	−6.0548170	2.2252260	0.0952360
H	−6.3031900	1.7151750	−0.8416920
H	−6.0805110	1.4902220	0.9008480
C	−0.8173050	−7.7308780	−0.3531860
H	−0.6818130	−7.8867990	−1.4256620
H	−1.5095360	−8.4867870	0.0147120
C	0.5383230	−7.7540470	0.3601870
H	1.2026410	−8.5361150	−0.0044440
H	0.3971450	−7.9004660	1.4332600
C	−6.9860100	3.4097460	0.3551090
H	−7.9941060	3.2251480	−0.0131220
H	−7.0460900	3.6045340	1.4280840
C	−6.2863430	4.5730140	−0.3551210
H	−6.4855730	4.5340030	−1.4282490
H	−6.5965630	5.5501190	0.0122150
C	6.4476740	4.3428680	0.3572880
H	6.6484610	4.2939860	1.4297720
H	6.7916390	5.3092000	−0.0085650
C	7.1032480	3.1572640	−0.3581040
H	8.1050710	2.9355760	0.0067950
H	7.1673340	3.3526990	−1.4307630

A−ADOTA^{+}, E = −1609.254186 au, G = −1608.717999 au

Symbol	X	Y	Z
H	0.0091380	−4.5347900	0.0365090
C	−0.5617830	−3.6208610	−0.0066820
C	−2.0405850	−1.1954720	−0.0910150
C	−1.9849430	−3.6308140	0.0035620
C	0.0872840	−2.4173020	−0.0410630
C	−0.6221430	−1.1995770	−0.0778420
C	−2.7080560	−2.4106210	−0.0357150
H	−3.7822060	−2.4480780	−0.0139490
C	0.0816880	−0.0009730	−0.0797160
C	1.4812700	−0.0200220	−0.0522870
C	2.1712520	−1.2395340	−0.0316840

O	1.4640390	−2.4181960	−0.0323650
C	3.5430050	−1.2805180	−0.0117400
C	4.2724600	−0.0580570	−0.0047020
C	3.5765130	1.1838460	−0.0120960
C	2.2042380	1.1802340	−0.0348210
H	4.0479030	−2.2336970	−0.0111440
H	4.1067820	2.1227520	0.0155480
C	−0.5899120	1.2161210	−0.0767500
C	−1.8851830	3.6834480	0.0068020
C	−2.0082150	1.2506830	−0.0936710
C	0.1527570	2.4139240	−0.0337220
C	−0.4629550	3.6347420	0.0001170
C	−2.6416490	2.4839430	−0.0334100
H	0.1323300	4.5339260	0.0169190
H	−3.7134130	2.5508060	0.0196300
N	−2.6923720	0.0363120	−0.1688180
O	1.5291000	2.3774950	−0.0300450
C	−4.1455830	0.0509050	−0.3174520
H	−4.4451650	0.9437700	−0.8564110
H	−4.4566750	−0.8056520	−0.9080100
H	−4.6481470	0.0256560	0.6519080
N	−2.5138320	4.8767430	0.0558680
N	−2.6463660	−4.8060840	0.0571030
N	5.6216730	−0.0762940	0.0130770
C	−1.8219500	6.1631840	0.2039890
H	−1.2946840	6.4213360	−0.7208930
H	−1.0896410	6.1163460	1.0113150
C	−3.9688130	5.0407490	−0.0344110
H	−4.4503690	4.6991140	0.8886820
H	−4.3709120	4.4558350	−0.8633990
C	−4.1051710	−4.9211070	0.1627240
H	−4.4878210	−4.2685710	0.9492820
H	−4.5797690	−4.6309270	−0.7813650
C	−1.9915200	−6.1192300	0.0109140
H	−1.4734190	−6.3206570	0.9548880
H	−1.2571150	−6.1558090	−0.7948280
C	6.4228230	−1.3012060	0.1162420
H	6.3757340	−1.8679730	−0.8202080
H	6.0491970	−1.9396840	0.9183950

C	6.4581020	1.1263260	−0.0700860
H	6.4064480	1.6931300	0.8661410
H	6.1194390	1.7756700	−0.8789820
C	−4.3309510	−6.4011530	0.4747010
H	−4.2855000	−6.5623930	1.5540130
H	−5.2995650	−6.7508020	0.1202390
C	−3.1493990	−7.0924940	−0.2131320
H	−3.3438740	−7.1956100	−1.2829840
H	−2.9362120	−8.0816360	0.1896130
C	7.8362940	−0.7862940	0.3915100
H	8.5997990	−1.4734320	0.0295690
H	7.9793410	−0.6548940	1.4663220
C	7.8625160	0.5729640	−0.3152890
H	8.0247330	0.4373340	−1.3868520
H	8.6366120	1.2390680	0.0631140
C	−4.1515050	6.5451590	−0.2385550
H	−5.1106610	6.8959600	0.1396870
H	−4.0980620	6.7831370	−1.3032770
C	−2.9525110	7.1496160	0.4993190
H	−3.1471440	7.1785320	1.5737060
H	−2.7101920	8.1594310	0.1712670

A−TATA^{+}, E = −1648.191328 au, G = −1647.576501 au

Symbol	X	Y	Z
H	−4.2087140	−1.7967990	0.0406850
C	−3.1496400	−1.9514130	−0.0580040
C	−0.3744810	−2.4180460	−0.1794880
C	−2.6416000	−3.2677150	0.0073940
C	−2.2850560	−0.8736530	−0.1790810
C	−0.8821380	−1.0919410	−0.2141000
C	−1.2480880	−3.4889170	−0.0612570
H	−0.8776950	−4.4955440	0.0048810
C	0.0002480	0.0000090	−0.2461230
C	−0.5041910	1.3100630	−0.2102270
C	−1.9062410	1.5332080	−0.1749510
N	−2.7542100	0.4335950	−0.2674110
C	−2.3979860	2.8240670	−0.0499690
C	−1.5103590	3.9206640	0.0192520

C	−0.1161860	3.7032010	−0.0489180
C	0.3859990	2.4160820	−0.1713260
H	−3.4535170	3.0016000	0.0478590
H	0.5460050	4.5468360	0.0200510
C	1.3871210	−0.2182080	−0.2166090
C	4.1521080	−0.6529540	−0.0063270
C	1.8997870	−1.5425210	−0.1842700
C	2.2814780	0.8846310	−0.1833260
C	3.6460670	0.6642770	−0.0678790
C	3.2664160	−1.7513610	−0.0722390
H	4.3287200	1.4886380	0.0297190
H	3.6668700	−2.7465270	−0.0082090
N	1.0020140	−2.6025390	−0.2736010
N	1.7524980	2.1693710	−0.2663580
C	−4.1870010	0.6595660	−0.4286990
H	−4.6175400	−0.1586970	−0.9980970
H	−4.3447990	1.5725260	−0.9950820
H	−4.6989540	0.7385630	0.5335730
C	1.5230900	−3.9569100	−0.4292740
H	2.4470780	−3.9239580	−0.9983450
H	0.8131000	−4.5530950	−0.9942510
H	1.7098570	−4.4353000	0.5353860
C	2.6631720	3.2992070	−0.4215430
H	2.9817460	3.7020040	0.5431720
H	3.5359960	2.9827110	−0.9843020
H	2.1717580	4.0814250	−0.9922440
N	−1.9953320	5.1778150	0.1620100
C	−3.4225310	5.5100670	0.1454190
C	−3.4377920	7.0348900	0.0267360
C	−2.1470510	7.4570590	0.7361870
C	−1.1532640	6.3637890	0.3405240
H	−3.9082260	5.1748140	1.0692380
H	−3.9229180	5.0238720	−0.6941900
H	−4.3332050	7.4721330	0.4666510
H	−3.4004040	7.3242060	−1.0259990
H	−1.8023080	8.4493050	0.4479540
H	−2.2931880	7.4493820	1.8187390
H	−0.6336560	6.6116040	−0.5925330
H	−0.3992420	6.1918130	1.1108540

N	5.4840940	−0.8621790	0.1280630
C	6.4853810	0.2076030	0.1099690
C	7.8125550	−0.5412910	−0.0207730
C	7.5375790	−1.8729360	0.6852470
C	6.0906360	−2.1850790	0.2998000
H	6.4436610	0.7918200	1.0366990
H	6.3093330	0.8877370	−0.7255130
H	8.0369680	−0.7140040	−1.0758240
H	8.6421140	0.0136140	0.4155520
H	8.2219650	−2.6666320	0.3883700
H	7.6126140	−1.7470510	1.7677310
H	6.0374150	−2.7575490	−0.6336710
H	5.5702820	−2.7530530	1.0733340
N	−3.4891780	−4.3155280	0.1476010
C	−3.0518360	−5.7028090	0.3254160
C	−4.3346980	−6.4403740	0.7128970
C	−5.4315450	−5.6393680	0.0037190
C	−4.9493130	−4.1934250	0.1300020
H	−2.2853730	−5.7716670	1.0997560
H	−2.6279790	−6.0955900	−0.6061930
H	−4.4753630	−6.3938020	1.7951590
H	−4.3099040	−7.4890870	0.4195760
H	−5.4816690	−5.9214990	−1.0504470
H	−6.4191770	−5.7827500	0.4401820
H	−5.2750350	−3.5730560	−0.7070600
H	−5.3096700	−3.7294760	1.0556220

TOTA-OH, E = −1031.322669 au, G = −1031.121501 au

Symbol	X	Y	Z
H	3.9185680	0.5201330	2.1591320
C	3.4080980	0.3650090	1.2184240
C	2.0614460	0.0286960	−1.2033580
C	4.0678030	0.5112760	0.0000000
C	2.0614460	0.0286960	1.2033580
C	1.4017030	−0.1862540	0.0000000
C	3.4080980	0.3650090	−1.2184240
H	5.1176140	0.7752770	0.0000000
H	3.9185680	0.5201330	−2.1591320

C	0.0024850	−0.6741070	0.0000000
C	−0.7002380	−0.1889210	1.2142510
C	0.0115850	0.0220130	2.3898570
O	1.3877920	−0.0748620	2.4036650
C	−0.6480760	0.3529480	3.5648320
C	−2.0331440	0.5030450	3.5282280
C	−2.7577810	0.3678310	2.3463010
C	−2.0712610	0.0377800	1.1857090
H	−0.0880010	0.5049290	4.4774560
H	−2.5573630	0.7634620	4.4387810
H	−3.8266690	0.5298820	2.3172990
C	−0.7002380	−0.1889210	−1.2142510
C	−2.0331440	0.5030450	−3.5282280
C	0.0115850	0.0220130	−2.3898570
C	−2.0712610	0.0377800	−1.1857090
C	−2.7577810	0.3678310	−2.3463010
C	−0.6480760	0.3529480	−3.5648320
H	−2.5573630	0.7634620	−4.4387810
H	−3.8266690	0.5298820	−2.3172990
H	−0.0880010	0.5049290	−4.4774560
O	−2.7743320	−0.0524670	0.0000000
O	1.3877920	−0.0748620	−2.4036650
O	0.0887970	−2.1338640	0.0000000
H	−0.8105800	−2.4899540	0.0000000

ADOTA-OH, E = −1050.788180 au, G = −1050.547701 au

Symbol	X	Y	Z
H	0.5121450	0.1940600	4.4849080
C	0.3714090	−0.3901810	3.5859090
C	0.0458880	−1.8828730	1.2122580
C	0.5166780	−1.7725170	3.5779320
C	0.0524380	0.2367490	2.3890520
C	−0.1450310	−0.4924310	1.2233250
C	0.3744020	−2.5227490	2.4146530
H	0.7748730	−2.2812300	4.4983280
H	0.5431920	−3.5880660	2.4510330
C	−0.6332320	0.1984670	0.0000000
C	−0.1815140	1.6129500	0.0000000

C	0.0178330	2.2835440	1.1998200
O	−0.0632690	1.6123180	2.3979860
C	0.3178270	3.6393120	1.2163390
C	0.4463350	4.3049650	0.0000000
C	0.3178270	3.6393120	−1.2163390
C	0.0178330	2.2835440	−1.1998200
H	0.4592310	4.1507570	2.1587440
H	0.6812810	5.3617310	0.0000000
H	0.4592310	4.1507570	−2.1587440
C	−0.1450310	−0.4924310	−1.2233250
C	0.5166780	−1.7725170	−3.5779320
C	0.0458880	−1.8828730	−1.2122580
C	0.0524380	0.2367490	−2.3890520
C	0.3714090	−0.3901810	−3.5859090
C	0.3744020	−2.5227490	−2.4146530
H	0.7748730	−2.2812300	−4.4983280
H	0.5121450	0.1940600	−4.4849080
H	0.5431920	−3.5880660	−2.4510330
N	−0.0944540	−2.5698270	0.0000000
O	−0.0632690	1.6123180	−2.3979860
C	−0.0783990	−4.0255710	0.0000000
H	−0.6057220	−4.3903560	−0.8778800
H	−0.6057220	−4.3903560	0.8778800
H	0.9377890	−4.4323950	0.0000000
O	−2.1024710	0.2523550	0.0000000
H	−2.4297260	−0.6579140	0.0000000

DAOTA-OH, E = −1070.251601 au, G = −1069.971675 au

Symbol	X	Y	Z
H	−2.2790140	−4.0790910	−0.4635610
C	−2.3349270	−3.0069710	−0.3333460
C	−2.4276920	−0.2070310	−0.0328890
C	−3.5310980	−2.3124210	−0.4596760
C	−1.1861920	−2.2802370	−0.0473260
C	−1.2219770	−0.9045310	0.1381740
C	−3.5918970	−0.9289190	−0.3292100
H	−4.4378590	−2.8567750	−0.6924350
H	−4.5342720	−0.4259310	−0.4826580

C	1.2213610	−0.9080030	0.1415630
C	1.1794730	−2.2821080	−0.0489800
O	−0.0040940	−2.9775910	0.0476790
C	2.3255050	−3.0115810	−0.3408230
C	3.5231650	−2.3198790	−0.4657780
C	3.5888670	−0.9372140	−0.3289260
C	2.4280580	−0.2123220	−0.0260310
H	2.2661490	−4.0830840	−0.4740770
H	4.4279790	−2.8659710	−0.7022290
H	4.5328640	−0.4369100	−0.4810710
C	0.0037340	1.2222640	0.1049230
C	0.0086540	3.9023070	−0.5647350
C	−1.2167890	1.8904490	−0.0765010
C	1.2274310	1.8875320	−0.0678990
C	1.2221370	3.2476280	−0.4055190
C	−1.2073350	3.2508170	−0.4138050
H	0.0109070	4.9501910	−0.8391910
H	2.1420400	3.7873330	−0.5681290
H	−2.1251400	3.7923310	−0.5818600
N	−2.4147310	1.1834770	0.0937250
C	−3.6761850	1.9087780	0.1149330
H	−4.4142920	1.3276040	0.6620620
H	−4.0594490	2.1142910	−0.8897370
H	−3.5410560	2.8504880	0.6410040
N	2.4205600	1.1767470	0.0985740
C	3.6845240	1.8969240	0.1290890
H	4.4175590	1.3103420	0.6771800
H	4.0734690	2.1060800	−0.8727170
H	3.5503450	2.8363850	0.6594390
C	0.0019890	−0.1852840	0.5961750
O	0.0647080	−0.2012980	2.0725390
H	−0.6807720	0.3210790	2.3996530

TATA-OH, E = −1089.712804 au, G = −1089.393443 au

Symbol	X	Y	Z
H	0.1548200	0.5212800	4.5384950
C	0.6814350	0.3682860	3.6094480
C	2.1020210	0.0657910	1.2097020

C	2.0603310	0.5143750	3.5734270
C	−0.0072390	0.0585260	2.4280010
C	0.7090340	−0.1002620	1.2316560
C	2.7812970	0.3750380	2.3968580
H	2.5863940	0.7683560	4.4857850
H	3.8485190	0.5324360	2.4047280
C	−0.0027690	−0.5627280	0.0000000
C	−1.4235830	−0.1035440	0.0000000
C	−2.0990180	0.0592030	1.2180080
N	−1.3934200	−0.0927300	2.4122800
C	−3.4659280	0.3727630	1.2124700
C	−4.1236950	0.5166750	0.0000000
C	−3.4659280	0.3727630	−1.2124700
C	−2.0990180	0.0592030	−1.2180080
H	−4.0067920	0.5278010	2.1329170
H	−5.1764810	0.7723090	0.0000000
H	−4.0067920	0.5278010	−2.1329170
C	0.7090340	−0.1002620	−1.2316560
C	2.0603310	0.5143750	−3.5734270
C	2.1020210	0.0657910	−1.2097020
C	−0.0072390	0.0585260	−2.4280010
C	0.6814350	0.3682860	−3.6094480
C	2.7812970	0.3750380	−2.3968580
H	2.5863940	0.7683560	−4.4857850
H	0.1548200	0.5212800	−4.5384950
H	3.8485190	0.5324360	−2.4047280
N	2.7833120	−0.0898600	0.0000000
N	−1.3934200	−0.0927300	−2.4122800
C	−2.1213670	−0.1585110	3.6699580
H	−2.3554900	0.8316710	4.0748540
H	−1.5291920	−0.7060890	4.3989410
H	−3.0486210	−0.7056810	3.5192970
C	4.2370540	−0.1455060	0.0000000
H	4.5752830	−0.6901210	−0.8780270
H	4.5752830	−0.6901210	0.8780270
H	4.6974210	0.8480050	0.0000000
C	−2.1213670	−0.1585110	−3.6699580
H	−2.3554900	0.8316710	−4.0748540
H	−3.0486210	−0.7056810	−3.5192970

H	−1.5291920	−0.7060890	−4.3989410
O	−0.0738430	−2.0461640	0.0000000
H	0.8358210	−2.3749530	0.0000000

MeO-TATA-OH, E = −1433.417570 au, G = −1433.012118 au

Symbol	X	Y	Z
H	4.5135620	−0.3420370	−0.3322390
C	3.5745240	−0.8415160	−0.1722730
C	1.1124560	−2.1526800	0.1319210
C	3.4761050	−2.2209130	−0.3177920
C	2.4195330	−0.1081960	0.1414200
C	1.1935530	−0.7617230	0.3041830
C	2.2597020	−2.8855330	−0.1770910
H	2.2376610	−3.9506270	−0.3447770
C	0.0002860	0.0020390	0.7711280
C	0.0644120	1.4162580	0.3103510
C	1.3104200	2.0398430	0.1428050
N	2.4723830	1.2786110	0.2917720
C	1.3713630	3.3987990	−0.1704770
C	0.1877930	4.1191820	−0.3169210
C	−1.0564260	3.5152720	−0.1741640
C	−1.1140660	2.1489520	0.1433510
H	2.3050240	3.9124330	−0.3363200
H	−1.9581900	4.0785390	−0.3366960
C	−1.2578550	−0.6502890	0.3053460
C	−3.6642910	−1.8952100	−0.3151320
C	−1.3051040	−2.0370970	0.1330700
C	−2.4232540	0.1166340	0.1432850
C	−3.6315020	−0.5102170	−0.1651940
C	−2.5182490	−2.6706300	−0.1796870
H	−4.5438830	0.0416520	−0.3267380
H	−2.5550620	−3.7325980	−0.3458800
N	−0.1289310	−2.7783990	0.2843470
N	−2.3432090	1.5023300	0.2929870
C	3.7620480	1.9479900	0.3491430
H	4.1733490	2.1588980	−0.6437260
H	4.4654710	1.3267760	0.8983480
H	3.6552620	2.8841580	0.8914490

C	−0.1945420	−4.2305350	0.3314230
H	−1.0858340	−4.5331230	0.8757190
H	0.6682490	−4.6102680	0.8731160
H	−0.2145740	−4.6849660	−0.6647490
C	−3.5665260	2.2863850	0.3511040
H	−3.9559850	2.5361690	−0.6415660
H	−3.3782440	3.2066250	0.8987540
H	−4.3240870	1.7277290	0.8952290
O	−4.8875510	−2.4137600	−0.6301680
O	4.5379140	−3.0189050	−0.6344920
O	0.3491520	5.4368240	−0.6368400
C	−4.9973270	−3.8226360	−0.8114090
H	−6.0433780	−4.0121490	−1.0390090
H	−4.3760670	−4.1634170	−1.6435310
H	−4.7185010	−4.3604900	0.0982630
C	5.8139420	−2.4083450	−0.8048790
H	6.5019140	−3.2177280	−1.0362250
H	5.8023140	−1.6928630	−1.6310000
H	6.1361030	−1.9057460	0.1105850
C	−0.8167570	6.2360060	−0.8150550
H	−1.4175790	6.2663400	0.0973460
H	−0.4586980	7.2358900	−1.0474240
H	−1.4264060	5.8658610	−1.6432420
O	0.0040430	0.0703880	2.2609320
H	−0.0340140	−0.8402530	2.5843790

A-TOTA-OH, E = −1665.761059 au, G = −1665.254850 au

Symbol	X	Y	Z
H	−2.1654200	−3.8776160	−0.0802390
C	−2.2547050	−2.8196960	0.1142770
C	−2.3830850	−0.0627490	0.4826990
C	−3.4904780	−2.1450780	−0.0312910
C	−1.1299270	−2.0978800	0.4688980
C	−1.1873690	−0.7318490	0.7137990
C	−3.5359220	−0.7393060	0.1306720
H	−4.4475840	−0.1838290	−0.0283040
C	0.0002070	0.0004040	1.2030490
C	1.2269040	−0.6638250	0.7132420

C	1.2456810	−2.0301490	0.4648280
O	0.0782670	−2.7717320	0.5595290
C	2.4100430	−2.6884400	0.1130200
C	3.6055140	−1.9453150	−0.0326670
C	3.5716280	−0.5389590	0.1293450
C	2.3839220	0.0713820	0.4850730
H	2.3847330	−3.7539440	−0.0572040
H	4.4447190	0.0684570	−0.0545490
C	−0.0391040	1.3925640	0.7155990
C	−0.1153290	4.0904160	−0.0319220
C	−1.2530140	2.0252350	0.4838750
C	1.1367780	2.0916190	0.4793970
C	1.1257390	3.4278620	0.1238830
C	−1.3171000	3.3587840	0.1252650
H	2.0616890	3.9400410	−0.0389990
H	−2.2789460	3.8115010	−0.0614120
O	−2.4392960	1.3168780	0.5856690
O	2.3613600	1.4523260	0.5841090
N	−0.1541340	5.4115090	−0.3676450
N	4.7709360	−2.5710930	−0.3633910
N	−4.6176190	−2.8376590	−0.3616620
C	1.0333460	6.2067580	−0.6716260
H	1.6798180	5.6879540	−1.3837660
H	1.6206350	6.3952950	0.2358690
C	−1.3888470	6.1853400	−0.4704140
H	−1.9588740	5.9004270	−1.3642250
H	−2.0276760	6.0156450	0.3994150
C	−5.9009780	−2.2051300	−0.6591950
H	−5.7767620	−1.3820670	−1.3672130
H	−6.3553070	−1.7956610	0.2517240
C	−4.6692270	−4.2927760	−0.4787250
H	−4.1975220	−4.7692250	0.3838410
H	−4.1421390	−4.6345310	−1.3789670
C	4.8663560	−3.9951860	−0.6765440
H	4.0967320	−4.2904530	−1.3940120
H	4.7314070	−4.6037910	0.2264420
C	6.0584480	−1.8878590	−0.4615200
H	6.0989130	−1.2499490	−1.3539410
H	6.2284310	−1.2516230	0.4101020

C	0.4615840	7.5031960	−1.2507300
H	0.3238440	7.3964960	−2.3293250
H	1.1159570	8.3567800	−1.0765000
C	−0.8992420	7.6322720	−0.5571140
H	−1.5970630	8.2731950	−1.0951490
H	−0.7710520	8.0391360	0.4487290
C	7.0669430	−3.0349950	−0.5485620
H	7.9732110	−2.7489580	−1.0815010
H	7.3507350	−3.3537780	0.4572050
C	6.2774280	−4.1457390	−1.2504080
H	6.2584690	−3.9682890	−2.3282870
H	6.6886230	−5.1400540	−1.0789440
C	−6.1671600	−4.5928340	−0.5605770
H	−6.5789480	−4.6929230	0.4464670
H	−6.3750580	−5.5137580	−1.1045030
C	−6.7395780	−3.3450920	−1.2425980
H	−7.8052850	−3.2071430	−1.0626710
H	−6.5831140	−3.4032710	−2.3223260
O	−0.0017410	0.0783220	2.6801170
H	0.0230860	−0.8275530	3.0175740

A-ADOTA-OH, E = −1685.224784 au, G = −1684.679825 au

Symbol	X	Y	Z
H	0.0575480	−4.4574900	−0.0860950
C	0.6299400	−3.5583640	0.0832710
C	2.0361660	−1.1432130	0.4276500
C	2.0327930	−3.5308440	−0.0666390
C	−0.0267940	−2.3873910	0.4167990
C	0.6494700	−1.1943230	0.6292690
C	2.7249850	−2.3082170	0.0880130
H	3.7877630	−2.2829030	−0.0816450
C	−0.0816380	−0.0038680	1.1207690
C	−1.4872260	−0.0538560	0.6660240
C	−2.1200670	−1.2691240	0.4445590
O	−1.4062370	−2.4479770	0.5277330
C	−3.4639340	−1.3446490	0.1239490
C	−4.2097490	−0.1507560	−0.0115670
C	−3.5517340	1.0934160	0.1296610

C	−2.2068640	1.1138020	0.4525830
H	−3.9169820	−2.3127090	−0.0267320
H	−4.0679590	2.0257680	−0.0418040
C	0.5620390	1.2369890	0.6314510
C	1.7729290	3.6666980	−0.0658910
C	1.9490370	1.2861530	0.4310290
C	−0.1985520	2.3778200	0.4175810
C	0.3721960	3.5939480	0.0864570
C	2.5512790	2.4966300	0.0869660
H	−0.2616440	4.4557710	−0.0557520
H	3.6086140	2.5425050	−0.1111990
N	2.6820610	0.0959370	0.5757540
O	−1.5782100	2.3403730	0.5352950
C	4.1339510	0.1476950	0.5468660
H	4.4717140	1.0425620	1.0644290
H	4.5351860	−0.7136680	1.0761170
H	4.5359570	0.1552430	−0.4722820
N	2.3712340	4.8509330	−0.3914390
N	2.7134010	−4.6703510	−0.3903680
N	−5.5400530	−0.1967730	−0.3113960
C	1.6324100	6.0738750	−0.6943480
H	1.1762130	6.4919240	0.2121680
H	0.8292130	5.8785580	−1.4092610
C	3.8169540	5.0324190	−0.4826960
H	4.2226070	4.5351420	−1.3736970
H	4.3189370	4.6087690	0.3907100
C	4.1429500	−4.7075940	−0.6860840
H	4.4161310	−3.9278400	−1.4017410
H	4.7367090	−4.5471580	0.2231720
C	2.0857990	−5.9850250	−0.4908320
H	1.4568400	−6.0548720	−1.3880420
H	1.4497650	−6.1802160	0.3758210
C	−6.2625250	−1.4314810	−0.6076140
H	−6.3944460	−2.0353420	0.2990870
H	−5.7174190	−2.0391000	−1.3343020
C	−6.3923650	0.9860550	−0.3954430
H	−6.1631280	1.5746820	−1.2934090
H	−6.2460080	1.6334610	0.4723570
C	4.3585090	−6.1117190	−1.2564700

H	4.1914650	−6.1009800	−2.3361840
H	5.3673280	−6.4811910	−1.0744410
C	3.2741470	−6.9458220	−0.5652640
H	3.5942860	−7.2156410	0.4439860
H	3.0313240	−7.8636630	−1.1000010
C	−7.6048370	−0.9420090	−1.1572140
H	−8.4110640	−1.6504600	−0.9691580
H	−7.5294580	−0.7934570	−2.2370490
C	−7.8065430	0.4051800	−0.4543560
H	−8.1831120	0.2474830	0.5591050
H	−8.5021310	1.0622860	−0.9755940
C	3.9843180	6.5511420	−0.5666610
H	4.8907890	6.8386910	−1.0986490
H	4.0333880	6.9730040	0.4400570
C	2.7001240	7.0089080	−1.2672610
H	2.7860540	6.8546060	−2.3455350
H	2.4661930	8.0589180	−1.0938300
O	−0.1310430	−0.0073470	2.6075670
H	0.7837720	0.0238570	2.9194390

A-TATA-OH, E = −1724.146313 au, G = −1723.523738 au

Symbol	X	Y	Z
H	4.3073050	−1.3463980	−0.1264390
C	3.2849030	−1.6266830	0.0592970
C	0.5992230	−2.3481890	0.3885420
C	2.8999690	−2.9725020	−0.0833970
C	2.3311540	−0.6562970	0.3766720
C	0.9871600	−1.0111470	0.5528560
C	1.5469640	−3.3255940	0.0748410
H	1.2471950	−4.3485510	−0.0727900
C	−0.0007370	0.0016860	1.0171570
C	0.3812120	1.3621280	0.5475730
C	1.7310120	1.6941710	0.3711430
N	2.6942060	0.6886280	0.5305550
C	2.1031940	3.0017190	0.0489170
C	1.1204630	3.9979370	−0.0981740
C	−0.2363530	3.6600090	0.0600410
C	−0.5999990	2.3488940	0.3776550

H	3.1349850	3.2452200	−0.1367920
H	−0.9896450	4.4135750	−0.0908880
C	−1.3709870	−0.3491100	0.5619720
C	−4.0231290	−1.0275150	−0.0741830
C	−1.7332700	−1.6916450	0.3931540
C	−2.3327240	0.6547090	0.3896950
C	−3.6518410	0.3217660	0.0715830
C	−3.0512740	−2.0334250	0.0787240
H	−4.3800330	1.0926730	−0.1121870
H	−3.3273050	−3.0625890	−0.0718390
N	−0.7512580	−2.6776340	0.5475390
N	−1.9432790	1.9915100	0.5353810
C	4.1008450	1.0479860	0.5730480
H	4.6507420	0.2820420	1.1151990
H	4.2155340	1.9857710	1.1119730
H	4.5425170	1.1588950	−0.4238520
C	−1.1442390	−4.0743710	0.6058090
H	−2.0804620	−4.1615140	1.1522950
H	−0.3893300	−4.6376680	1.1495220
H	−1.2719660	−4.5229170	−0.3860990
C	−2.9575590	3.0294780	0.5877190
H	−3.2782740	3.3623480	−0.4061370
H	−3.8245390	2.6567370	1.1281590
H	−2.5680070	3.8855720	1.1339780
N	1.4805070	5.2793770	−0.4211360
C	2.8644580	5.7334300	−0.5066380
C	2.7412840	7.2573790	−0.5759950
C	1.3907400	7.4705420	−1.2687620
C	0.5229120	6.3433150	−0.7039760
H	3.3599990	5.3308340	−1.4003400
H	3.4378860	5.4053740	0.3642530
H	3.5747270	7.7167760	−1.1070000
H	2.7136460	7.6717580	0.4347340
H	0.9625100	8.4553770	−1.0834690
H	1.4999540	7.3464950	−2.3489150
H	0.0004030	6.6582800	0.2091930
H	−0.2342690	6.0104150	−1.4187720
N	−5.3142080	−1.3566300	−0.3917100
C	−6.4013000	−0.3862860	−0.4670000

C	−7.6591390	−1.2564110	−0.5234100
C	−7.1738840	−2.5325110	−1.2200930
C	−5.7582560	−2.7185380	−0.6686260
H	−6.3100150	0.2437770	−1.3620020
H	−6.3959260	0.2747360	0.4034980
H	−7.9937160	−1.4873030	0.4908860
H	−8.4796360	−0.7656680	−1.0465060
H	−7.8099370	−3.3963460	−1.0280950
H	−7.1315960	−2.3766270	−2.3008250
H	−5.7605580	−3.3273640	0.2454110
H	−5.0976700	−3.2080770	−1.3891210
N	3.8302420	−3.9258990	−0.4022130
C	3.4995170	−5.3190800	−0.6827540
C	4.8010570	−5.8935020	−1.2474730
C	5.8847940	−5.0571490	−0.5580430
C	5.2621560	−3.6606720	−0.4916550
H	2.6750780	−5.3908480	−1.3970680
H	3.1923080	−5.8445050	0.2313550
H	4.8362510	−5.7348870	−2.3280430
H	4.8976790	−6.9626230	−1.0597180
H	6.0603860	−5.4314240	0.4534600
H	6.8358410	−5.0620310	−1.0901370
H	5.6098220	−3.0950170	0.3766940
H	5.5018540	−3.0725960	−1.3878190
O	−0.0604510	−0.0103700	2.5197770
H	0.8264280	0.2186640	2.8297970

1.11 References

[1] B. W. Laursen and F. C. Krebs, *Angew. Chem., Int. Ed.* **2000**, *39*, 3432-3434.
[2] H. E. Gottlieb, V. Kotlyar and A. Nudelman, *J. Org. Chem.* **1997**, *62*, 7512-7515.
[3] Z. Gryczynski and I. Gryczynski, *Practical Fluorescence Spectroscopy*. 1st ed., Taylor & Francis Group: **2019**.
[4] M. Fischer and J. Georges, *Chem. Phys. Lett.* **1996**, *260*, 115-118.
[5] K. Rurack and M. Spieles, *Anal. Chem.* **2011**, *83*, 1232-1242.
[6] M. J. Frisch, G. W. Trucks, H. B. Schlegel, G. E. Scuseria, M. A. Robb, J. R. Cheeseman, G. Scalmani, V. Barone, G. A. Petersson, H. Nakatsuji, X. Li, M. Caricato, A. V. Marenich, J. Bloino, B. G. Janesko, R. Gomperts, B. Mennucci, H. P. Hratchian, J. V. Ortiz, A. F. Izmaylov, J. L. Sonnenberg, Williams, F. Ding, F. Lipparini, F. Egidi, J. Goings, B. Peng, A. Petrone, T. Henderson, D. Ranasinghe, V. G. Zakrzewski, J. Gao, N. Rega, G. Zheng, W. Liang, M. Hada, M. Ehara, K. Toyota, R. Fukuda, J. Hasegawa, M. Ishida, T. Nakajima, Y. Honda, O. Kitao, H. Nakai, T. Vreven, K.

Throssell, J. A. Montgomery Jr., J. E. Peralta, F. Ogliaro, M. J. Bearpark, J. J. Heyd, E. N. Brothers, K. N. Kudin, V. N. Staroverov, T. A. Keith, R. Kobayashi, J. Normand, K. Raghavachari, A. P. Rendell, J. C. Burant, S. S. Iyengar, J. Tomasi, M. Cossi, J. M. Millam, M. Klene, C. Adamo, R. Cammi, J. W. Ochterski, R. L. Martin, K. Morokuma, O. Farkas, J. B. Foresman and D. J. Fox, Gaussian 16, Revision C.01, 2016,Wallingford, CT,
[7] N. G. Limas and T. A. Manz, ChargeMol, Program for Performing DDEC Analysis, v3.5, 2017,ddec.sourceforge.net.,
[8] S. Ito, F. J. White, E. Okunishi, Y. Aoyama, A. Yamano, H. Sato, J. D. Ferrara, M. Jasnowski and M. Meyer, *CrystEngComm* **2021**, *23*, 8622-8630.
[9] Rigaku Corporation, CrysAlisPro, v171.44.122a, Rigaku Oxford Difraction Ltd, Wroclaw, Poland, 2025,
[10] O. V. Dolomanov, L. J. Bourhis, R. J. Gildea, J. A. K. Howard and H. Puschmann, *J. Appl. Crystallogr.* **2009**, *42*, 339-341.
[11] G. Sheldrick, *Acta Crystallogr. A* **2015**, *71*, 3-8.
[12] G. Sheldrick, *Acta Crystallogr. C* **2015**, *71*, 3-8.
[13] L. M. Peng, *Micron* **1999**, *30*, 625-648.
[14] F. H. Allen and I. J. Bruno, *Acta Crystallogr. B* **2010**, *66*, 380-386.
[15] D. N. Rainer and J. Hester, CIVET - CIF Validation and Editing Tool, v1.1, 2026, DOI: 10.5281/zenodo.18178135.
[16] H. Noguchi, T. Hirose, S. Yokoyama and K. Matsuda, *CrystEngComm* **2016**, *18*, 7377-7383.
[17] V. V. Pavlishchuk and A. W. Addison, *Inorganica Chim. Acta* **2000**, *298*, 97-102.
[18] S. Ito, S. Kikuchi, N. Morita and T. Asao, *Chem. Lett.* **1996**, *25*, 175-176.
[19] S. Ito, S. Kikuchi, N. Morita and T. Asao, *J. Org. Chem.* **1999**, *64*, 5815-5821.
[20] S. Ito, S. Kikuchi, N. Morita and T. Asao, *Bull. Chem. Soc. Jpn.* **1999**, *72*, 839-849.
[21] E. M. Arnett, R. A. Flowers, R. T. Ludwig, A. E. Meekhof and S. A. Walek, *J. Phys. Org. Chem.* **1997**, *10*, 499-513.
[22] B. W. Laursen, F. C. Krebs, M. F. Nielsen, K. Bechgaard, J. B. Christensen and N. Harrit, *J. Am. Chem. Soc.* **1998**, *120*, 12255-12263.
[23] B. W. Laursen and F. C. Krebs, *Chem. Eur. J.* **2001**, *7*, 1773-1783.
[24] B. W. Laursen and T. J. Sørensen, *J. Org. Chem.* **2009**, *74*, 3183-3185.
[25] J. C. Martin and R. G. Smith, *J. Am. Chem. Soc.* **1964**, *86*, 2252-2256.